WL-TM-97-3084

PROGRESS AND NEW TECHNIQUES IN BUFFET ALLEVIATION

WLADIMIRO CALARESE
Unsteady Aerodynamics
Integrated Product Team
Chairman - Retired

ELIJAH TURNER
Vibration and Aeroelasticity Branch

FINAL
Technical Memorandum
for Period
October 1994 to September 1997

SEPTEMBER 1997

Approved for public release; distribution unlimited.

FLIGHT DYNAMICS DIRECTORATE
WRIGHT LABORATORY
AIR FORCE MATERIEL COMMAND
WRIGHT-PATTERSON AFB, OH 45433-7542

NOTICE

THIS TECHNICAL REPORT HAS BEEN REVIEWED AND IS APPROVED FOR PUBLICATION.

Wladimiro Calarese
Chief Scientist - Retired
Flight Dynamics Directorate

Elijah Turner
Vibration and Aeroelasticity Branch
Structures Division

Terry M. Harris
Chief - Vibration and Aeroelasticity Branch
Structures Division

L. J. Huttsell
Leader - Unsteady Aero IPT
Vibration and Aeroelasticity Branch

REPORT DOCUMENTATION PAGE

Form Approved
OMB No. 0704-0188

1. AGENCY USE ONLY *(Leave blank)*

2. REPORT DATE: September 1997

3. REPORT TYPE AND DATES COVERED: FINAL Oct 94 to Sep 97

4. TITLE AND SUBTITLE

PROGRESS AND NEW TECHNIQUES IN BUFFET ALLEVIATION

5. FUNDING NUMBERS

PE 65502
PR 2404
TA 49
WU 51

6. AUTHOR(S)

Wladimiro Calarese
Elijah Turner

7. PERFORMING ORGANIZATION NAME(S) AND ADDRESS(ES)

Flight Dynamics Directorate
Wright Laboratory
Air Force Materiel Command
Wright-Patterson AFB OH 45433-7542

8. PERFORMING ORGANIZATION REPORT NUMBER

9. SPONSORING/MONITORING AGENCY NAME(S) AND ADDRESS(ES)

Flight Dynamics Directorate
Wright Laboratory
Air Force Materiel Command
Wright-Patterson AFB OH 45433-7542

10. SPONSORING/MONITORING AGENCY REPORT NUMBER

WL-TM-97-3084

11. SUPPLEMENTARY NOTES

12a. DISTRIBUTION/AVAILABILITY STATEMENT

Approved for public release: Distribution unlimited.

12b. DISTRIBUTION CODE

13. ABSTRACT *(Maximum 200 words)*

Research for twin-tail buffet alleviation is centered on ground tests, wind tunnel tests, and computational fluid dynamics (CFD) analysis. The objective of the research is to improve present technology to obtain a significant reduction in vibration due to buffet. One of the techniques for active control of buffet is the use of smart structures with piezoelectric actuators. The actuators are embedded in the vertical tails in the most advantageous locations to reduce the response of the various structural modes of vibration due to buffet excitation. Ground and wind tunnel tests are necessary to ascertain the piezoelectric actuator's authority at full loads. It is also necessary to evaluate the increase in weight compared with the increase in damping. Two companies, ACX and Rohini International, are investigating tail buffet and buffet alleviation. The results using two different types of piezoelectric actuators are encouraging. In-house wind tunnel tests on a 4.7% scale model of an F-15C aircraft were also conducted to ascertain the effects of tangential blowing and piezoelectric actuators. The tests were performed in the SARL (Subsonic Aerodynamics Research Laboratory) wind tunnel. Tangential blowing had some effect at lower angles of attack. The tests with the actuators are scheduled for October 1997. A numerical investigation was conducted simultaneously. This report presents an overview of the buffet research at various organizations, results of the in-house wind tunnel test, and a summary of the computational effort.

14. SUBJECT TERMS

CFD, Buffet, Buffet alleviation, Buffet test, Unsteady aerodynamics

15. NUMBER OF PAGES: 76

16. PRICE CODE

17. SECURITY CLASSIFICATION OF REPORT	18. SECURITY CLASSIFICATION OF THIS PAGE	19. SECURITY CLASSIFICATION OF ABSTRACT	20. LIMITATION OF ABSTRACT
UNCLASSIFIED	UNCLASSIFIED	UNCLASSIFIED	SAR

NSN 7540-01-280-5500

Standard Form 298 (Rev. 2-89)
Prescribed by ANSI Std Z39-18
298-102

TABLE OF CONTENTS

Section	Title	Page
I	Introduction	1
II	Background	2
III	F-16 Unsteady Aerodynamic Investigation	6
IV	Techniques for Buffet Attenuation	7
V	Role of WL/FI Research Team	10
VI	Summary	16
VII	UAIPT Active Members	17
VIII	References	18
APPENDIX	Figures and Tables	23

LIST OF FIGURES

Section	Title	Page
1.	Unsteady Aerodynamics IPT	A-1
2.	Technology Interaction, Buffet Research	A-2
3.	Vertical Tail Buffet Research	A-3
4.	F-15 Twin Fin Buffet Model	A-4
5.	Wind Tunnel Model Assembly	A-5
6.	Flexible Vertical Spar	A-6
7.	Left and Right Vertical Tail Dynamic Pressure Transducer Location	A-7
8-14.	Measured Dynamic Pressure Distributions Versus Angles of Attack	A-8
15.	Photograph of Vortices Impinging on the Tails During Wind Tunnel Testing	A-15
16.	F-15 Vertical Tail Buffet Data	A-16
17.	a. Sketch of Vertical Tail Showing Modal Patterns	A-17
	b. Damping Versus Velocity for the First Three Modes	A-17
	c. Frequency Versus Velocity for the First Three Modes	A-17
18.	Response of Bending Mode Versus Angle of Attack	A-18
19.	Response of Torsion Mode Versus Angle of Attack	A-19
20.	Response of Bending Mode for Various Levels of Blowing	A-20
21.	Response of Torsion Mode for Various Levels of Blowing	A-21
22.	Structural Response due to First Bending Actuators	A-22
23.	Structural Response due to Second Bending Actuators	A-23
24.	Structural Response due to First and Second Bending Actuators	A-24
25.	Structural Response due to First Torsion Actuators	A-25
26.	F-15 Tail Buffet Study	A-26
27.	Unstructured Grid Using the Tetmesh Grid Generator	A-27
28.	Flow Sweeping over the Gun Bump Fairing	A-28
29.	Vortical Flow Outside the Vertical Tails	A-29
30.	Vortical Flow Impacting the Vertical Tails	A-30
31.	Streamline Traces from the Inlet and Wing's Leading Edge	A-31
32.	Streamline Traces from the Inlet and Wing Top	..A-32
33.	Pressure on Vertical Tails from Aircraft Right	A-33
34.	Pressure on Vertical Tails from Aircraft Left	A-34
35.	Vortical Flow over the Vertical Tails for the Engine-on Case	A-35
36.	Strain Intensity on the Vertical Tail for the First Bending Mode	A-36
37.	Strain Intensity on the Vertical Tail for the First Torsion Mode	A-37
38.	Strain Intensity on the Vertical Tail for the Second Bending Mode	A-38

LIST OF TABLES

Section	Title	Page
1-4.	Representative Test Conditions with and without Blowing	A-39
5.	Additional Data for Different Test Conditions	A-43
6.	Comparison of Analysis and Test	A-44
7.	Vertical Tail Static Pressure Comparison	A-45

FOREWORD

This technical memorandum documents the activities of the Unsteady Aerodynamics Integrated Product Team (UAIPT). Dr. Wladimiro Calarese, Chairman of the UAIPT from September 1993 until his retirement in January 1997, and Elijah Turner, a member of the UAIPT from October 1994 to the present, prepared this memorandum based on the work of the UAIPT. The study reported herein was conducted under work unit 24044951.

The support of all of the members of the UAIPT, SARL wind tunnel personnel, and other Flight Dynamics Directorate personnel is gratefully acknowledged. Bob Weyer (ASC/ENFT) performed the Euler simulations while working in WL/FIMC.

This manuscript was released by the authors in August 1997 for publication as a Wright Laboratory Technical Memorandum.

I INTRODUCTION

The problem of buffet excitation on vertical twin tails at high angle of attack has been studied by many scientists for many years with various degrees of success. Shock wave-boundary layer interaction, separated flows at high angles of attack, vortex interaction and bursting are phenomena responsible for buffet excitation and structural response of vertical twin tails of aircraft flying and maneuvering at high angles of attack. The magnitude of the structural loads can approach limiting values and would considerably reduce the fatigue life of the structure.

Various techniques for buffet attenuation have been developed. Unfortunately, the problem has not been solved. Advanced fighter aircraft capable of maneuvering at high angles of attack and high g's experience strong multiple-mode tail buffeting. Buffet attenuation and possible elimination must be studied both theoretically and experimentally. In order to achieve reliable results, the different static and dynamic effects on an aircraft structure must be analyzed simultaneously.

The first studies of buffeting started in the 1930's and both the USA and European countries showed a lot of interest in the problem (Ref 1). Later on, some predictions of tail buffet loads and fatigue damage experienced by fighter aircraft during high angle of attack maneuvering were reported for design application (Ref 2). Predictions were obtained for the F-111 using forcing functions derived by integration of pressure time histories with the natural buffeting modes, correlation of predicted and measured damping, and correlation of predicted and measured buffet response (Ref 3).

Wind tunnel testing was used extensively to measure unsteady pressures present on the tails of aircraft at high angles of attack and the buffeting response (Refs 4-5). Experimental research was carried out separately by the structures and aerodynamics scientists. Huston (Ref 6) used traditional methods to correlate wind tunnel data with flight buffeting response while Mabey (Ref 7) presented an evaluation of dynamic loads due to the separation of the flow field. Investigations of buffet on wings, fuselage, and weapon bays of aircraft were also reported by various researchers (Refs 8-11).

This report refers, in chronological order, to studies of buffet excitation on advanced fighter aircraft tails and, in particular, to the F-15 twin vertical tails.

II BACKGROUND

Aircraft can experience buffet when unsteady pressures associated with separated flow excite modes of vibration of the aircraft structure. For twin tail fighter aircraft, buffet can be severe when maneuvering at high angles of attack, due to separation at the leading edge of the wing being convected down stream and impinging on the vertical tail. This buffet is a function of the geometry of the wing, fuselage, and vertical tails. Triplett (Ref 5) performed wind tunnel tests to obtain the buffeting pressures on the vertical tail surfaces of a 13 percent F-15 model equipped with a rigid and a flexible tail. The MCAIR low speed tunnel was used. The research indicated that, for the configuration tested, the pressures and the buffet response levels reached a maximum at 22 degree angle of attack, and the predominant mode was the first torsion. Kulite pressure transducers were used to measure both steady and unsteady pressures. These pressures on the flexible tail were different in magnitude and distribution when compared to the rigid tail. For the same tail incidence, the lift was three times as large for the flexible tail. The results obtained were very valuable for the analysis and design of a torsional oscillation suppression system for the vertical tails.

At first, aerodynamicists and structures experts researched vortex-dominated and buffet flows separately. As mentioned in the introduction, Huston (Ref 6) indicates the traditional methods used to correlate wind tunnel and flight buffeting response; Mabey (Ref 7) gives an assessment of dynamic loads due to flow separation.

Other researchers tried to predict buffet on empennage by theoretical and experimental techniques. Edwards (Ref 12) assessed the validity of Euler as well as Navier-Stokes equations in modeling vortex-dominated flows conducive to buffet. He stressed the importance of grid density to obtain accurate, converged calculations, and showed that computational finite difference methods can provide accurate solutions of the thin-layer Navier-Stokes equations for flows about complex aircraft. Ferman et al. (Ref 13) developed a unified approach for predicting buffet response of a fighter aircraft empennage operating at high AOA. Ferman derived two approaches for predicting buffet response of a fighter aircraft empennage. The first one used elastically scaled models in wind tunnel tests to provide full scale prediction. The second was based on calculations using measured pressure data from wind tunnel tests. The latter method was considered to be more versatile.

Zimmerman et al. (Ref 14) show the buffet pressure frequency responses for an advance fighter aircraft; the peak frequency decreases with increasing angle of attack. Cunningham et al. (Ref 15) report unsteady pressure and flow visualization tests on oscillating delta wing models, with particular reference to the vortex systems (strake and wing vortices). Vortex lift augmentation is shown to occur between 8 and 18 deg angle of attack and the downward break in the lift curve slope indicates the onset of burst vortex flow over the planform. The maximum normal force coefficient, C_n, occurs at 35 degree AOA; at higher angles the flow is fully separated and the value of C_n falls. The aerodynamic community is trying to understand the physics of separated vortical flows, and data bases are being gathered which can be used to validate CFD codes. Experiments have been performed on static, rigid models.

Elsenaar et al. (Ref 16) report results of vortex flow development on a 65 degree cropped delta wing at Mach 0.4 to 4.0. Both sharp and rounded leading edges were tested for validation of Euler and Navier-Stokes codes. Other experiments have used non-intrusive 3-D laser Doppler velocimeters to improve the data quality for code validation. Pagan and Solignа (Ref 17) investigated in detail the bursting of vortices generated by a 75 degree delta wing. RMS velocity components were reported together with mean velocity. This was done in order to study the unsteady aspects of the flow field. The region downstream of the vortex burst generated strong fluctuations.

Komerath (Ref 18) reported a quantitative study on the low speed flow environment of a scaled model of an F-15 fighter aircraft at high angles of attack. Laser sheet flow visualization was used to observe the various locations of vortex generation, and the evolution of these vortex flows. Laser Doppler velocimetry was used to obtain quantitative values of the velocity field. Although the vertical tails were immersed in rotational flow, no concentrated vortex was observed. At 22 degrees AOA, the flow separated on the outside surfaces of the vertical tails. Mabey (Ref 19) performed extensive studies of tail buffeting at high angles of incidence on a complete scale model with a single fin. He found that the buffet excitation in the first bending mode was controlled by the wing flow separations and contained a peak at a well-defined frequency parameter. Adding trapezoidal or gothic canards strongly influenced the fin buffeting, and sideslip or strakes increased it.

Other researchers studied, both theoretically and experimentally, the tail buffet characteristics on the F-18 (Refs 20-22). Komerath et al. (Ref 20) observed sharply peaked spectra both inboard and outboard of the upper portion of the vertical tails. The narrow-band fluctuations appeared to originate in the separated flow over the wing surfaces. This demonstrated that the tail oscillations were driven by narrow-band fluid dynamic oscillations, whose frequency varied with angle of attack and flight velocity.

Zan (Ref 23) measured the buffeting on a single-tail generic fighter aircraft, such as the F-16. The results were correlated in terms of the buffet excitation parameter $\sqrt{nG(n)}$. At low angle of attack, where the flow on the forebody remained attached, the buffeting on the tail was negligible. The beginning of buffeting coincided with the onset of symmetric vortices and increased with increasing angle of attack, up to the onset of asymmetric vortices. At higher angles of attack, the buffeting decreased considerably. It was evident that the buffeting was directly connected with the vortex flow in the vicinity of the tail. Bean (Ref 24) then tried tangential leading edge blowing to alter the vortex flow pattern and characteristics on a single fin model with the intent of attenuating the fin buffet. Blowing at a constant rate delayed vortex breakdown and shifted the maximum buffet response to higher angles of attack. It is probable that the optimum blowing profile would be wing dependent and change with flight condition. Using an optimum blowing profile might completely suppress the buffeting response without significantly changing the wing characteristics.

Jacobs (Ref 25) used artificial intelligence for predicting empennage buffeting pressures and elastic response as a function of upstream flow field and geometric conditions. The effort employed a combined neural network and finite element modeling to predict flexible tail response based on rigid pressure information. Weeks and Nagaraja (Ref 26) surveyed a number of numerical codes used for linear and nonlinear problems which can analyze vertical tail buffet and the aeroelastic responses of 3-D vehicles at high angles of attack.

Other studies were conducted during the time span 1993-1995 on vertical tail buffet for existing fighter aircraft, such as the F-15 and F-18. Some were directed towards the analysis of the vortex flow surrounding the tail, and vortex burst over the wings and tails (Refs 27-43). Cornelius (Ref 40) evaluated criteria for vortex breakdown. The parameters that govern stability were formulated in terms of the local vortex flow variables. Laser measurements were taken and showed that the critical parameters, such as the ratio of axial-to-crossflow energy, decreased downstream from the adverse pressure gradient along the vortex trajectory, providing conditions that correlate with the location of vortex breakdown. Visbal (Ref 38) ascertained that breakdown emerged from the growth and upstream propagation of essentially axisymmetric disturbances which subsequently lose stability to helical modes. Both spiral and bubble modes of breakdown were compared with experimental measurements. Compressibility was shown to have a significant effect on the flow structure above a 75 degree swept wing at incidences corresponding to breakdown onset. Others studied the characteristics of surface pressures due to buffet (Refs 44-45). Correlation of wind tunnel and flight data were obtained for the F/A-18 vertical tail buffet (Ref 46). Mabey et al. (Ref 47) performed measurements in a cryogenic wind tunnel in order to find out the importance of the variations in frequency parameter and Reynolds number, the choice of model material (considering stiffness and damping), and the effect of static aeroelastic distortion. The choice of the wind tunnel gave them the opportunity to obtain conditions independent of temperature effects and to test at higher Reynolds numbers. Dima and Jacobs (Ref 48) investigated the effects of dynamic pitch-up maneuvers on empennage environment by means of a system of local-stationary equations based on the steady-state response equivalence. This system constituted a design tool to obtain more accurate values of buffet response and structural fatigue. Wolfe et al. (Ref 49) investigated the surface pressure loading on buffeting fins and concluded that the onset of vortex breakdown played a major role in dictating the spectral content of the pressure fluctuations on the fin. Pendelton et. al (Ref 45) and Meyn et. al (Ref 50) performed wind tunnel buffet studies on a full scale F/A-18 with and without a LEX fence. The fence significantly reduced the magnitude of the rms pressures and bending moments for angles of attack up to 22 degrees. The importance of this experiment lay in the comparison of the full-scale results with small-scale tests. It showed that the tail buffet frequency scales very well with length and velocity. Moses and Pendleton (Ref 51) also compared the pressure measurement results of a full-scale and a 1/6 scale F/A-18 twin tail during buffet. In 1995/96, multidisciplinary methods were used to compute the vertical tail buffet (Ref 52). Three sets of equations were used on a multi-block grid structure. The first set was the unsteady, compressible, full Navier-Stokes equations. The second set was the coupled aeroelastic equations for bending and torsional responses. The third set was the grid-displacement equations used to update the grid coordinates due to the tail deflections. This system allowed the computation of coupled and uncoupled bending-torsional responses. Cunningham (Ref 53) illustrated problems associated with nonlinear aerodynamic effects and their impact on structural integrity.

III F-16 UNSTEADY AERODYNAMICS INVESTIGATION

Fighter aircraft can experience oscillations of external stores that critically affect structural integrity and result in performance limitations. Limit Cycle Oscillations (LCO) result from a variety of phenomena that produce unsteady separated flow for some store configurations. The F-16 experienced LCO for several store configurations due to shock induced trailing edge separation on the wing. Engine spillage during throttle transients can cause vibration on the down stream structures such as store fins and antennas, resulting in fatigue damage.

Cunningham (Ref 53) performed a detailed investigation with regard to the fatigue life of the ventral fins of the F-16 fighter aircraft. The fatigue life was shortened considerably with the use of LANTIRN pods upstream of the fins. Inlet spillage also contributed to the deterioration of the fins. Airflow separating and reattaching continuously ahead of the fins (caused by strong turbulence) was another cause of the fins fatigue problem. Modification of the aircraft, such as increased inlet size for larger engines, inlet thin lip effects (such as severe flow separation) during throttle chops, and the addition of the cooling system exhaust deflector accentuated the buffet loads even more and led to fatigue problems on the fins. As a result, the ventral fins had to be re-designed. Using a semi-empirical model, various modifications were investigated, such as increasing the stiffness by 40%, leading edge nose cap, and using a constant NACA airfoil section from root to tip for the fins. Results showed that the solution that takes into consideration the aeroelastic nonlinearity has the best chance to solve the fin problem. As stated above, it is important to limit the effects of two types of nonlinear aeroelastic problems, i.e. limit cycle oscillations and large amplitude buffet.

IV TECHNIQUES FOR BUFFET ATTENUATION

Various techniques for buffet attenuation have been developed with some degree of success. Unfortunately, the problem has not been solved. Advanced fighter aircraft capable of maneuvering at high angles of attack and acceleration experience strong multiple-mode tail buffeting.

Ferman (Ref 54), referring to the vertical tail buffet, stated that "traditional fixes related to structural fatigue consisted of reinforcing the broken structure. This tended to merely chase cracking in the secondary structure from one area to another on the tail. With the use of composite material technology and adhesive bonding technology, it was possible to improve the F-15 vertical tail durability". He then tried to reduce the strong buffeting of the F-15 vertical tails by using a bond-on composite stiffening doubler called Exoskin. This approach should reduce the tail vibration response created by high angle of attack buffeting forces. However, this patch has not been in use long enough to determine its effectiveness.

Mabey and Pyne (Ref 55) performed some new research on the effects of wing leading edge blowing, similar to what had been done before by Bean et al. (Ref 24). The buffet excitation parameter $\sqrt{nG(n)}$ decreased consistently with increasing blowing momentum coefficient C_μ, up to the attainment of an optimum C_μ for a given angle of incidence. The indication was that buffeting could be attenuated. In addition, the overall L/D increased. They believed that this technique was promising.

Rock and Ashley (Ref 56) presented a technique that used active control to reduce the fin buffet response on the F/A-18 vertical tail. They first developed a model for control design generated by finite element structural analysis and linearized potential aerodynamic theory. With this model they designed a feedback control law that affected the movement of the rudder by means of feedback signals received from an accelerometer mounted on a fin-tip vane. They proved that it was possible to reduce the bending moment associated with the first modal frequency by 34% with the rudder motion limited to 2 degrees. A similar model was also effective on the F-15 aircraft. This result was based on theoretical analysis and was not proven in practice. However, there was a potential for enhancing the fatigue life of the empennage structure of aircraft operating at high angles of attack. Later on, RANN Corporation and McDonnell Douglas (MDA) suggested the use of adaptive feedback neural network controllers to activate the rudder command signal.

Barrett et al. (Ref 57) tried to reduce the buffet response of an advanced fighter tail section by passive damping, i.e. they started a research and development program whose goal was the development of buffet and fatigue resistant structure. They applied passive damping technology to redesign structural components. The specific components addressed included the beavertail section of the F-14D and the spars of the F/A-18 vertical tails. The damping material used consisted of advanced composites. Benefits can be obtained by including damping as a parameter in the design of parts of the structure that are subjected to dynamic loads.

Hauch et al. (Ref 58) studied the possibility of reducing tail buffet response by using integrated piezoelectric actuators. They performed their experiments on a 5%-scale aeroelastically-tailored structure that had similar vibration response to a full-scale aircraft structure. At high angles of attack, the leading edge vortices generate severe buffet pressures on the vertical tails, causing excitation of the first few natural modes of the flexible tail. Simple control algorithms were used with piezoelectric actuators and sensors to attenuate the strain at the root of the tail. Spectral analysis showed that the peak response was 65% less than the one without actuators.

Lazarus et al. (Ref 59) also addressed the feasibility of using active piezoelectric buffet suppression system to reduce buffet vibration in the vertical tails of aircraft. Full-scale piezoelectric buffet suppression systems were designed and evaluated. Many different actuator distributions, sensor locations and controller architectures were examined. Significant performance improvement was achieved (greater than 70%) with minimal weight penalties. This study showed that the tail vibrations could be reduced and the fatigue life extended.

It is important to list past and on-going WL efforts on techniques for tail buffet attenuation. The past efforts included a contracted F-15 buffet test in 1982 on a 13% scale-model with one rigid and one flexible vertical tail by Triplett (Ref 5), and a RANN analytical effort for active control using rudder on the F/A 18 and a tip vane on the F-15 (Ref 60). WL supported NASA Ames wind tunnel tests on a full-scale F-18 by conducting ground vibration tests on the vertical tails and measuring buffet data on one of the vertical tails (Ref 45). WL also supported NASA Langley Research Center's (LaRC) test on a 16% scale F-18 model through the supplying of a technician and test equipment and by supplying a control law through a data exchange agreement (DEA) with Germany. WL supported ACX and Rohini International with SBIR contracts for research on buffet load alleviation, provided an in-house numerical simulation of the interaction between leading edge vortex and a rigid vertical tail (Ref 61), awarded a grant to Dr. Singh (Clark Atlantic University), Dr. Sankar (Georgia Tech University) and Dr. Smith (Georgia Tech Research Institute) to modify an Euler/Navier-Stokes computer code (ENS3DAE) and include a trim module in order to perform trimmed and untrimmed aeroelastic analyses. Funding was also provided to Georgia Tech Research Institute to improve the computer code FASIT (Fluid and Structures Interface Toolkit), which is used to transfer data between different computational grids; specifically, it transfers data between CFD and structural grids in order to perform static aeroelastic calculations. FASIT is being enhanced to include data transfer for solutions of dynamic aeroelastic problems, as well as data transfer to/from unstructured CDF grids. On-going WL efforts include RANN analytical research on the F-22, ACX Phase II SBIR research for buffet load alleviation on the F-18 vertical tails, and Rohini International Phase II SBIR research for buffet load alleviation on the F-15 vertical tails.

Another on-going effort is NASA LaRC's ACROBAT (Actively Controlled Response of Buffet Affected Tails) program. This program consists of wind tunnel tests in NASA LaRC's 16-foot transonic dynamic tunnel to ascertain the effect of piezoelectric actuators and rudder on vertical tail buffeting. Moses (Ref 62) performed the experiment and recently presented some preliminary results, which indicated a reduction in power spectral density (PSD) of the root strain (bending moment) of up to 60% for certain angles of attack. In the Active Vertical Tail (AVT) tests, McDonnel Douglas Aircraft (MDA) and NASA LaRC conducted buffet suppression tests using integrated piezoelectric actuators. The model was a generic fighter that could be assembled into different configurations. MDA chose an F/A-18 to pursue the Buffet Load Alleviation System Technology (BLAST) program which refers to vertical tail buffet. An adaptive neural network is proposed for control of the rudder actuator . The Navy also conducted in-house wind tunnel tests and CFD simulations on a generic fighter configuration similar to the MDA/NASA model.

V ROLE OF WL/FI RESEARCH TEAM

In view of the importance of obtaining solutions of unsteady aerodynamic problems, WL decided at the beginning of 1994 to establish the "Unsteady Aerodynamics Integrated Product Team" (UAIPT). This team was formed by scientists and engineers from three different divisions in order to coordinate multidisciplinary research. The three divisions were the Aeromechanics Division, mostly involved in experimental and computational aerodynamic problems, the Structures Division, involved in both metallic and composite structures development, and the Flight Control Division, mainly involved in establishing and evaluating flight control laws (Fig 1).

The UAIPT was considered the center for coordinating and integrating unsteady aerodynamic research at WL (Fig 2). It initiated contacts with the various System Program Offices (SPOs) at Wright-Patterson AF Base, such as the F-15 SPO, the F-16 SPO, the F-22 SPO, the C-17 SPO, and the B-2 SPO. Among the many problems in unsteady aerodynamics, such as Limit Cycle Oscillations (LCO), buffet, flutter, separated flow, etc., the buffet problem seemed to be the most important due to the many requests received for immediate attention and support (Fig 3). Buffet attenuation and possible elimination had to be studied both theoretically and experimentally in-house and by contract. In order to achieve reliable results, the different static and dynamic effects on an aircraft structure had to be studied simultaneously. Team members had to work together and interact with each other to define and conduct an in-house program. Support was received by another service, the Navy, by a Government agency, NASA, and private companies, such as Rohini International, RANN Corporation, ACX, and MDA (Fig 2). Research was centered on computational fluid dynamics (CFD), finite element research, vibration tests, and wind tunnel tests. The first project selected by the UAIPT consisted in improving present technology to obtain significant buffet vibration reduction.

Twin tail buffeting problems are quite different for different aircraft. For example, the F/A-18 problems are attributed to the bursting of strong vortices and the attendant high intensity turbulence which drive the structural dynamics modes at high angles of attack. F-15 aircraft investigations show a concentration of energy fluctuation over the wing at high angles of attack, which then propagates downstream in a narrow band of frequencies enveloping the vertical tails.

Rohini International was awarded a Phase II SBIR contract for research on buffet load alleviation on the F-15 vertical tail (Ref 63). Under this contract the use of stacked piezoelectric actuators was investigated as a means of suppressing buffet. Structural dynamic tests were conducted on a full scale F-15 vertical tail subassembly with piezoelectric actuators and reported by Hanagud et al. (Ref 64). Hanagud was able to determine the vertical stabilizer dynamic response characteristics. Natural frequencies, mode shapes, and damping ratios of the modes were studied to determine their interaction. The results of these vibration tests correlated well with data from an operational F-15 aircraft. Modes from the laboratory test article (F-15 subassembly) and the aircraft were identified and found to be the same. The nonlinearities that were observed in the F-15 vertical tail structure appeared to be quadratic. Therefore, the laboratory subassembly could be used to predict the effects of structural modifications of the vertical stabilizer and the effects of active or passive vibration controllers on the full scale aircraft (Ref 63). Since stiffening of the tail structure alone is not an effective means of reducing the vibrations, it may be necessary to use an active vibration absorber capable of sensing the buffet induced structural dynamics reducing the multi-mode vibration.

In the Rohini/Georgia Tech effort, lateral and torsional vibrations in the plane of the vertical tail were controlled by applying stresses and strains with piezoelectric actuators. The optimum locations for the actuators that would give a maximum response to lateral and torsional vibrations of the vertical tail had to be determined. That was accomplished by using in-plane actuators and measuring lateral and torsional deflections at various desired locations. In this way the best locations for controlling the vibrations at each individual mode were found. The force disturbances were generated by a shaker mounted on the outboard trailing edge of the vertical tail. Transfer functions between the accelerometer and the actuator were determined. A control system was designed whose purpose was to reduce the bending response (2nd bending at 39.8 Hz) of the tail as measured by a tip mounted accelerometer. Tests results showed that the magnitude of the acceleration at the tip could be reduced by nearly 40%.

A computer program was developed to construct a finite element model from the measured experimental modal data. The first step in the program was to input the experimentally measured modes and natural frequencies. The second step in the program was to construct the mass matrix from the data provided in the vertical tail drawings, the densities of different components, and the total weight of the vertical tail. In the third step, the measured relative modal amplitudes were normalized with respect to the mass matrix. Next, the damping and stiffness matrices were calculated, and the natural frequencies were calculated from the reconstructed mass, damping, and stiffness matrices. This experimentally-based finite element model yielded a range of frequencies which were reasonably accurate.

ACX, Inc. was also supported by WL in their research on buffet load alleviation with distributed piezoelectric actuators applied to the vertical tails of an F-18 aircraft. SBIR Phase I and Phase II contracts were awarded, with the goal to conduct ground vibration tests on a full scale structure, measure the vibration level reduction, and demonstrate piezoelectric actuators' authority at full loads.

In Phase I (1994), ACX assessed the feasibility of employing piezoelectric actuators. This was demonstrated on a scale model with simple geometry by Lazarus (Ref 59). Design and feasibility studies were conducted on a full scale tail. A distribution of actuators in the vertical tail was selected in the areas of maximum strain. ACX demonstrated the effectiveness of buffet suppression using piezoelectric actuators and active control. Power requirements and weights were expected to have minimal impact on aircraft operation. For an 8% increase in tail weight, the damping of the first mode was increased by 60% which would significantly reduce structural damage and fatigue.

In Phase II, ACX addressed the fabrication and integration of the actuators, the electronics, and power conditioning. They evaluated the controller implementation, testing, and performance. The controller did not have to be inserted in the flight control system since it could be dedicated to the actuators only. In the meantime, McDonnel Douglas Aerospace (MDA) studied the cost benefits of equipping the tail with actuators instead of replacing it. The actuators should last the life of the tail to reduce maintenance of the buffet suppression system and the added weight should be less than 25 pounds per tail, with a maximum added weight to the aircraft of 100 pounds for both tails. The actuators were embedded in the aircraft skin and thermal control had to be addressed. The cable between the amplifiers and the actuators had to be shielded to avoid electro-magnetic countermeasures (EMC) problems. Accelerometers and strain gauges were used as sensors; the accelerometers turned out to be more reliable. The NASTRAN finite element code was used for modeling the mode shapes, frequencies, and actuator modal influence. A linear unsteady aerodynamics code was used to compute the aerodynamic forces. The actuators were limited to peak actuation strain of 400 microstrain. In the case of least disturbance energy, up to 75% of buffet reduction was achieved, and in most severe cases, a 20 % reduction was still attained.

ACX, through The Technical Cooperation Program (TTCP), has set up a test program with the Defense Science and Technology Organization (DSTO), to be performed at the International Follow-On Structural Testing Project (IFOSTP) facility at the Aeronautical and Maritime Research Laboratory (AMRL) in Melbourne, Australia. This program is the Buffet Load Alleviation (BLA) experimental investigation. The USAF Technical Project Officers are Mark Hopkins and Doug Henderson, members of the UAIPT. The reasons to conduct ground tests in Australia are twofold: (1) A full size F/A-18 test aircraft is tested, i.e. a full size empennage is attached to the vehicle and not to a structure; (2) Even though this is going to be a ground test, the facility has the capability of applying realistic flight loads. It may be possible to go directly to flight testing upon completion of the ground tests. This international cooperative program will benefit a number of different aircraft, namely the F-14, F-15, F/A-18, F-22, and F-117. This program will be completed by March 1999.

The UAIPT decided to conduct an in-house experiment on a 4.7% scale- model of an F-15C aircraft to investigate the tail buffeting. The tests were performed in the SARL (Subsonic Aerodynamics Research Laboratory) wind tunnel located at Wright-Patterson AFB. A numerical investigation was conducted simultaneously.

The experiment used tangential blowing and later piezoelectric actuators to alleviate the buffeting response from the tail structure. The first test was limited to tangential blowing with sonic jets from the model's nose, gun bump, and a portion of the wing's leading edge near the root (See Fig 4). The model was equipped with one stiff vertical tail (the right tail) and one flexible tail. Fig 17 is a sketch of the modal patterns on the flexible vertical tail; damping and frequencies for the first 3 modes are shown. The rigid tail was equipped with 12 dynamic pressure transducers, while the flexible one was equipped with 2 strain gauges, 2 accelerometers, and 12 dynamic pressure transducers. Fig 5 shows the model assembly in the wind tunnel. The second entry will include piezoelectric actuators. The locations of the actuators are shown in Fig 6 (note the axis location for the first torsion and second bending modes). A NASTRAN code was used to identify areas of high strain gradients which are effective locations for the piezoelectric actuators. Figs 36-38 are plots showing the strain intensity on the vertical tail for the first three modes. The accelerometer signals were used to determine the buffet excitation parameter, $\sqrt{nG(n)}$, in the vertical tail first bending mode according to the equation:

$$\sqrt{nG(n)} = \frac{2}{\sqrt{\pi}}\left(\frac{m\ddot{z}}{qS_f}\right)\xi^{1/2}$$

$G(n)$	=	power spectral density
n	=	reduced frequency
m	=	generalized mass in mode with respect to motion at tip (for accelerometer mounted on tip)
$\ddot{z}$	=	rms tip acceleration in mode
q	=	dynamic pressure
S_f	=	exposed tail area
ξ	=	total damping as a ratio of critical damping

The blowing tests were performed at Mach 0.2, angles of attack from zero to 32 degrees, sideslip angles from -4 to 4 degrees, and dynamic pressures up to 56 psf. Pressures on both the rigid and flexible tails were measured as a function of angles of attack with and without blowing. Fig 7 shows the location of the pressure transducers on the vertical tails. Representative test conditions are shown in Tables 1-4. The $\beta = 0$ degree cases are show in Figs 8-14 as plots of rms pressures acting on the flexible and rigid tails for different conditions (with and without blowing). The pressure plots in general show an increase in pressure with angle of attack, but the increase is more pronounced for the rigid tail (the values on the rigid tail are higher than the values on the flexible tail at the corresponding locations). Blowing had a beneficial effect at some conditions; at alpha = 32 and beta =0, blowing at 45 psi from the wing's leading edge reduced the rms buffet response for the first bending mode; at alpha=32 and beta=4, the same amount of blowing from the wing's leading edge decreased the rms buffet response for the second bending mode. For other combinations of alpha and beta decreases of up to 36% were observed. Fig 15 is a laser light sheet photograph taken during the tests and showing a typical vortex pattern and the impingement of the vortices on the vertical tails. The buffet response from the tails was measured and power spectral densities are plotted for the first bending and first torsion modes in Fig 16. Additional data are presented in

Table 5. Figs 18-21 show the response of the different modes to the angle of attack variation for different sideslip angles and blowing coefficients. For the bending mode, the response increased with angle of attack up to the maximum test condition of 32 degrees, while for the torsion mode it increased up to an angle of attack of 24 degrees, then decreased drastically. Positive sideslip generally reduced the bending mode response; the torsion mode response decreased with a positive sideslip up to 24 degrees. At an angle of attack of 32 degrees the negative sideslip gave the smallest response for the torsion mode. The higher the blowing coefficient, the lower the bending mode response. The same occurred for the torsion mode up to 24 degrees. At higher angles of attack the blowing was detrimental. Specifically, for alpha (angle of attack)=32 and beta (sideslip)=0, the tests showed the largest buffet response. Results showed that: 1) Blowing from the wing leading edge with 45 psi of pressure reduced the rms buffet response by 2.9% and the peak frequency by 0.2% in the range of the first bending mode frequency; 2) For alpha=24 and beta=0, in the range of the first torsion frequency, the blowing had an adverse effect, increasing the buffet response by 7.8%; and 3) For alpha=32 and beta=4, in the range of the second bending frequency, the blowing decreased the buffet response by 7.2%, even though the peak frequency increased by 20%. Rms buffet responses were reduced for four different conditions from 6.2 to 36.1%. Only one other condition produced an increase of 1.7%.

The second phase of the in-house buffet test will investigate the use of piezoelectric actuation to reduce the response due to buffet. To evaluate the effectiveness of the actuators at various locations, frequency response tests were conducted. Figs 22-25 show the frequency response of the structure at the first bending, second bending, first torsion, and first and second bending actuator locations.

The numerical simulations were conducted by Bob Weyer, a UAIPT member (Ref 65). The computational model of a clean F-15C aircraft was similar to the wind tunnel model (Fig 26). Both models had flow through ducts, and the inlets and internal ramps were set for the subsonic high angle of attack condition. The engine sections on the inlet grid were bottlenecked to limit the mass flow without choking it. The geometry for this project was generated by a CAD system. This system retains the actual aircraft surfaces as files. The files are converted to discretized structured surface panels. All details of the aircraft were retained including the horizontal tail notch, inlet diverter gap, pods atop the vertical tails, separation between the horizontal tail and fuselage. A new unstructured grid generator (TETMESH) was used to create the grid around the complex configuration (see Fig 27). Computationally, a farfield boundary condition was modeled; therefore, tunnel effects were not modeled. An inviscid solution was obtained using the COBALT unstructured grid flow solver.

Fig 28 shows the flow over the gun bump. The vector components are colored to denote various pressures. From the top of the inlet the vortex core develops and moves downstream, then lifts over the wing and envelops the vertical tails (Fig 29). Fig 30 shows the same vortex pattern but the smaller vortices at the root of the tails are also visible. The streamline traces are shown in Figs 31-32.

The pressure on the vertical tails is shown in Figs 33-34. It is evident that the bottom of the left tail has outboard flow while the top has inboard flow. The right tail instead experiences outboard flow. For most of the conditions, the computational and measured pressure coefficients differed by about 20% (Table 7).

The computations for the flow-through case were compared to the experimental data for the forces and moments of the entire aircraft (Table 6). For alpha = 24 degrees and beta = -4 degrees, the lift coefficients differed by only 1% (computed value being larger), while the drag coefficients differed by 34% (computed value smaller). The pitching moments differed by only 7% (computed value less negative), but the rolling moments differed by 126% (computed value negative and measured value positive).

The follow-on computational effort included the engine-on case since the mass flow rate through the inlet with the engine on in similar flight conditions is seven times larger than the mass flow obtained with the flow-through inlet. Comparisons were made between the two cases. With the engine operating, the lift increased 6% but the drag increased by 10%. The pitching moment increased by 7%. The influence of the engine suction consisted in changing the location of the vortex origin. The origin moved forward on the leeward side while it moved aft on the windward side. The vortical flowfield is similar to the one with flow-through, but it is tighter and closer to the vertical tails (Fig 35).

The computational solution accurately described the flow field around an F-15 aircraft at high angles of attack and sideslip. The favorable comparison between computations and measurements indicated that the unstructured grid approach and an inviscid solution could be useful in further research.

VI SUMMARY

The review of research performed on the buffet problems of fighter aircraft has revealed a continuous and steady progress toward the partial or full elimination of buffet on the vertical tails at high angles of attack. Tangential blowing had some beneficial effects at some conditions.

The latest, most promising technique of using piezoelectric actuators for active buffet control is being applied to the empennage of scale-models and full size aircraft. Preliminary results show that with a minimal weight increase due to the actuators, a considerable reduction in buffet is obtained with attendant increase of vertical tail fatigue life. The UAIPT is working in-house and with companies which are involved in different buffet load alleviation systems and on aerodynamic nonlinear effects.

Work in this area is continuing at present at a fast pace and the new results covering the performance of the actuators in ground tests and wind tunnel experiments will be presented as soon as they become available.

VII UAIPT MEMBERS

Dr Wladimiro Calarese (IPT Chair)
Capt Deborah Grismer
Mr Terry Harris
Mr Douglas Henderson
Dr Mark Hopkins
Capt Alexander Hsia
Mr Lawrence Huttsell
Dr Charles Jobe
Lt Joel Luker
Capt Mark Lutton
Mr Juan Martinez
Capt Kenneth Moran
Mr Dieter Multhopp
Mr Stanley Palmere
Mr Norman Scaggs
Mr Thomas Tighe
Capt Brad Buxton
Mr Jon Tinapple
Mr Elijah Turner
Mr Matthew Wagner
Capt Scott Morton
Dr Reid Melville

VIII REFERENCES

1. Accident Investigation Sub-Committee: Accident to the Aeroplane G-AAZK at Meopham, Kent, 21 July 1930. R. & M. No. 1360, British A.R.C., 1931.

2. Zimmerman, N.H., and Ferman, M.A., "Prediction of Tail Buffet Loads for Design Application." NADC-88043-60, July 1987.

3. Coe, C.F., and Cunningham, A.M. Jr., "Predictions of F-111 TACT Aircraft Buffet Response and Correlations of Fluctuating Pressures Measured on Aluminum and Steel Models and the Aircraft." NASA CR-4069, May 1987.

4. McDonnell Aircraft Company, F-15 Loads-Aerodynamic Data Group. "High Speed Aeroelastic Effects Loads Test, 4.7 Percent Scale F-15 Model." MDC A1171, July 1971.

5. Triplett, W.E., "Pressure Measurements on Twin Vertical Tails in Buffeting Flow." AFWAL-TR-82-3015 Vol 1, April 1982.

6. Huston, W.B., "A Study of the Correlation Between Flight and Wind Tunnel Buffet Loads." AGARD Structures and Material Panel Meeting, April-May 1957.

7. Mabey, D.G., "Some Aspects of Aircraft Dynamic Loads Due to Flow Separation." Royal Aircraft Establishment, Tech Memo Aero 2110, July 1987.

8. Becker, J., and Gravelle, A., "Some Results of Experimental and Analytical Buffeting Investigations on a Delta Wing." Contribution to the International Symposium on Aeroelasticity at Aachen, April 1-3, 1985.

9. Mabey, D.G., "Elimination of Buffeting on the Rear Fuselage of the Hercules Tanker." The Aeronautical Journal of the Royal Aeronautical Society, November 1985.

10. Shaw, L., Clark, R., Talmadge, D., "F-111 Generic Weapons Bay Acoustic Environment." Journal of Aircraft, Vol 25, No 2, February 1988, Pages 147-153.

11. Zan, S.J., and Maull, D.J., "Buffet Excitation of Wings at Low Speeds." Journal of Aircraft. Vol 29, No 6, Nov-Dec 1992.

12. Edwards, J.W., "Assessment of Computational Prediction of Tail Buffeting." NASA Technical Memorandum 101613, January 1990.

13. Ferman, M.A., Patel, S.R., Zimmerman, N.H., and Gerstenkorn, G., "A Unified Approach to Buffet Response of Fighter Aircraft Empennage." Mcair 90-004, 70th Meeting of the Structures and Materials Panel for Aircraft Dynamic Loads due to Flow Separation, 2-4 April 1990, Sorrento, Italy, AGARD paper No 17.

14. Zimmerman, N.H., Ferman, M.A., and Yurkovich, R.N., "Prediction of Tail Buffet Loads for Design Application." AIAA Paper No 89-1378, AIAA Structures Structural Dynamics and Materials Conference, Mobile, Alabama, 3-5 April 1989.

15. Cunningham, A.M., den Boer, R.G., Dogger, C.S.G., Geurtis, E.G.M., Persoon, A.J., Retel, A.P., and Zwaan, R.J., "Unsteady Low-Speed Wind Tunnel Test on a Straked Delta Wing, Oscillating in Pitch." Part I General Description and Discussion of Results, AFWAL TR-87-3098, April 1988.

16. Elsenaar, A., Hjelmber, L., Butefisch, K., and Bannink, W.J., " The International Vortex Flow Experiment." Paper No 9 in AGARD Conference Proceedings No 437, Validation of Computational Fluid Dynamics, Vol 1, presented at Fluid Dynamics Panel Symposium, Lisbon, Portugal, 2-5 May 1988.

17. Pagan,D., and Soligna, J.L., "Experimental Study of the Breakdown of a Vortex Generated by a Delta Wing." Rech. Aerosp. (English Edition), 1986.

18. Komerath, N., McMahon, H., Schwartz, R., Liou, S., and Kim, J., "Flow Field Measurements Near a Fighter Model at High Angles of Attack." AIAA Paper 90-1431, AIAA 16th Aerodynamic Ground Testing Conference, Seattle, WA,18-20 June 1990.

19. Mabey, D.G., and Pyne, C.R., "Buffeting on the Single Fin of a Combat Aircraft Configuration at High Angles of Incidence." Technical Report 91006, Royal Aerospace Establishment, January 1991.

20. Komerath, N.M., Schwartz, R.J., and Kim, J.M., "Flow Over a Twin-Tailed Aircraft at Angle of Attack, Part II: Temporal Characteristics." Journal of Aircraft, Vol 29, No 4, July-August 1992.

21. Lee, B.H.K., Brown, D., Tang, F.C., and Plosenski, M., "Flowfield in the Vicinity of an F/A-18 Vertical Fin at High Angles of Attack." Journal of Aircraft, Vol 30, No 1, January-February 1993.

22. Rizk, Y.M., Guruswamy, G.P., and Gee, K., "Numerical Investigation of Tail Buffet on F-18 Aircraft." AIAA-92-2673-CP, 1992.

23. Zan, S.J., "Measurements of Single-Fin Buffeting on a Generic Fighter Aircraft Configuration." International Forum on Aeroelasticity at Strasburg, 1993.

24. Bean, D.E., Greenwell, D.I., and Wood, N.J., "Vortex Control Technique for the Attenuation of Fin Buffet." Journal of Aircraft, Vol 30, No 6, November-December 1993.

25. Jacobs, J.H., Hedgecock, C.E., Lichtenwalner, P.F., Pado, L.E., and Washburn, A.E., "The Use of Artificial Intelligence for Buffet Environments." AIAA-93-1534-CP, 1993.

26. Weeks, T.M., and Nagaraja, K.S., "Unsteady Aerodynamics for Air Force Needs." AIAA 93-3622, AIAA Atmospheric Flight Mechanics Conference, Monterey, CA, 9-11 August 1993.

27. Hebbar, S., Platzer, M., and Frink, W.Jr., "Vortex Wake Investigation of a Twin-Tail Fighter Aircraft Model at High Angles of Attack with and without Lex Fences." AIAA 93-0868, 31st Aerospace Sciences Meeting & Exhibit, Reno, NV, 11-14 January 1993.

28. Breitsamter, C., and Laschka, B., "Turbulent Flow Structure Associated with Vortex-Induced Fin Buffeting." FLM-93, Lehrstuhl fur Fluidmechanik, Technische Universitat Munchen, 1993.

29. Hebbar, S.K., Platzer, M.F., and Cavazos, O.V., "Pitch Rate/Sideslip Effects on Leading-Edge Extension Vortices of an F/A-18 Aircraft Model." Journal of Aircraft, Vol 29, No 4, July-August 1992, pp. 720-723.

30. Hebbar, S.K., Platzer, M.F., and Kim, C.H., "Water Tunnel Visualization of Dynamic Effects During Sideslipping of a Canard-Configured Fighter Model." The Fifth Asian Congress of Fluid Mechanics, Taejon, Korea, 10-14 August 1992.

31. Hebbar, S.K., Platzer, M.F., and Kwon, H.M., "Vortex Breakdown Studies of a Canard-Configured X-31A-Like Fighter Aircraft Model." Journal of Aircraft, Vol 30, No 3, May-June 1993, pp. 405-408.

32. Bernhardt, J., and Williams, D., "The Effect of Reynolds Number on Control of Forebody Asymmetry by Suction and Bleed." AIAA 93-3265, AIAA Shear Flow Conference, Orlando, FL, 6-9 July 1993.

33. Hebbar, S.K., and Platzer, M.F., "A Visualization Study of the Vortical Flow over a Double-Delta Wing in Dynamic Motion." AIAA 93-3425, AIAA 11th Applied Aerodynamics Conference, Monterey, CA 9-11 August 1993.

34. Hebbar, S.K., and Platzer, M.F., "Effect of Canard Oscillations on the Vortical Flowfield of an X-31A-Like Fighter Model in Dynamic Motion." AIAA 93-3427, AIAA 11th Applied Aerodynamics Conference, Monterey, CA, 9-11 August 1993.

35. Hebbar, S.K., Platzer, M.F., and Frink, W.D. Jr, "Effect of Leading-Edge Extension Fences on the Vortex Wake of an F/A-18 Model." Journal of Aircraft, Vol 32, No 3, Engineering Notes, Vol 32, No 3, May-June 1995.

36. Mayori, A., and Rockwell, D., "Interaction of a Streamwise Vortex with a Thin Plate: A Source of Turbulent Buffeting." AIAA Journal, Vol 32, No 10, October 1994.

37. Beyers, M.E., "Interpretation of Experimental High-Alpha Aerodynamics - Implications for Flight Prediction." Journal of Aircraft, Vol 32, No 2, March-April 1995.

38. Visbal, M.R., "Computational and Physical Aspects of Vortex Breakdown on Delta Wings." AIAA 95-0585, 33rd Aerospace Sciences Meeting and Exhibit, Reno, NV, 9-12 January 1995.

39. Murri, D.G., Shah, G.H., and DiCarlo, D.J., "Actuated Forebody Strake Controls for the F-18 High-Alpha Research Vehicle." Journal of Aircraft, Vol 32, No 3, May-June 1995.

40. Cornelius, K.C., "Analysis of Vortex Bursting Utilizing Three-Dimensional Laser Measurements." Journal of Aircraft, Vol 32, No 2, March-April 1995.

41. Lowson, M.V., and Riley, A.J., "Vortex Breakdown Control by Delta Wing Geometry." Journal of Aircraft, Vol 32, No 4, July-August 1995.

42. Canbazoglu, S., Lin, J. -C., Wolfe, S., and Rockwell, D., "Buffeting of a Fin: Streamwise Evolution of Flow Structure." AIAA Journal, Vol 33, No 1, January 1995.

43. Canbazoglu, S., Lin, J. -C., Wolfe, S., and Rockwell, D., "Buffeting of Fin: Distortion of Incident Vortex." AIAA Journal, Vol 33, No 11, November 1995.

44. Lee, B.H.K., and Tang, F.C., "Characteristics of the Surface Pressures on an F/A-18 Vertical Fin Due to Buffet." Journal of Aircraft, Vol 31, No 1, January-February 1994.

45. Pettit, C., Banford, M., Brown, D., and Pendleton E., "Pressure Measurements on an F/A-18 Twin Vertical Tail in a Buffeting Flow." WL-TM-94-3039, August 1994.

46. Bean, D.E., and Lee, B.H.K., "Correlation of Wind Tunnel and Flight Test Data for F/A-18 Vertical Tail Buffet." AIAA-94-1800-CP, 1994.

47. Mabey, D.G., Boyden, R.P., and Johnson, W.G., "Buffeting Tests in a Cryogenic Windtunnel." Aeronautical Journal, January 1995.

48. Dima, C., and Jacobs, J.H., "The Characterization of Non-Stationary Buffet Environments." AIAA-95-1339-CP, 1995.

49. Wolfe, S., Canbazoglu, S., Lin, J.-C., and Rockwell, D., "Buffeting of Fins: An Assessment of Surface Pressure Loading." AIAA Journal, Vol 33, No 11, November 1995.

50. Meyn, L.A., and James, K.D., "Full-Scale Wind-Tunnel Studies of F/A-18 Tail Buffet." Journal of Aircraft, Vol 33, No 3, May-June 1996.

51. Moses, R.W., and Pendleton, E., "A Comparison of Pressure Measurements Between a Full-Scale and a 1/6-Scale F/A-18 Twin Tail During Buffet." AGARD 83rd Structure and Materials Panel Meeting, September 1996.

52. Kandil, O.A., Sheta, E.F., and Massey, S.J., "Twin Tail/Delta Wing Configuration Buffet due to Unsteady Vortex Breakdown Flow." AIAA 96-2517-CP, 14th AIAA Applied Aerodynamics Conference, New Orleans, LA 18-20 June, 1996.

53. Cunningham, A.M. Jr, "Nonlinear Aeroelastic Problems and Their Impact on Structural Integrity." Paper presented at the Air Force 4th Aging Aircraft Conference, U.S. Air Force Academy, Colorado, 9-11 July 1996.

54. Ferman, M.A., Liguore, S.L., Colvin, B.J., and Smith, C.M., "Composite 'Exoskin' Doubler Extends F-15 Vertical Tail Fatigue Life." AIAA-93-1341-CP, 34th annual Structural Dynamics and Materials Conference, LaJolla, CA, 19-22 April 1993.

55. Mabey, D.G., and Pyne, C.R., "Tangetial Leading-Edge Blowing on a Combat Aircraft Configuration." Defense Research Agency Report, 1994.

56. Rock, S.M., and Ashley, H., "Active Control for Fin Buffet Alleviation." AIAA-93-3817-CP, 1993.

57. Barrett, D.J., Ray, H., and Arocho, A., "Highly Damped Structures." Report No. NAWCADWAR-94126-60, 22 June 1994.

58. Hauch, R.M., Jacobs, J.H., Ravindra, K., and Dima, C., "Reduction of Vertical Tail Buffet Response Using Active Control." AIAA-95-1080-CP.

59. Lazarus, K.B., Saarmaa, E., and Agnes, G.S., "An Active Smart Material System for Buffet Load Alleviation." SPIE Conference, 1995.

60. Ashley, H., Rock, S.M., Digumarthi, R., Chaney, K., and Eggers, A.J. Jr, "Active Control for Fin Buffet Alleviation." WL-TR-93-3099, January 1994.

61. Rizzetta, D.P., "Numerical Simulation of the Interaction between a Leading-Edge Vortex and a Vertical Tail." AIAA 96-2012, 27th AIAA Fluid Dynamics Conference, New Orleans, LA, 17-20 June 1996.

62. Moses R., "Vertical Tail Buffeting Alleviation Using Piezoelectric Actuators and Rudder." High Angle of Attack Technology Conference, NASA LaRC, 17-19 September 1996.

63. Nagaraja, K.S., and Hanagud, S.V., "F-15 Twin Tail Buffet Alleviation Using Smart Structures." WL-TR-96-3097, April 1996.

64. Hanagud, S. et al., "F-15 Modal Analysis Tests." Technical Report E-16-A07, F09603-85-6-3104-0030, 1990.

65. Weyer, R., "F-15 Tail Buffet Study." Informal paper for UAIPT, 28 August 1996.

APPENDIX

Figures and Tables

UNSTEADY AERODYNAMICS IPT

- Goal: Coordinate unsteady aerodynamic research and focus an in-house multidisciplinary (Aeromechanics, Flight Controls, and Structures) team on key problems such as buffet, LCO, and aerodynamics-structural interaction.
- On-Going Project: Buffet Investigations Using a 4.7% Model of F-15
  - Experimental (SARL Wind Tunnel)
    - Characterization of buffet
    - Suppression tangential blowing/piezoelectric actuators
  - CFD Simulations
    - Euler
    - Navier-Stokes
    - Blowing

Fig 1. Unsteady Aerodynamics IPT

TECHNOLOGY INTERACTION
BUFFET RESEARCH

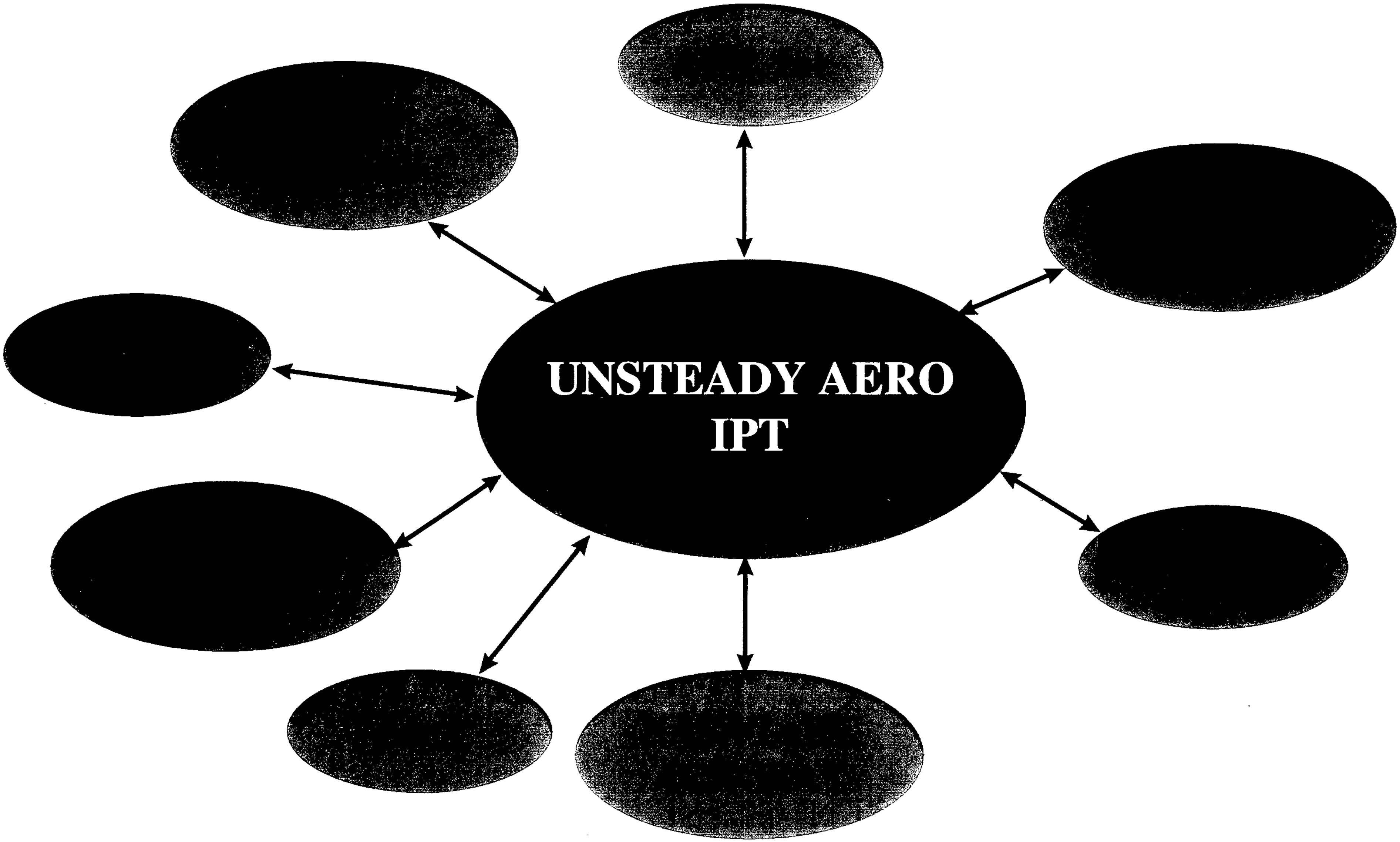

Fig 2. Technology Interaction, Buffet Research

4-7-02

VERTICAL TAIL BUFFET RESEARCH

Past Efforts:

- F-15 Buffet Tests on 13% Model
- Active Rudder Control Study for F/A-18 & F-15
- NASA Ames Wind Tunnel Tests of Full Scale F/A-18
- NASA Langley's F/A-18 Tests on 16% Model

Current:

- Phase II SBIR's
  - ACX - Buffet Alleviation (F/A-18)
  - Rohini - Buffet Alleviation (F-15)
- In-House Buffet Suppression Tests on 4.7% F-15 Model
  - Phase I - Blowing
  - Phase II - Piezoelectric Actuators
- Analytical Studies
  - Active Rudder Control Study of F-22
  - Application of CFD Methods for Loads Prediction

Fig 3. Vertical Tail Buffet Research

F-15 Twin Fin Buffet Model

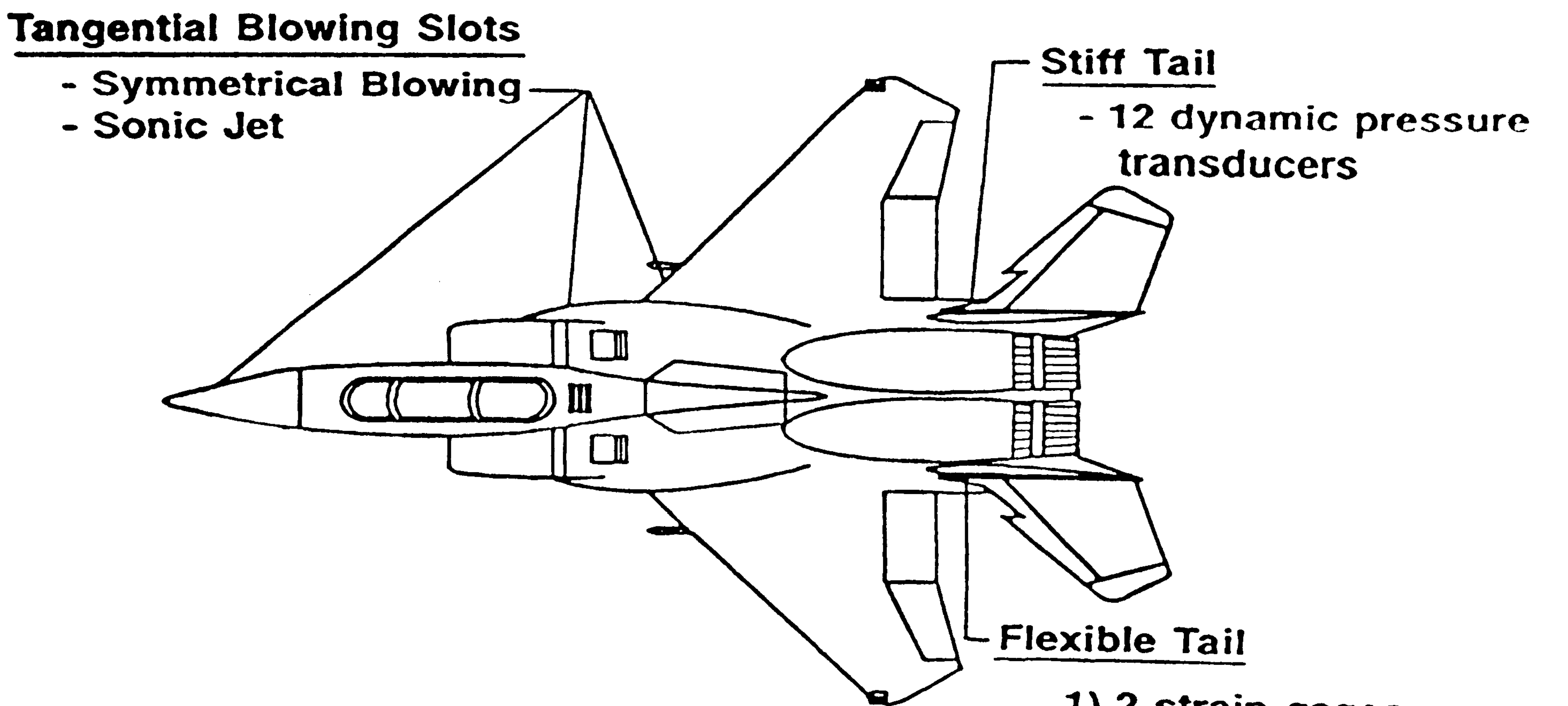

Fig 4. F-15 Twin Fin Buffet Model

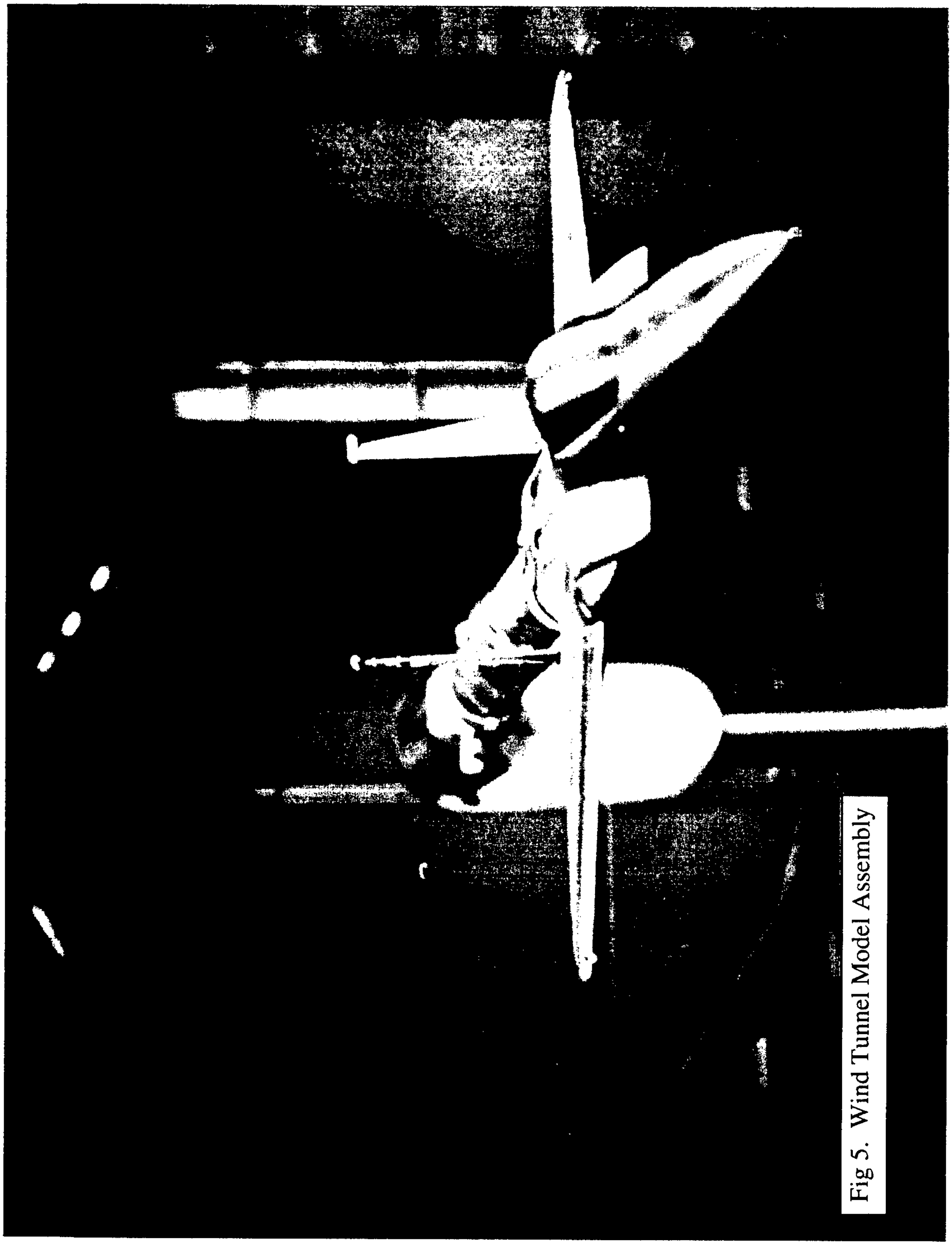

Fig 5. Wind Tunnel Model Assembly

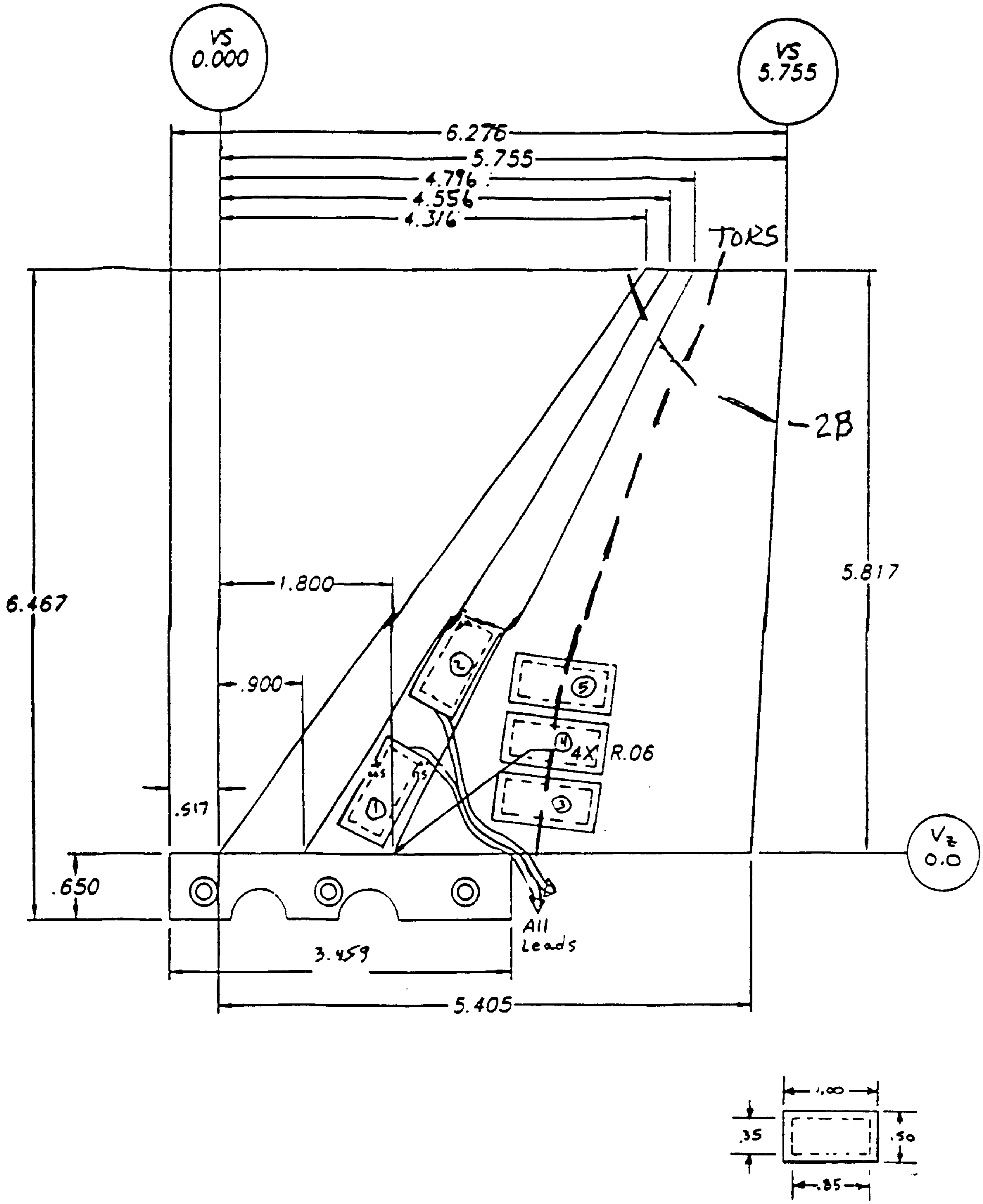

Fig 6. Flexible Vertical Spar

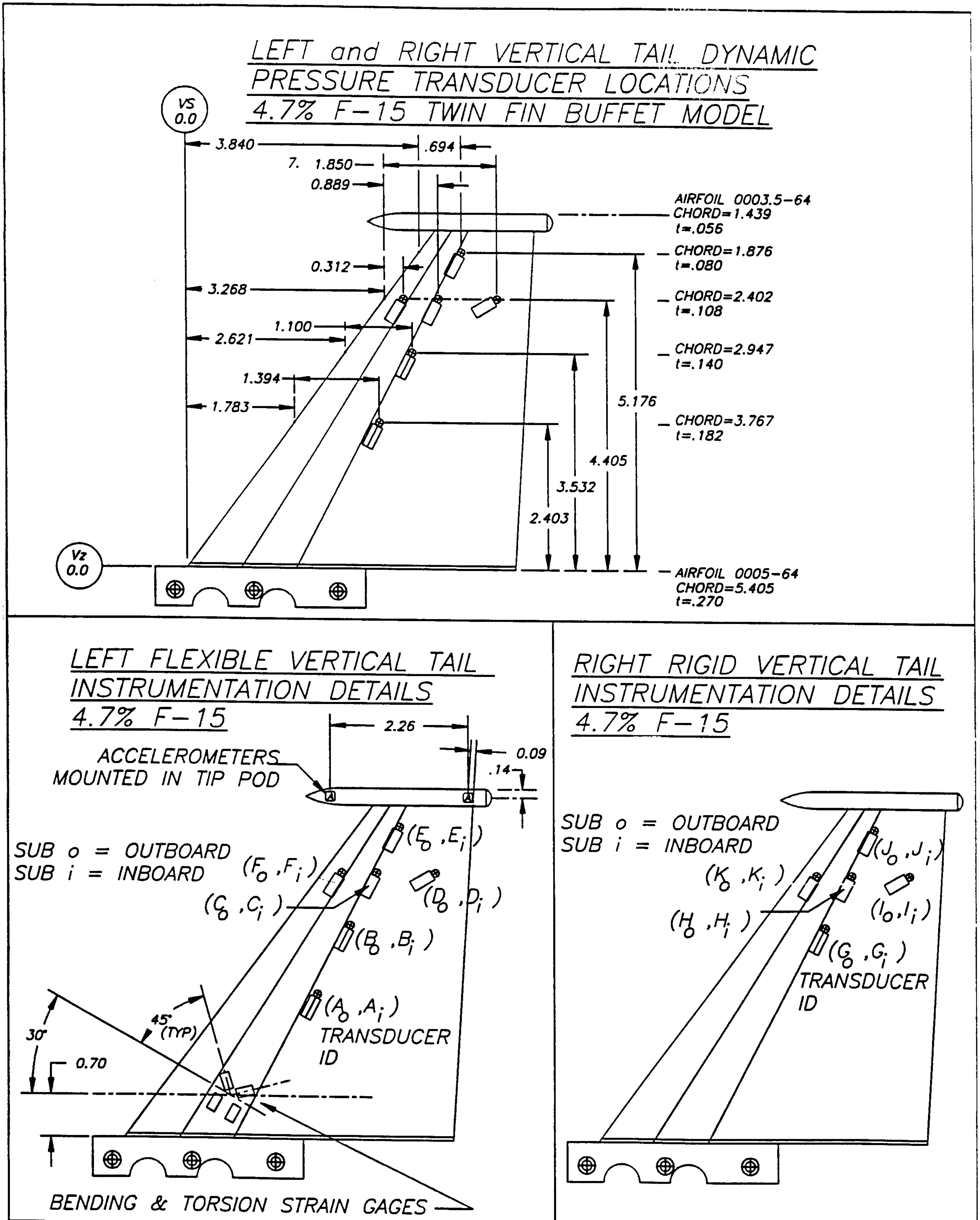

Fig 7. Left and Right Vertical Tail Dynamic Pressure Transducer Location

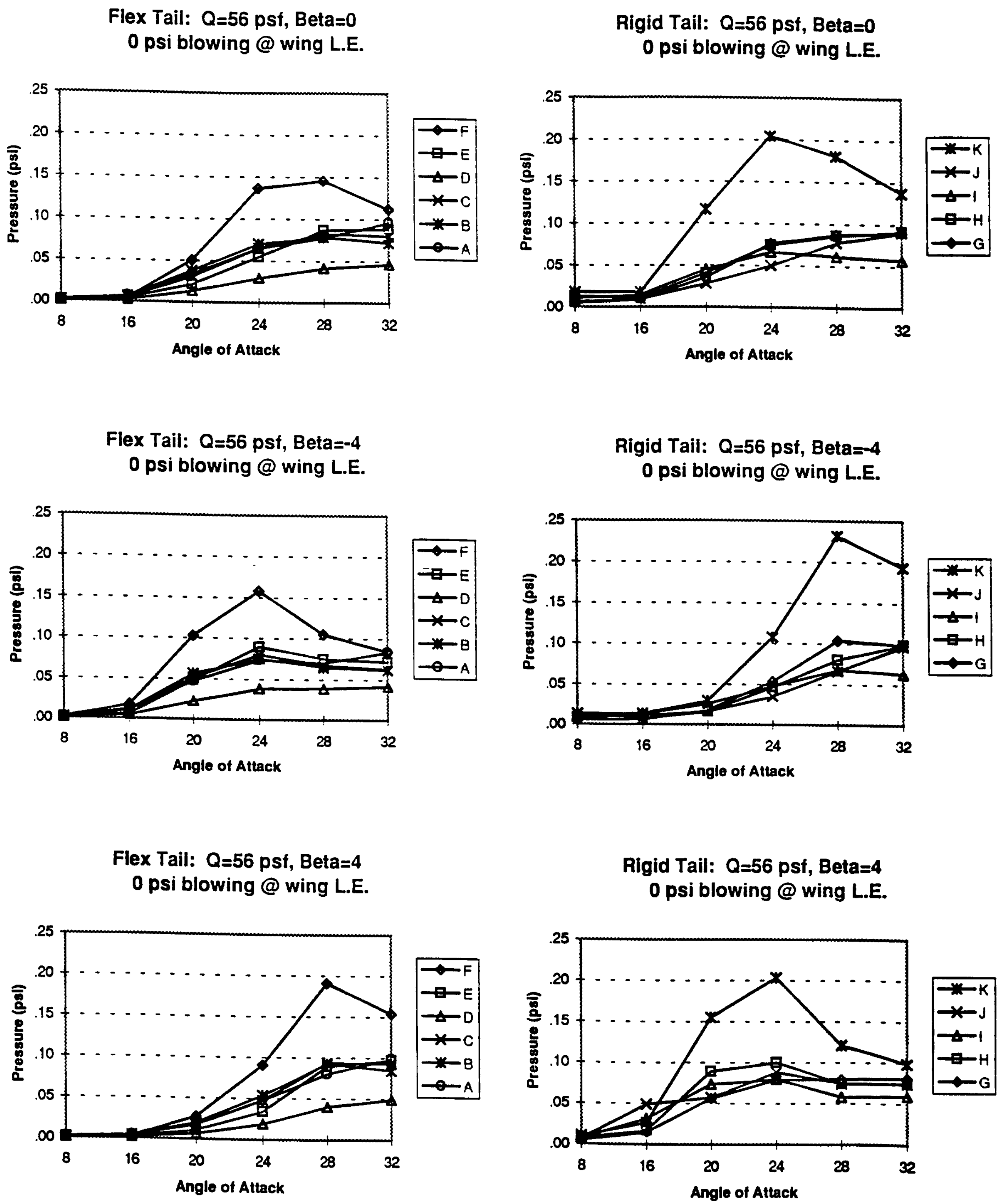

Fig 8. Measured Dynamic Pressure Distribution versus Angle of Attack

Flex Tail: Q=56 psf, Beta=0
45 psi blowing @ wing L.E.

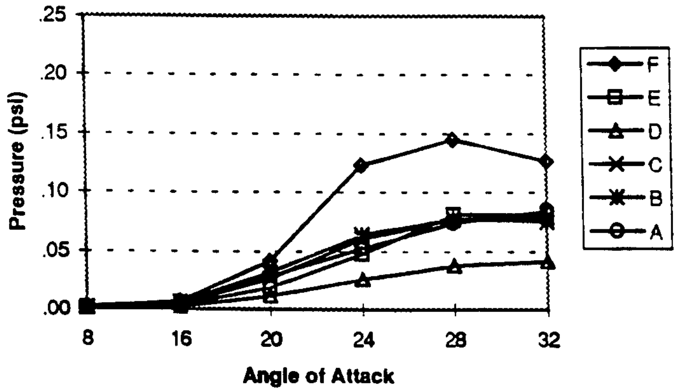

Rigid Tail: Q=56 psf, Beta=0
45 psi blowing @ wing L.E.

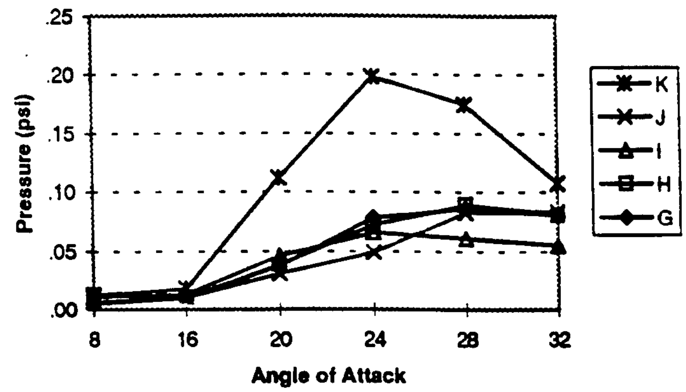

Flex Tail: Q=56 psf, Beta=-4
45 psi blowing @ wing L.E.

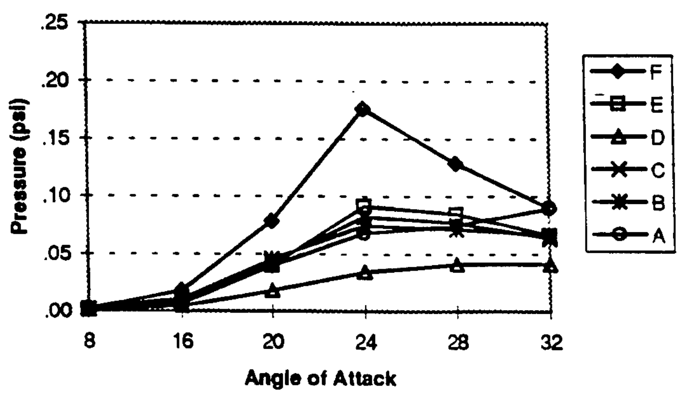

Rigid Tail: Q=56 psf, Beta=-4
45 psi blowing @ wing L.E.

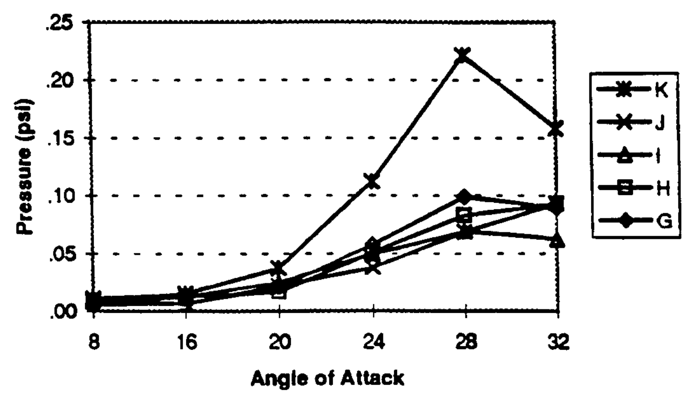

Flex Tail: Q=56 psf, Beta=4
45 psi blowing @ wing L.E.

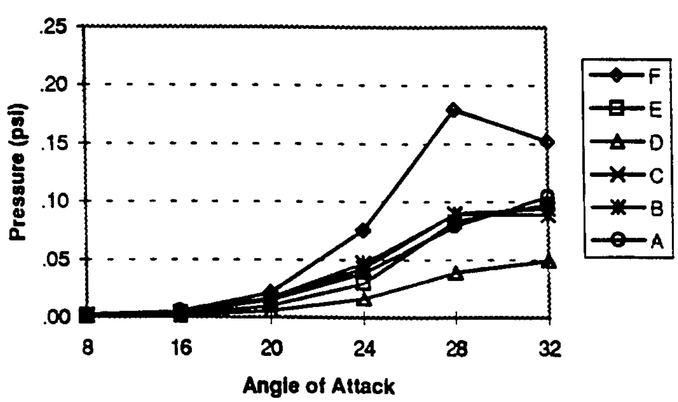

Rigid Tail: Q=56 psf, Beta=4
45 psi blowing @ wing L.E.

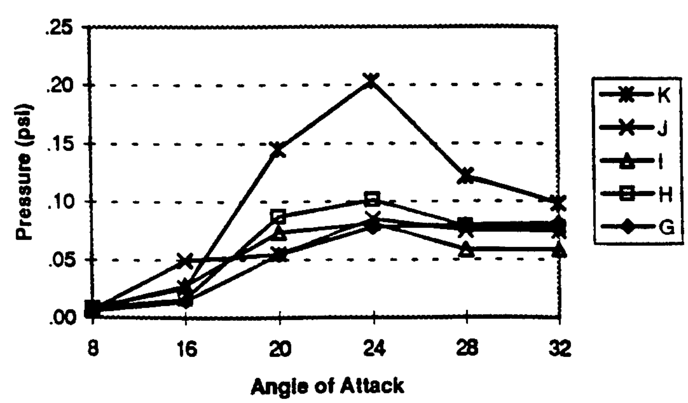

Fig 9. Measured Dynamic Pressure Distribution versus Angle of Attack

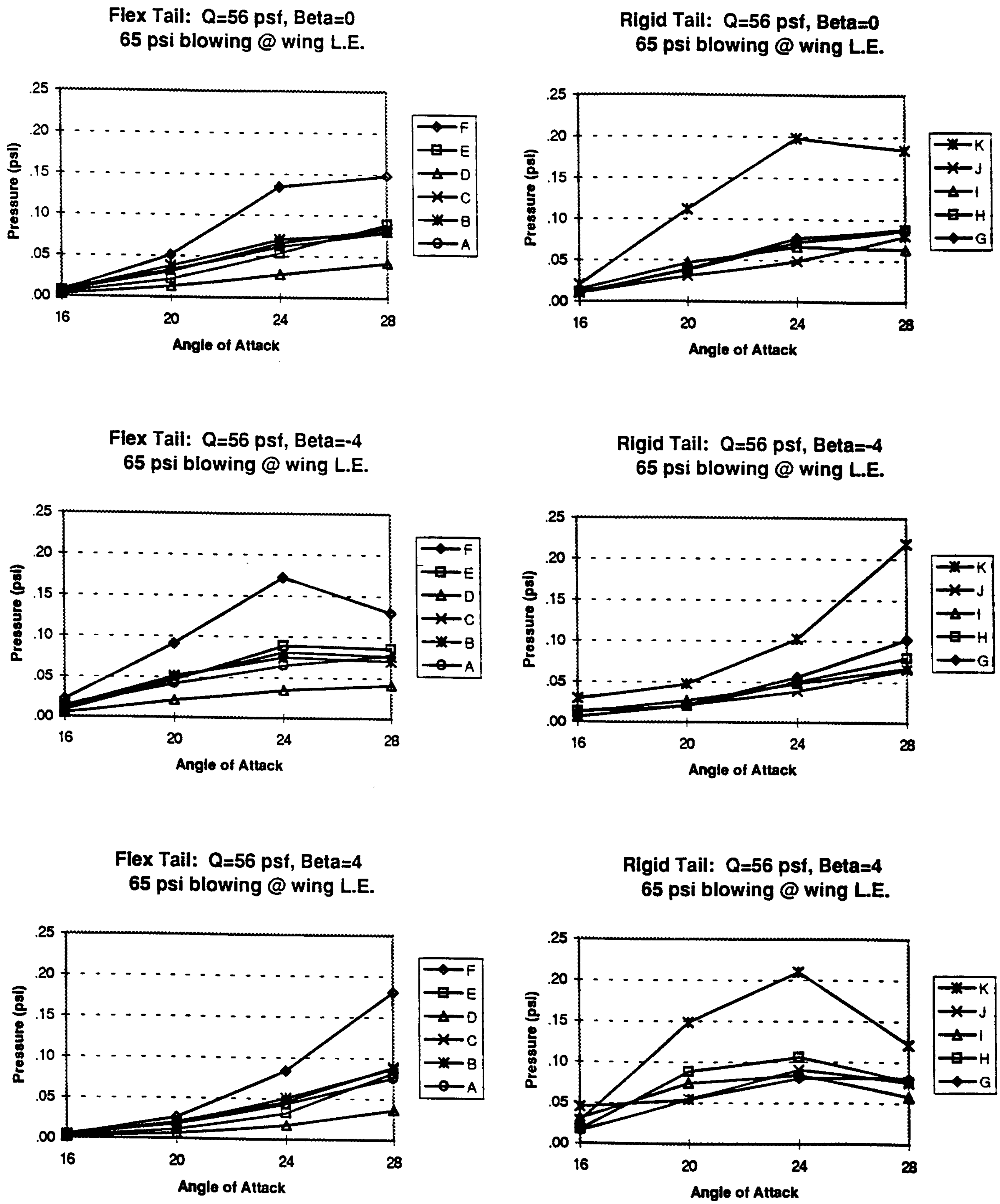

Fig 10. Measured Dynamic Pressure Distribution versus Angle of Attack

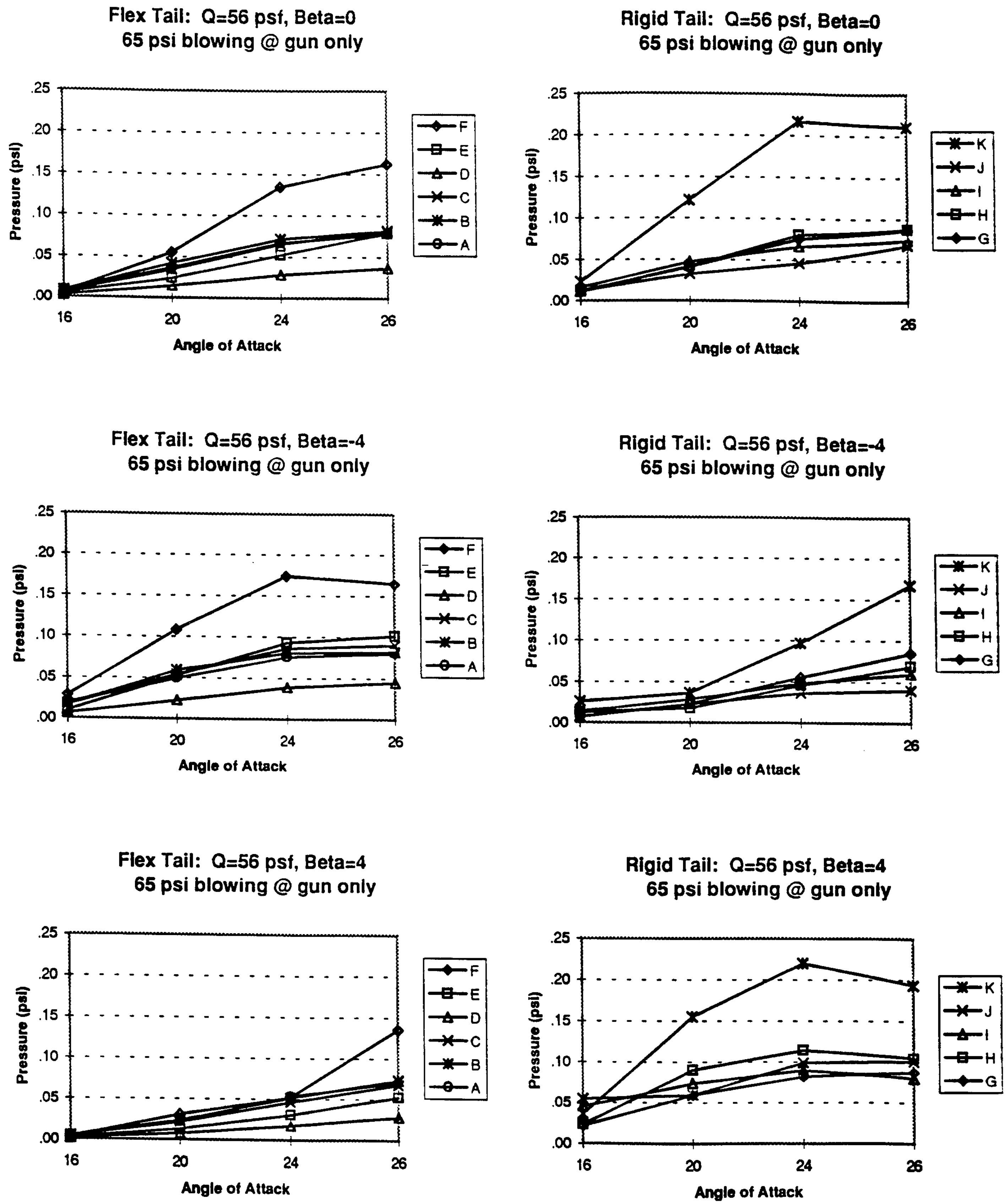

Fig 11. Measured Dynamic Pressure Distribution versus Angle of Attack

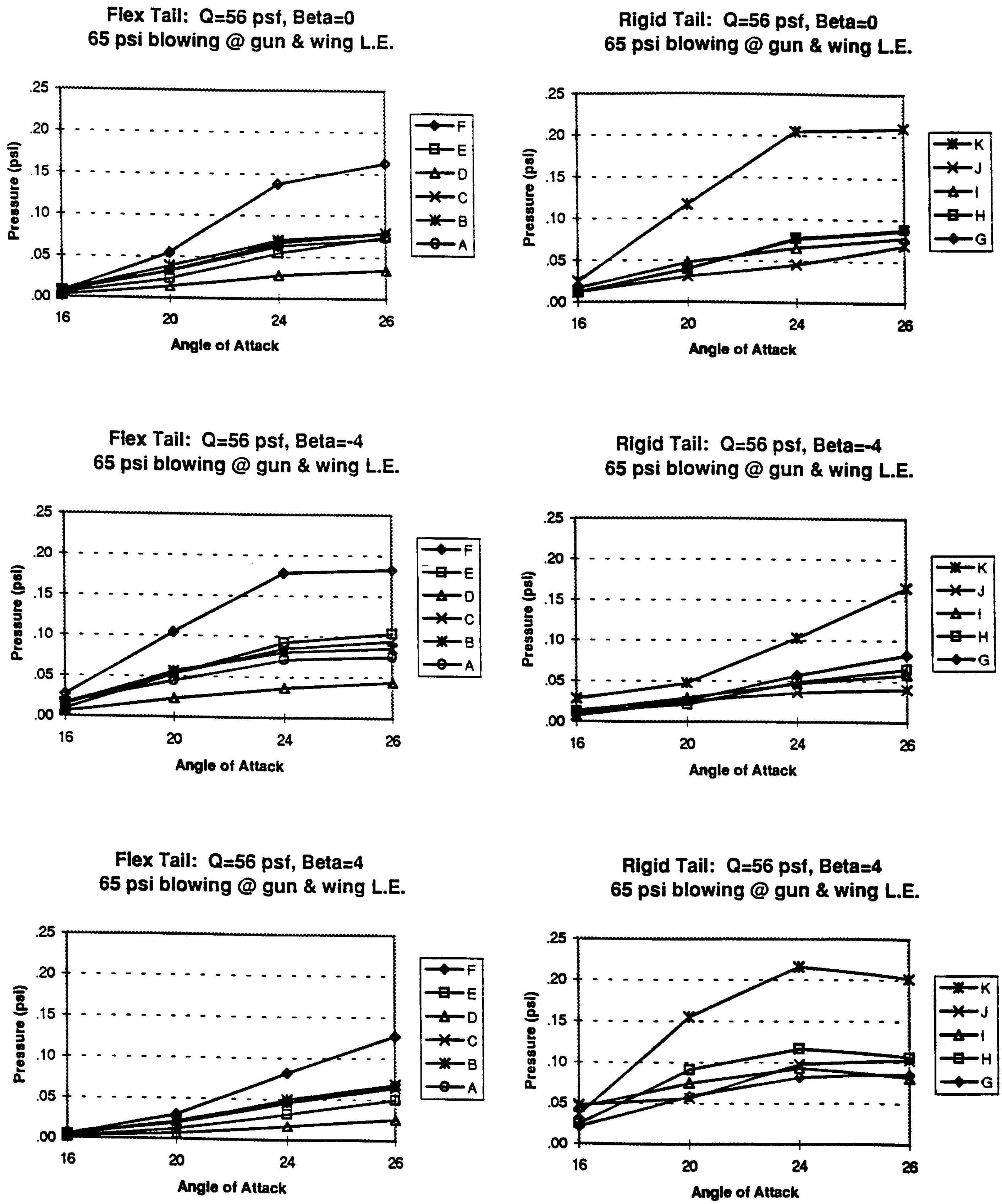

Fig 12. Measured Dynamic Pressure Distribution versus Angle of Attack

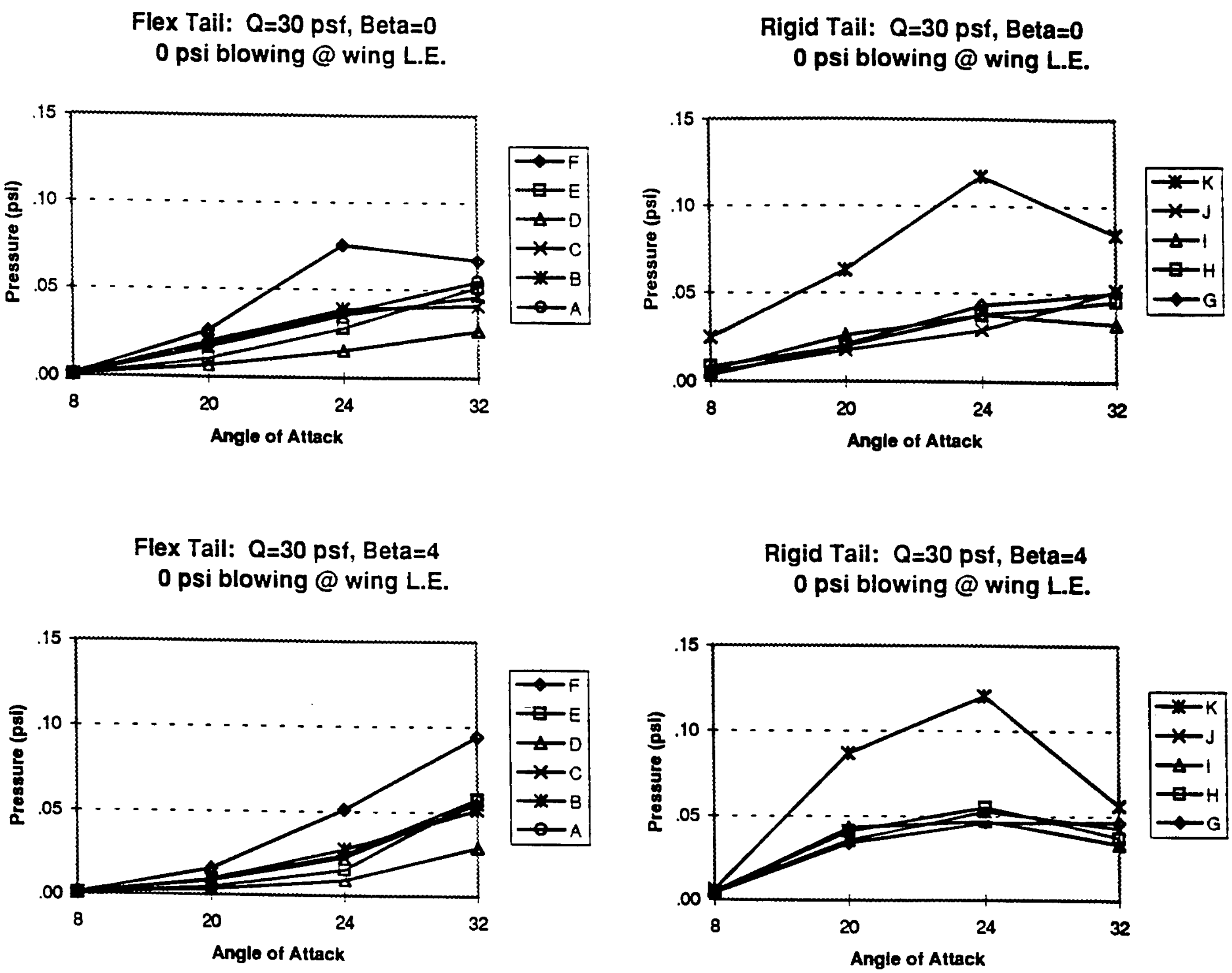

Fig 13. Measured Dynamic Pressure Distribution versus Angle of Attack

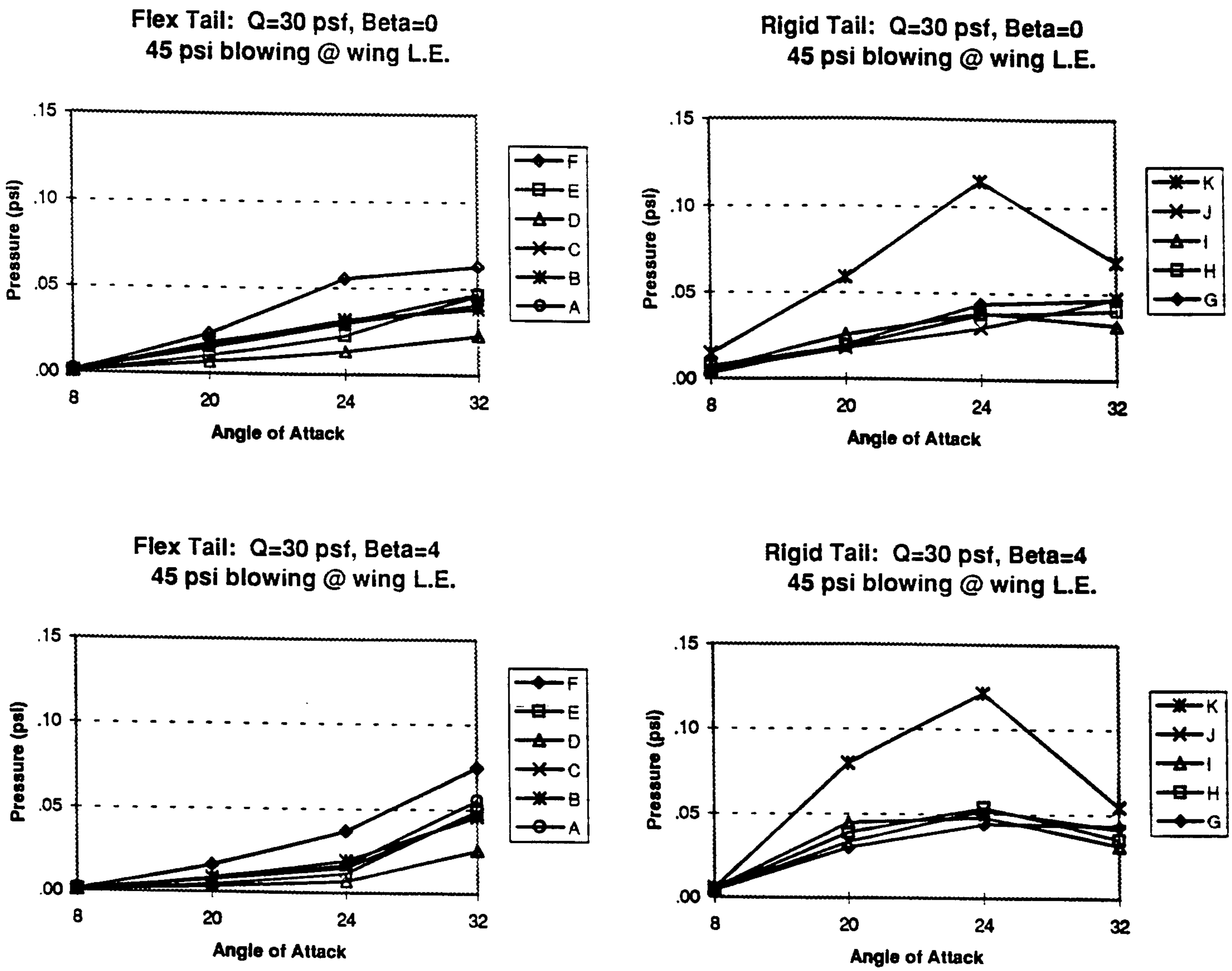

Fig 14. Measured Dynamic Pressure Distribution versus Angle of Attack

Fig 15. Photograph of Vortices Impinging on the Tail during Wind Tunnel Testing

F-15 VERTICAL TAIL BUFFET DATA

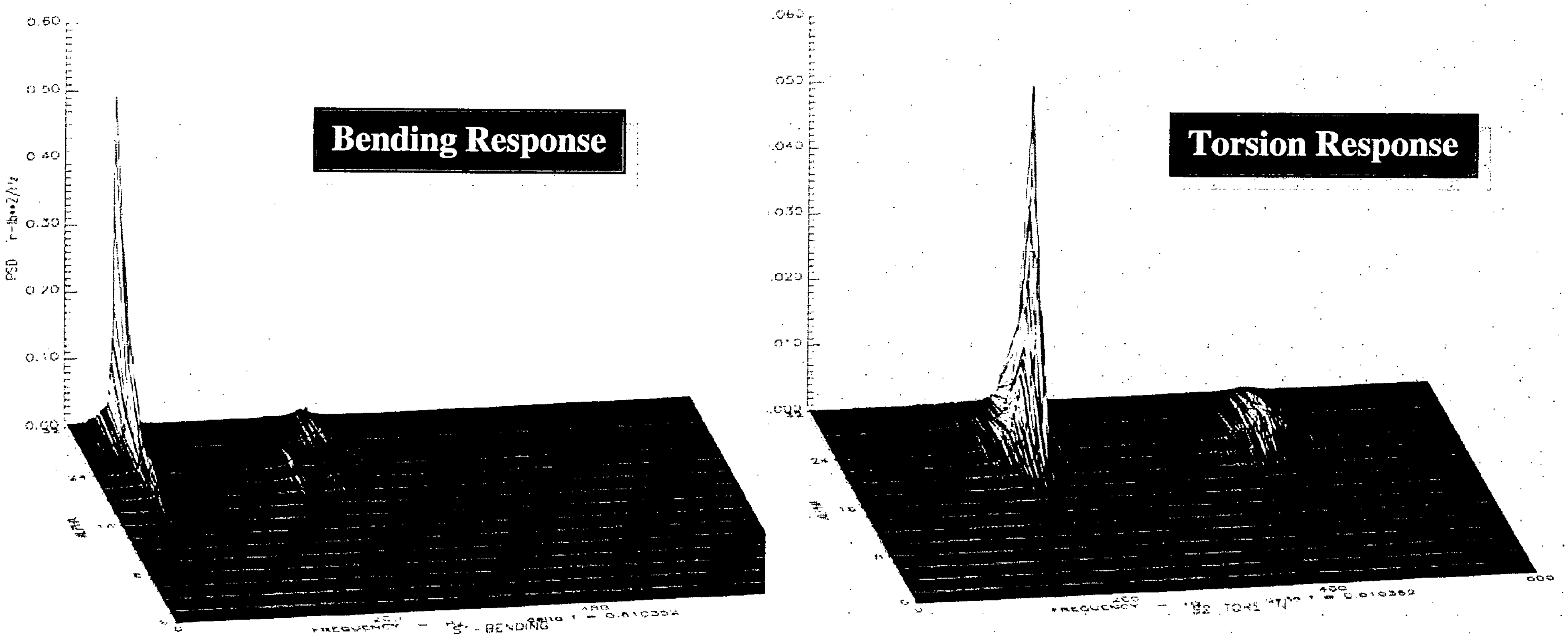

Fig 16. F-15 Vertical Tail Buffet Data

96064TMC-20

a

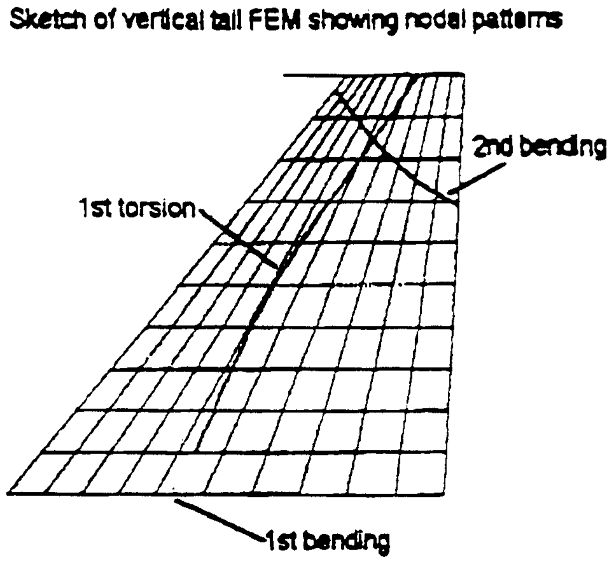

b

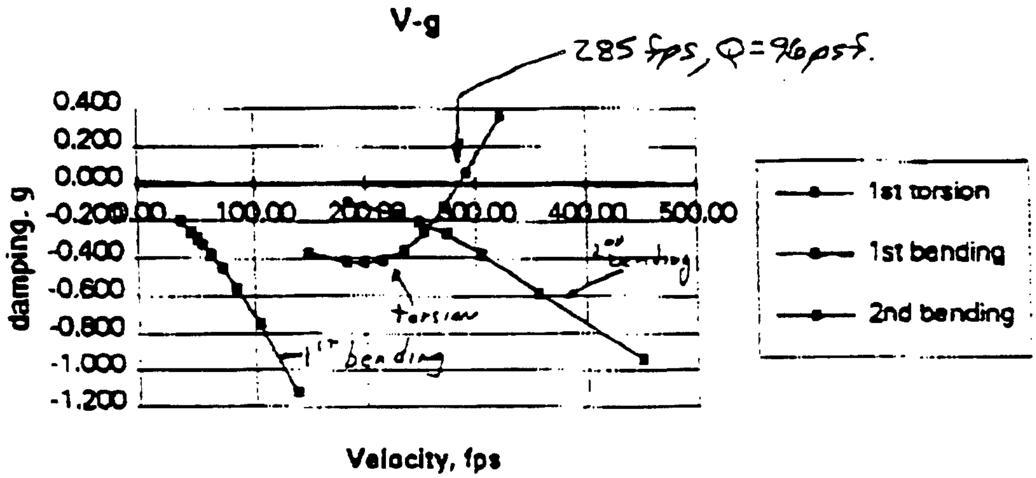

c

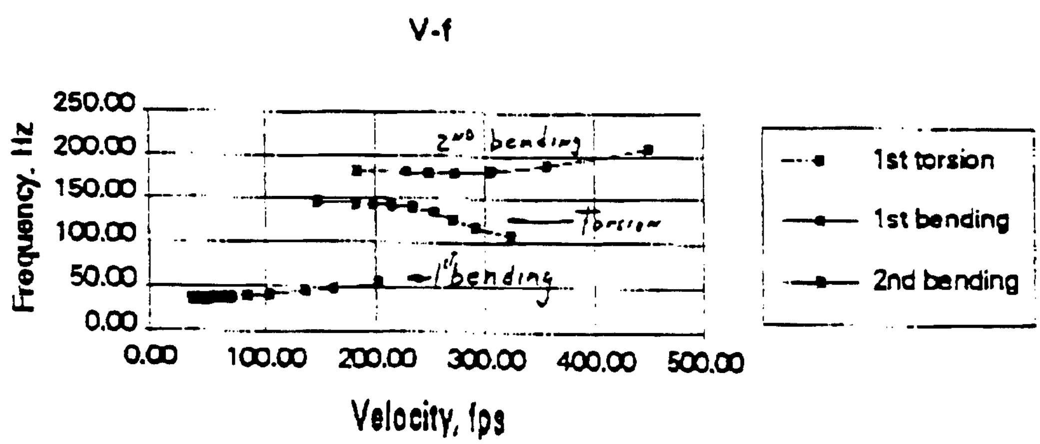

Fig 17. a) Sketch of Vertical Tail Showing Modal Pattern, b) Damping versus Velocity for the First Three Modes, c) Frequency versus Velocity for the First Three Modes

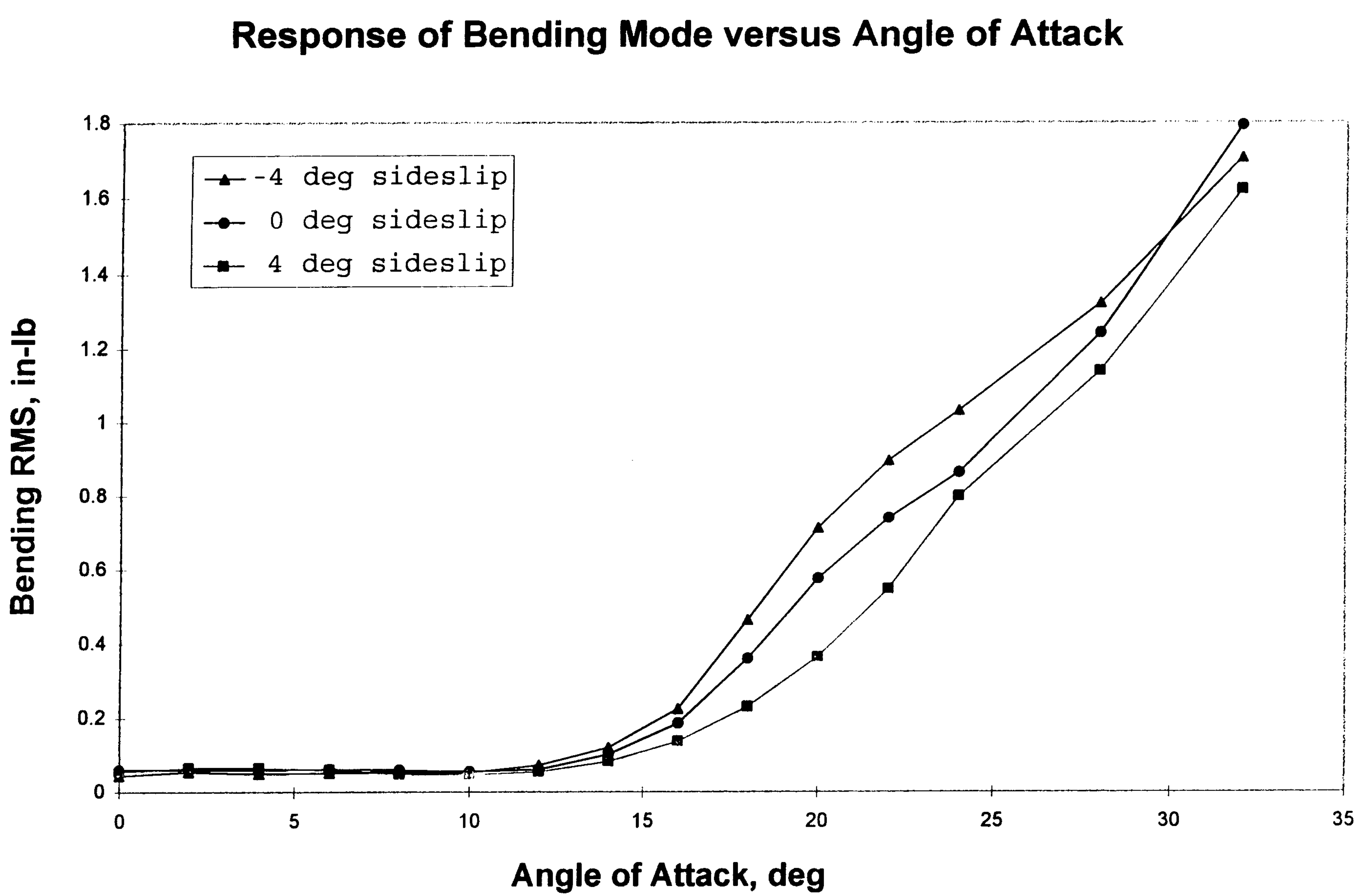

Fig 18. Response of Bending Mode versus Angle of Attack

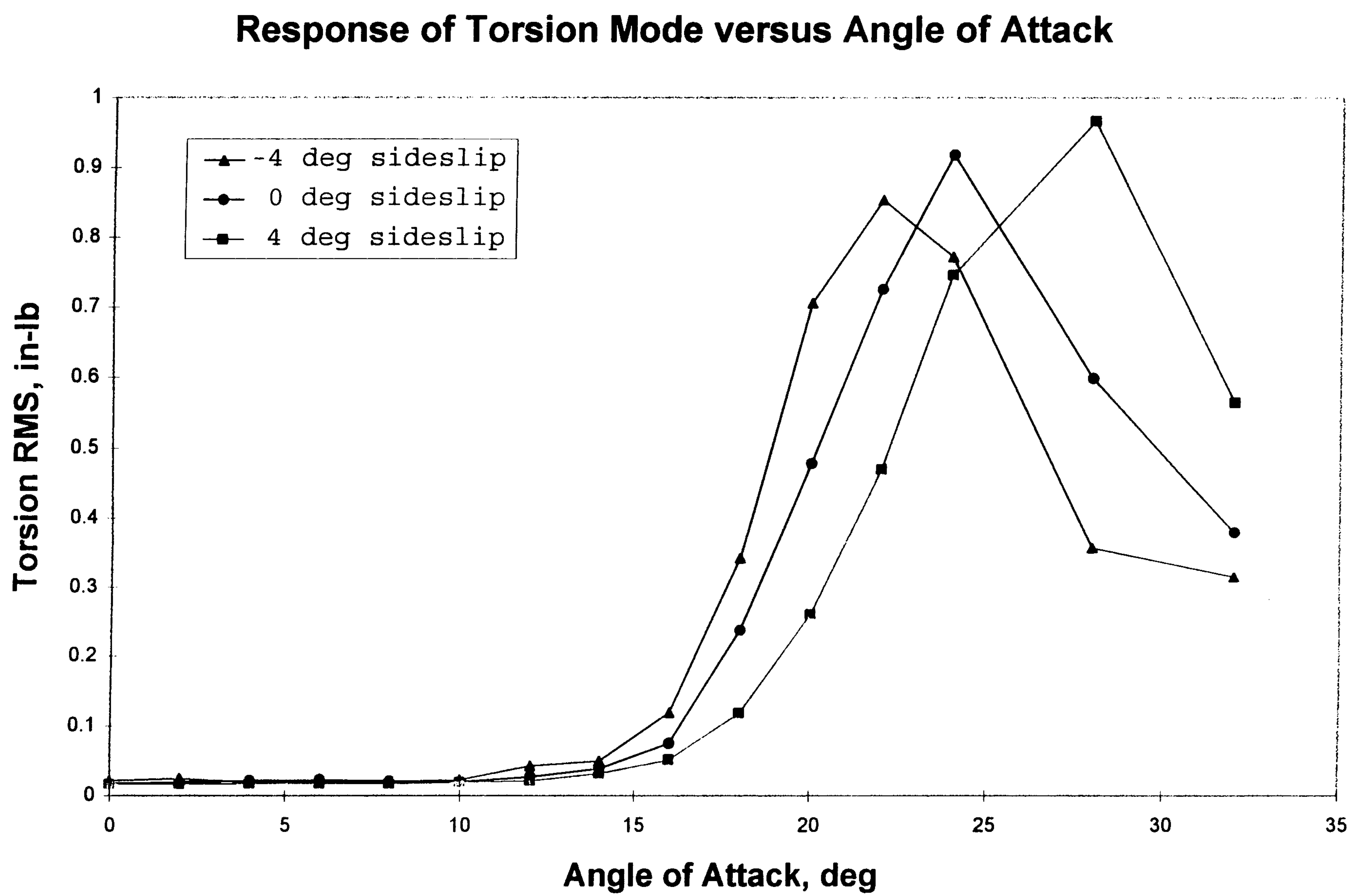

Fig 19. Response of Torsion Mode versus Angle of Attack

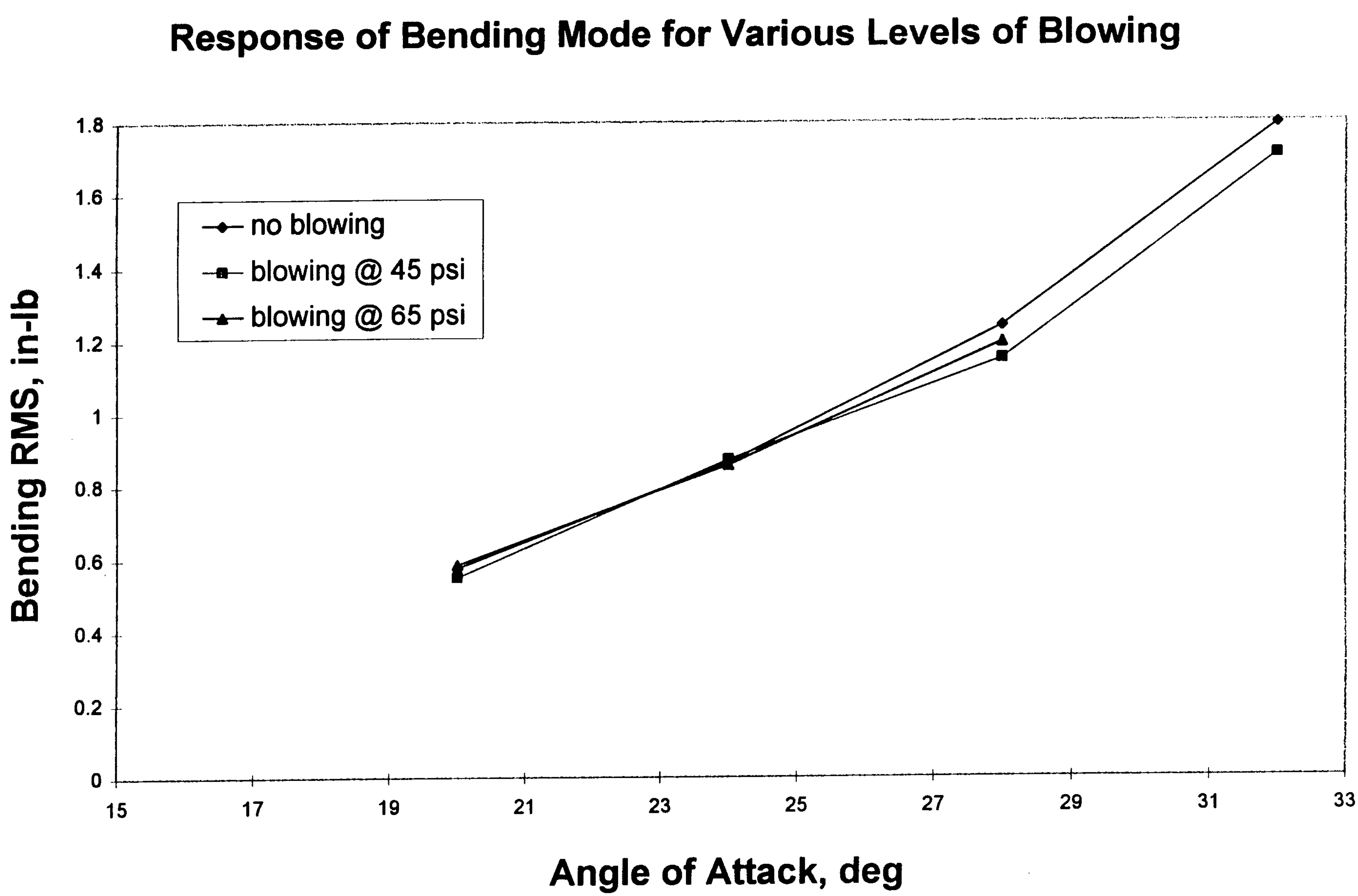

Fig 20. Response of Bending Mode for Various Levels of Blowing

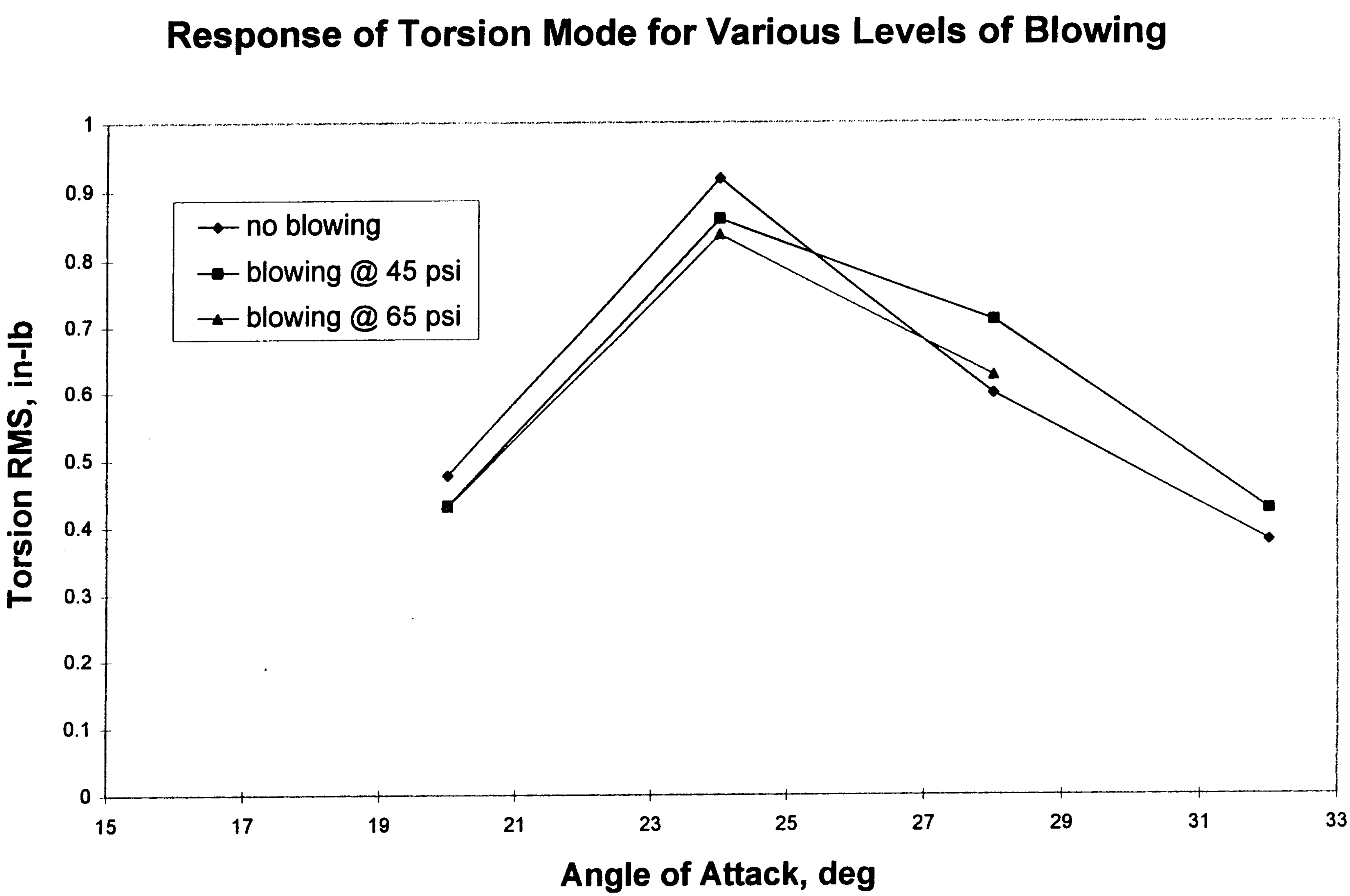

Fig 21. Response of Torsion Mode for Various Levels of Blowing

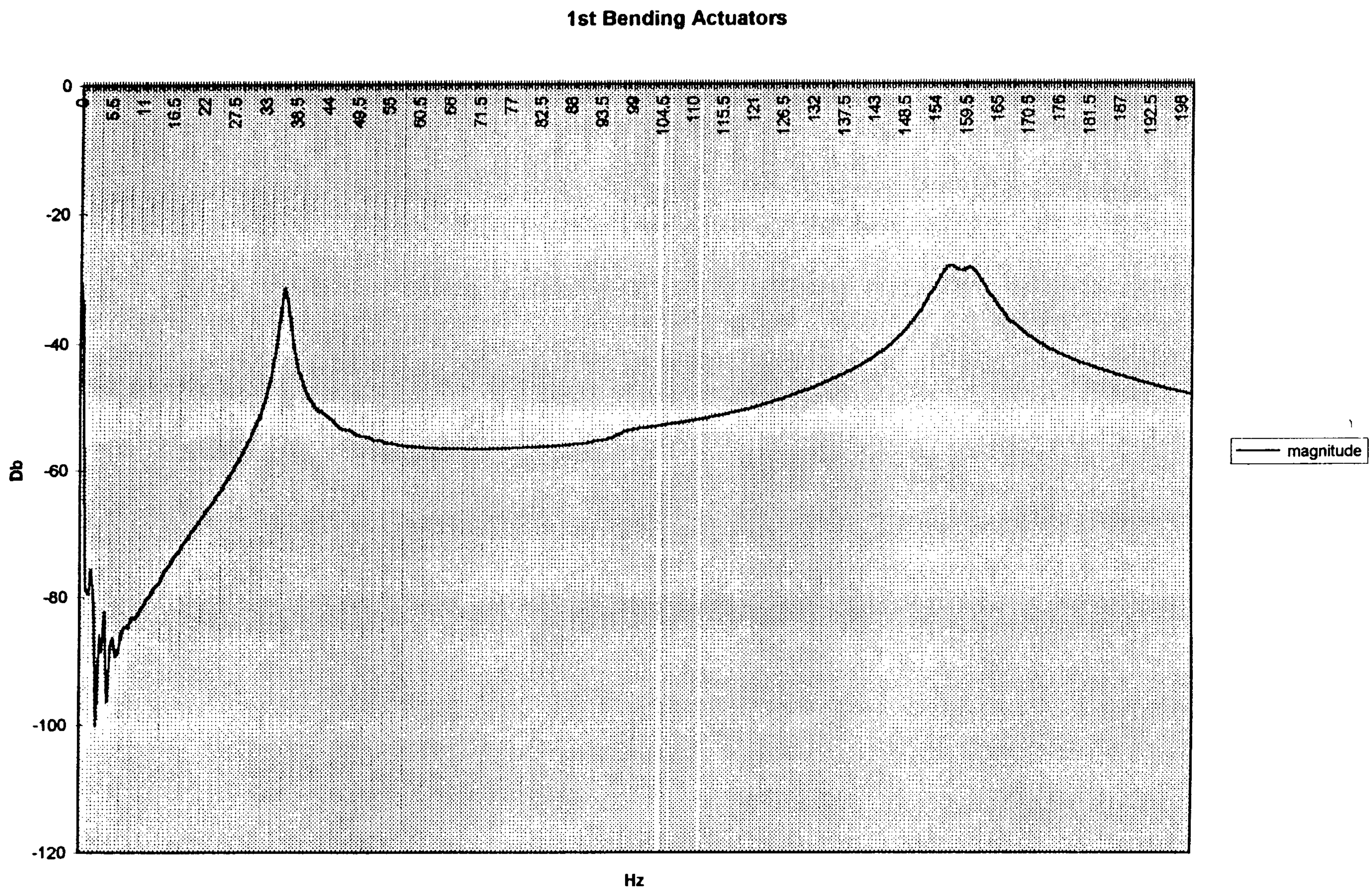

Fig 22. Structural Response due to First Bending Actuators

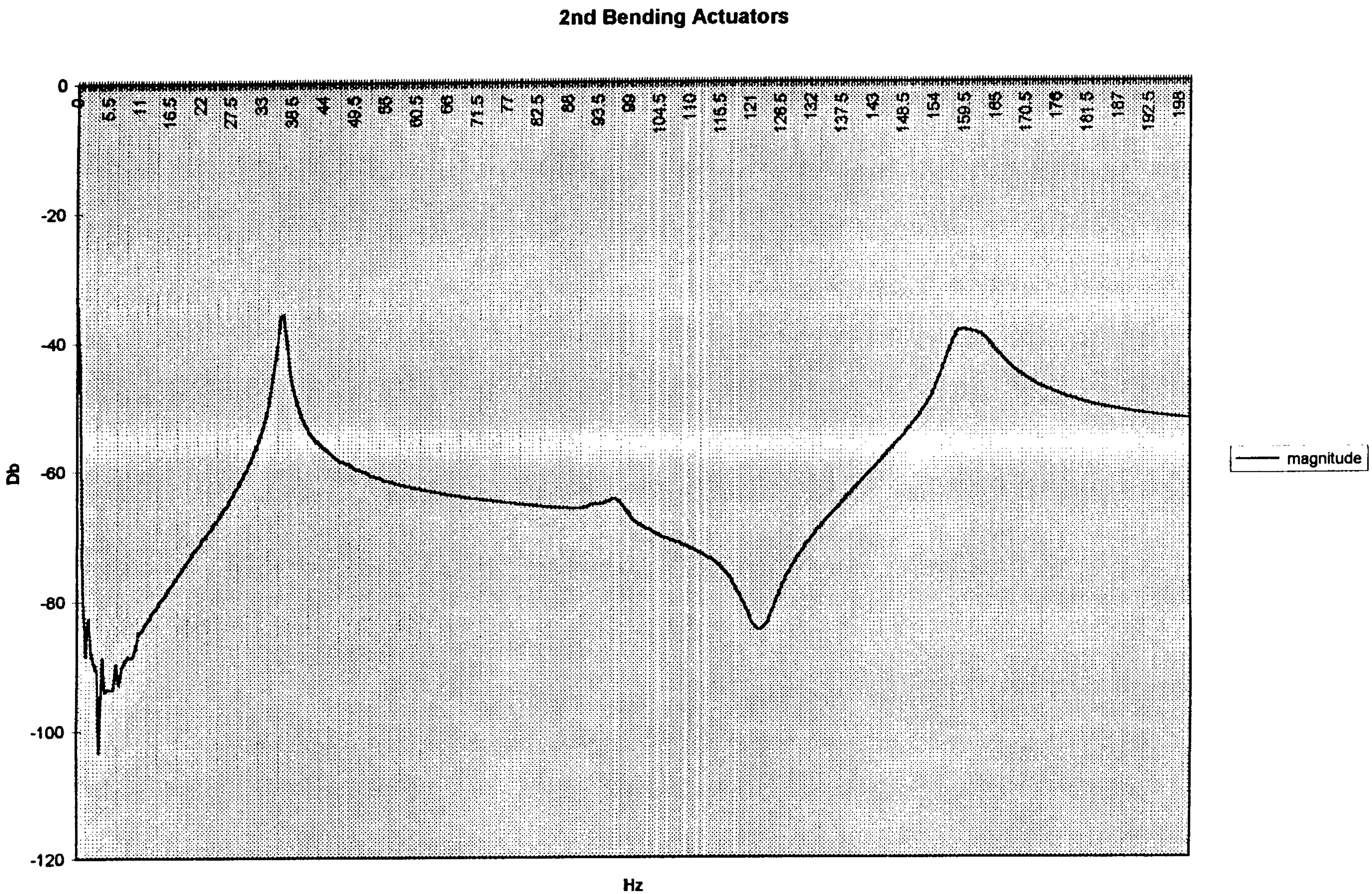

Fig 23. Structural Response due to Second Bending Actuators

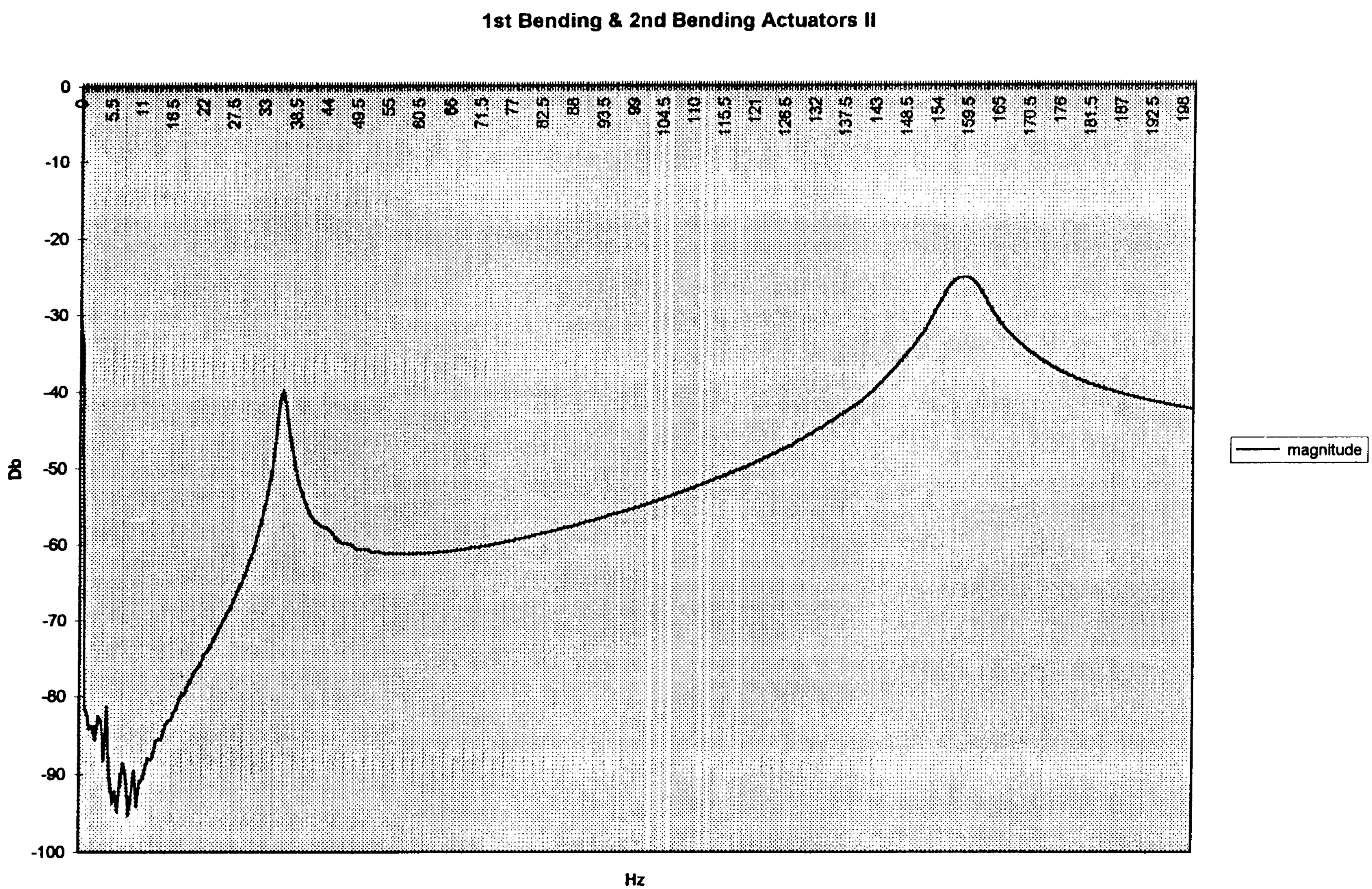

Fig 24. Structural Response due to First and Second Bending Actuators

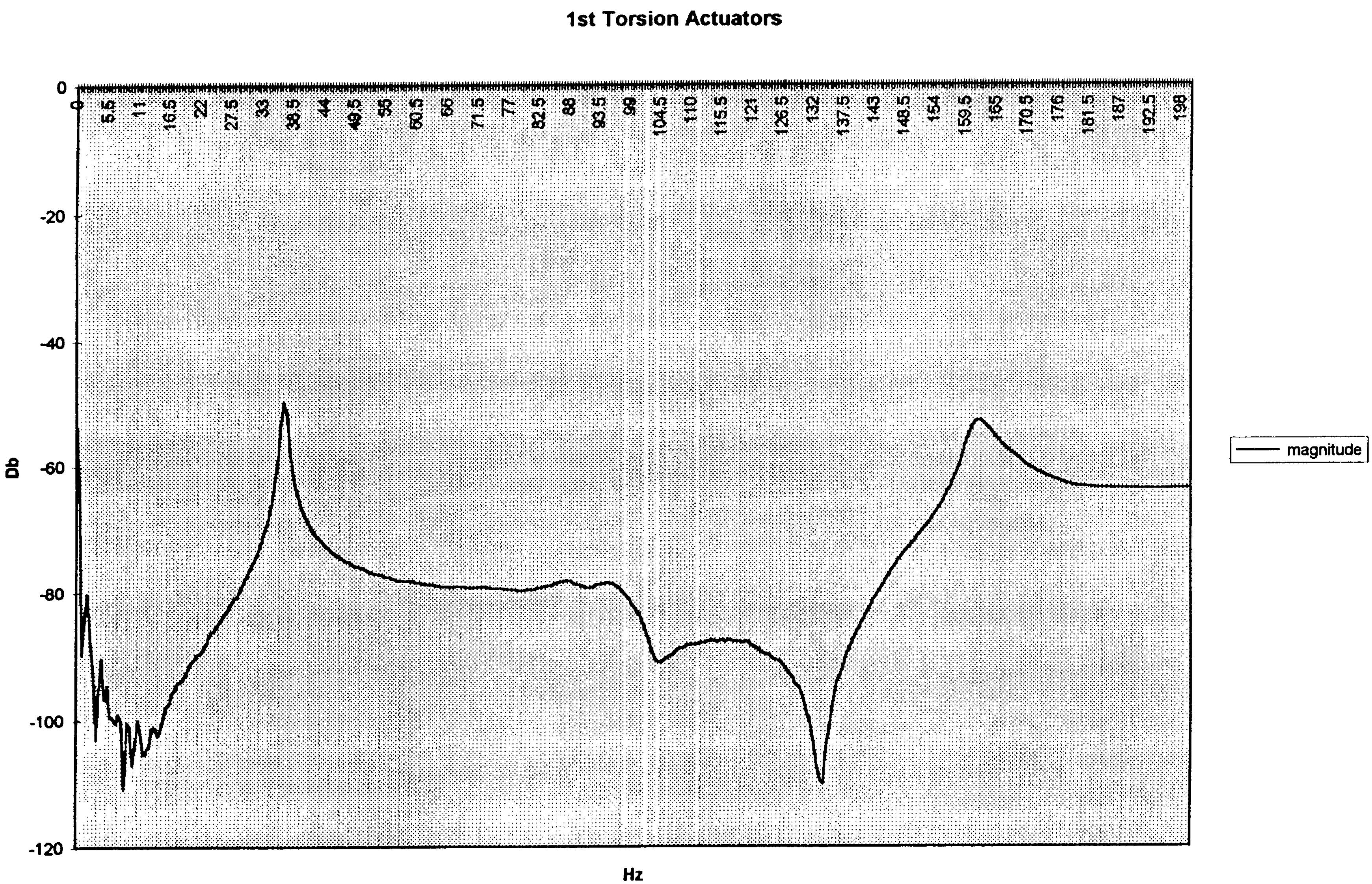

Fig 25. Structural Response due to First Torsion Actuators

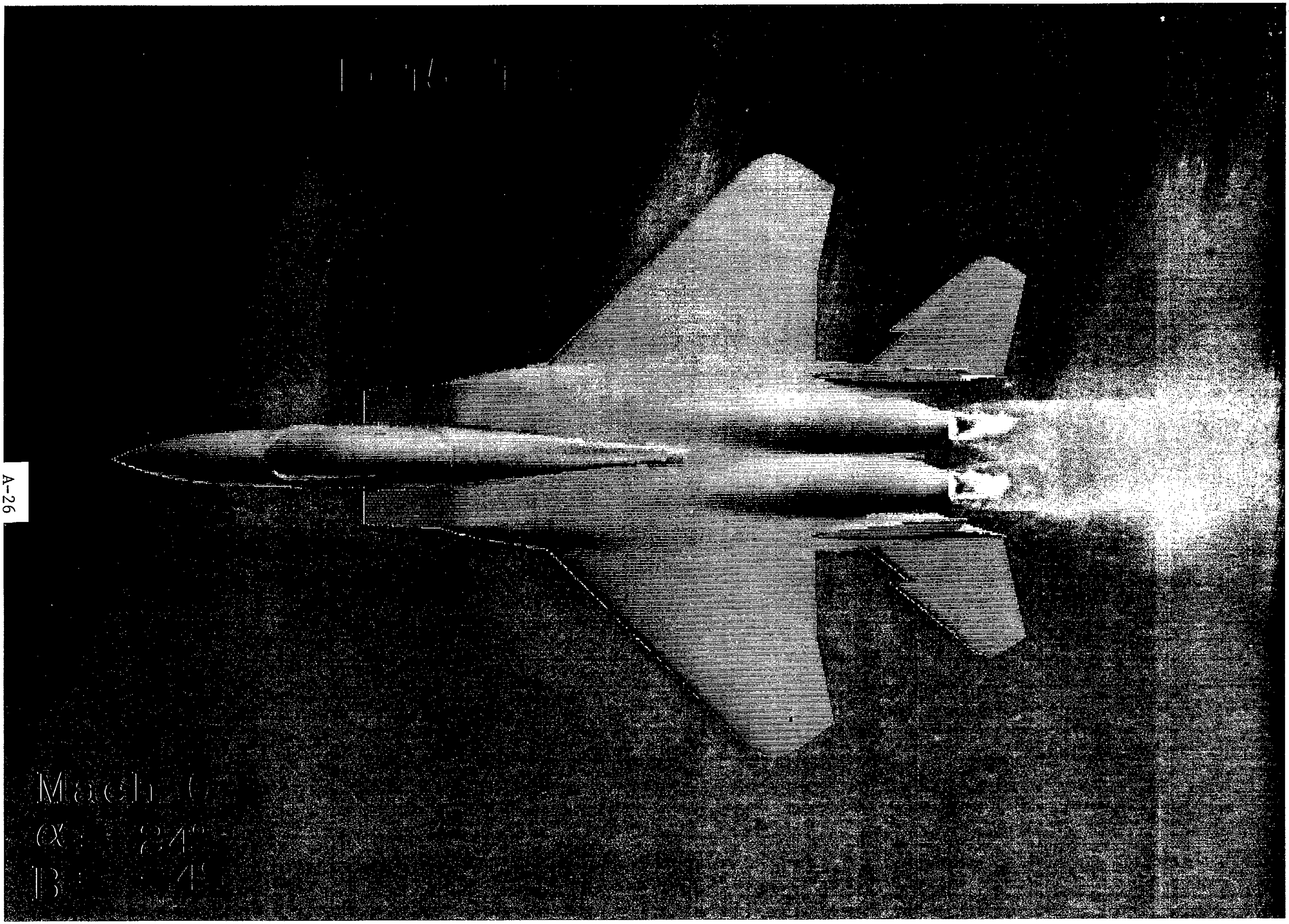

Fig 26. F-15 Tail Buffet Study

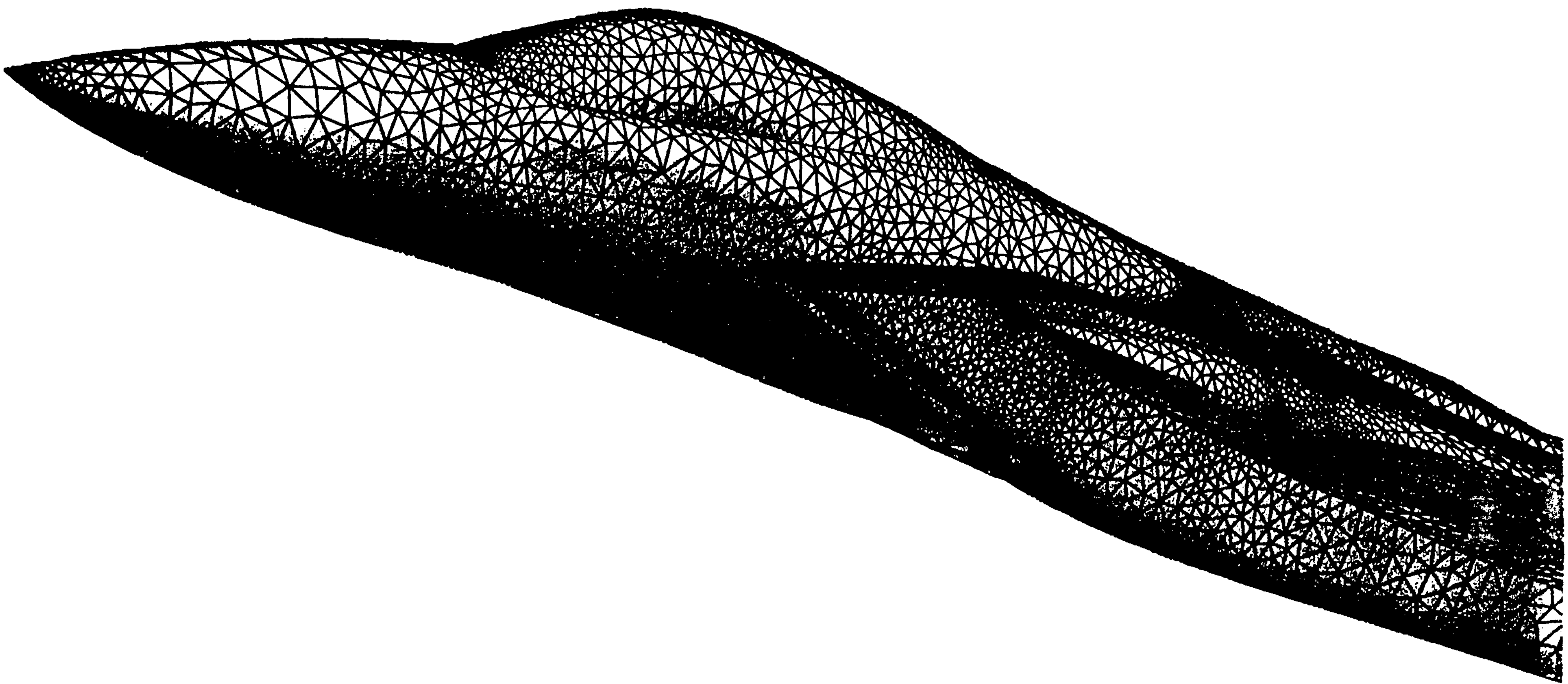

Fig 27. Unstructured Grid Using the Tetmesh Grid Generator

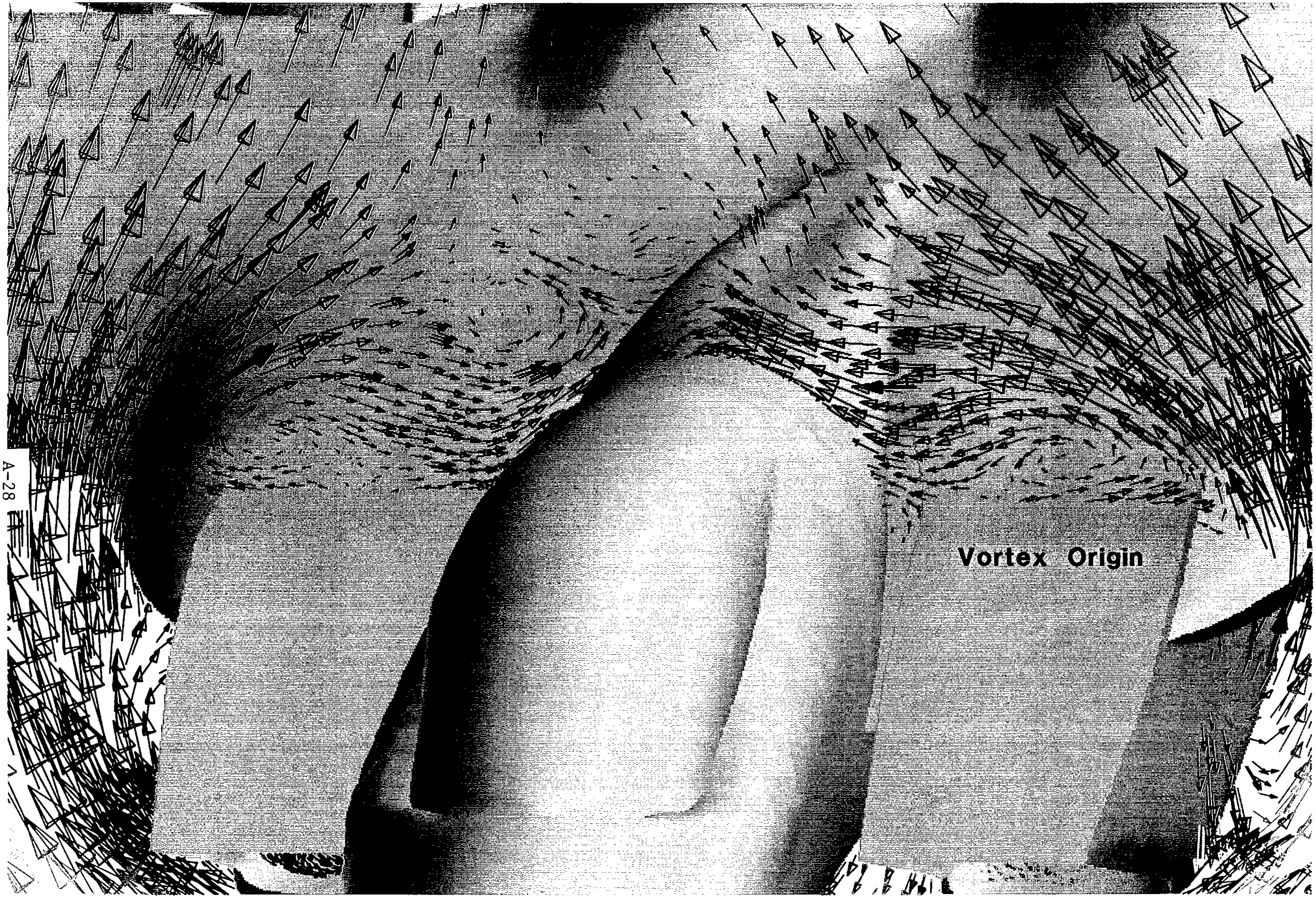

Fig 28. Flow Sweeping over the Gun Bump Fairing

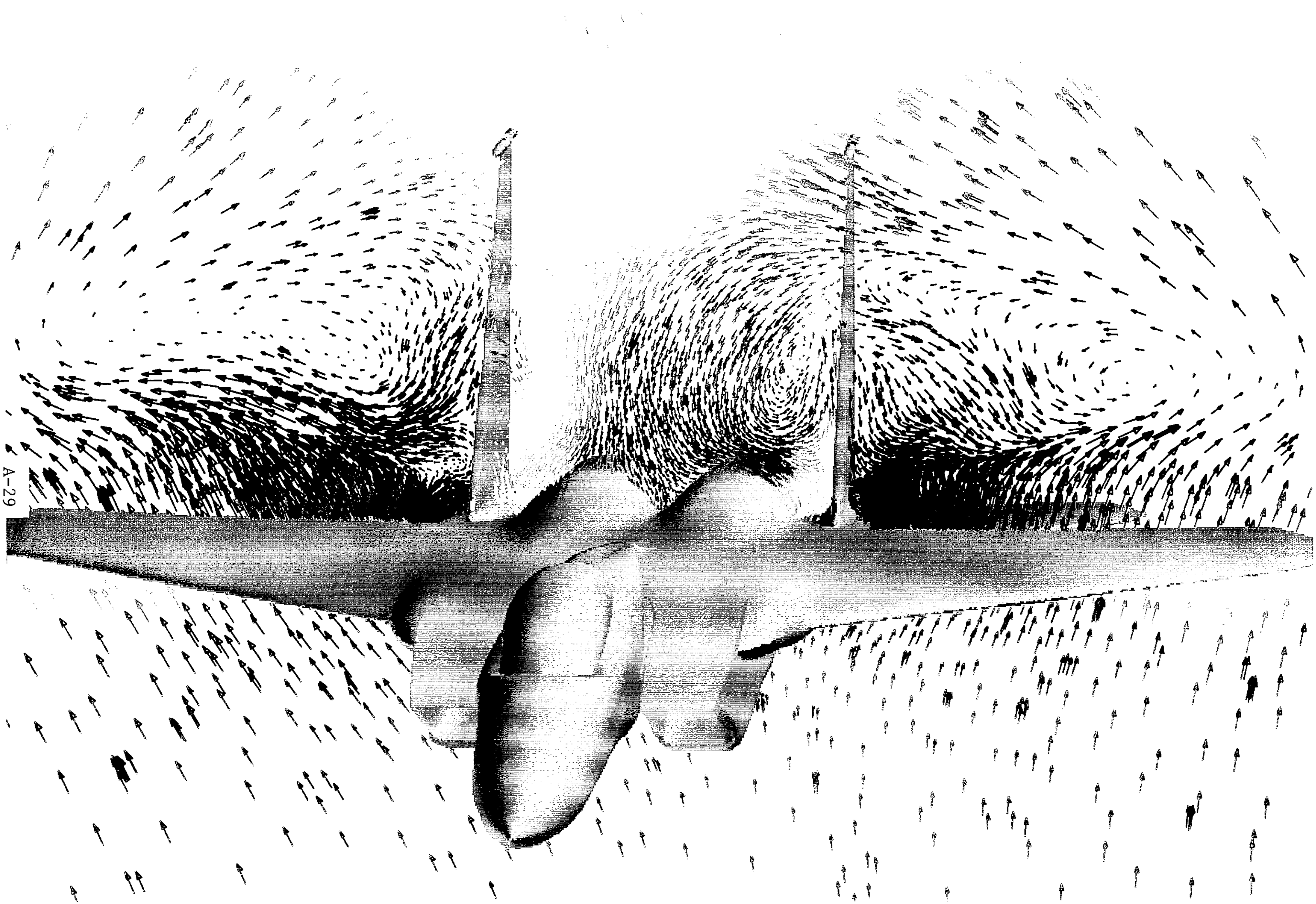

Fig 29. Vortical Flow Outside the Vertical Tails

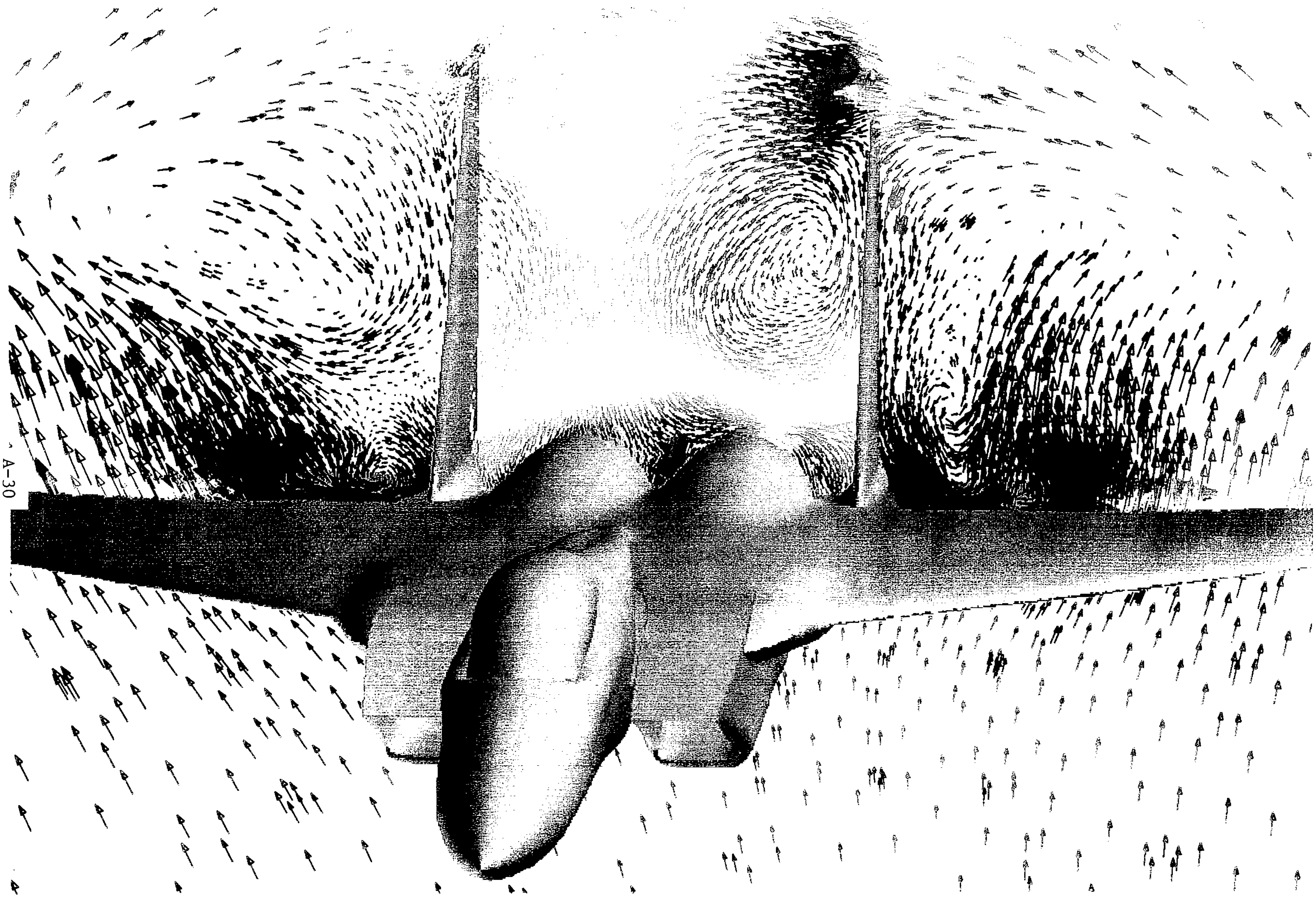

Fig 30. Vortical Flow Impacting the Vertical Tails

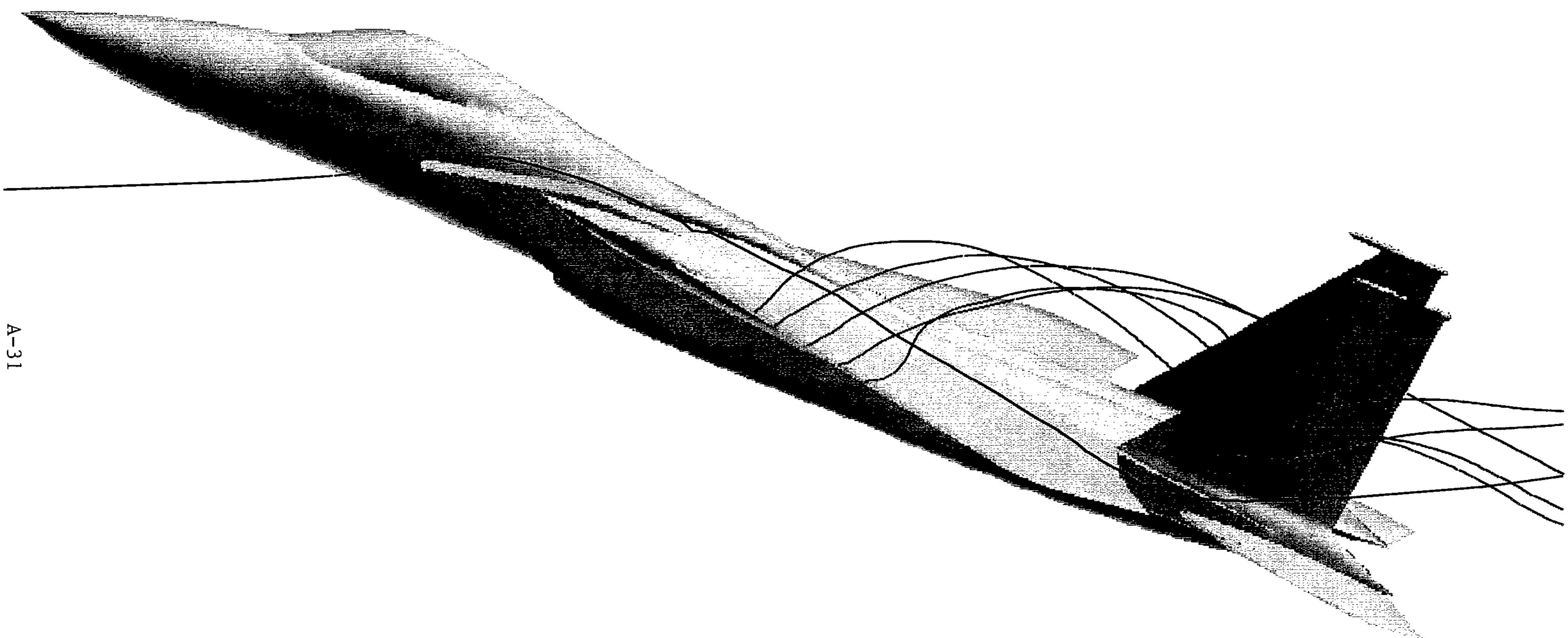

Fig 31. Streamline Traces from the Inlet and Wing's Leading Edge

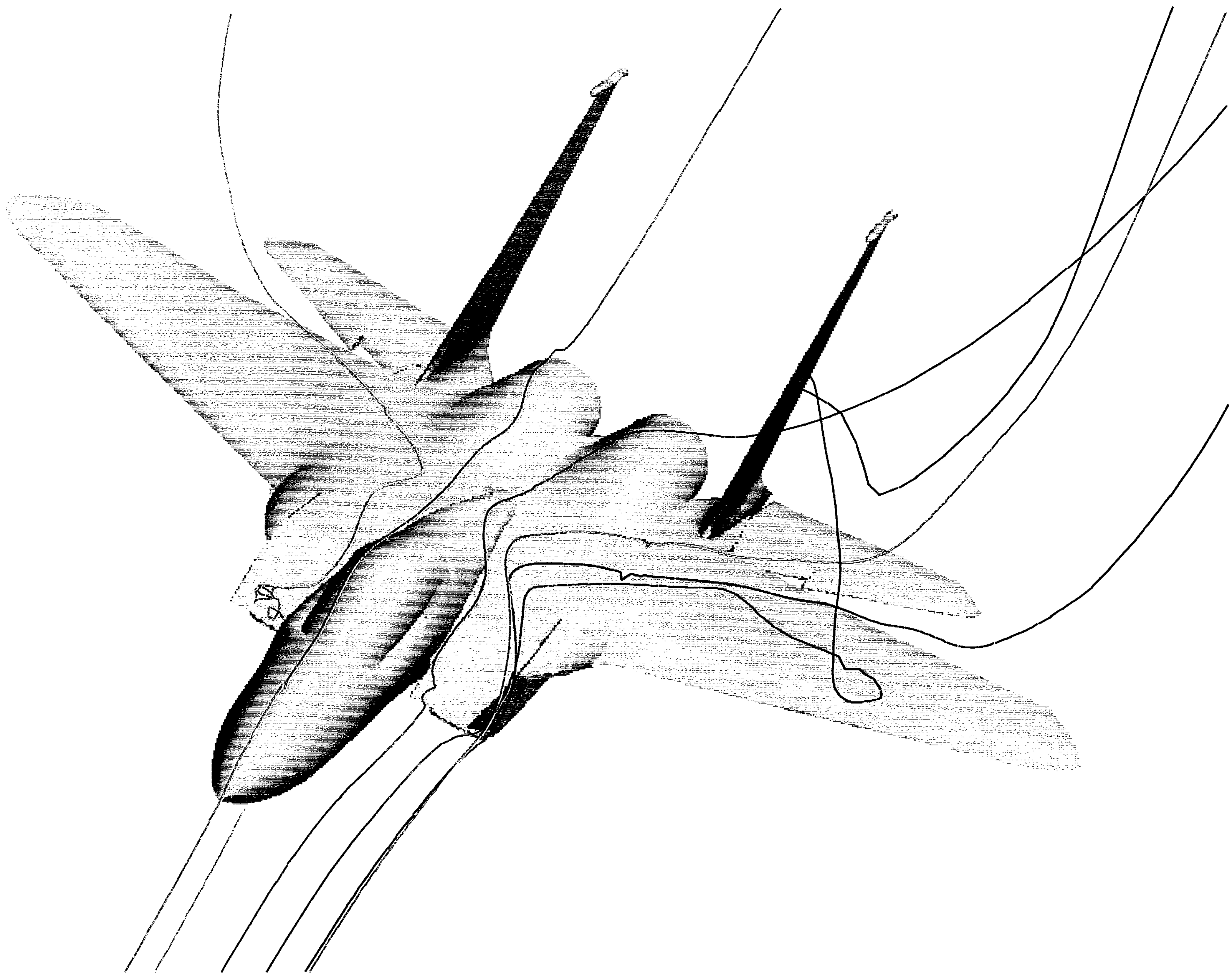

Fig 32. Streamline Traces from the Inlet and Wing Top

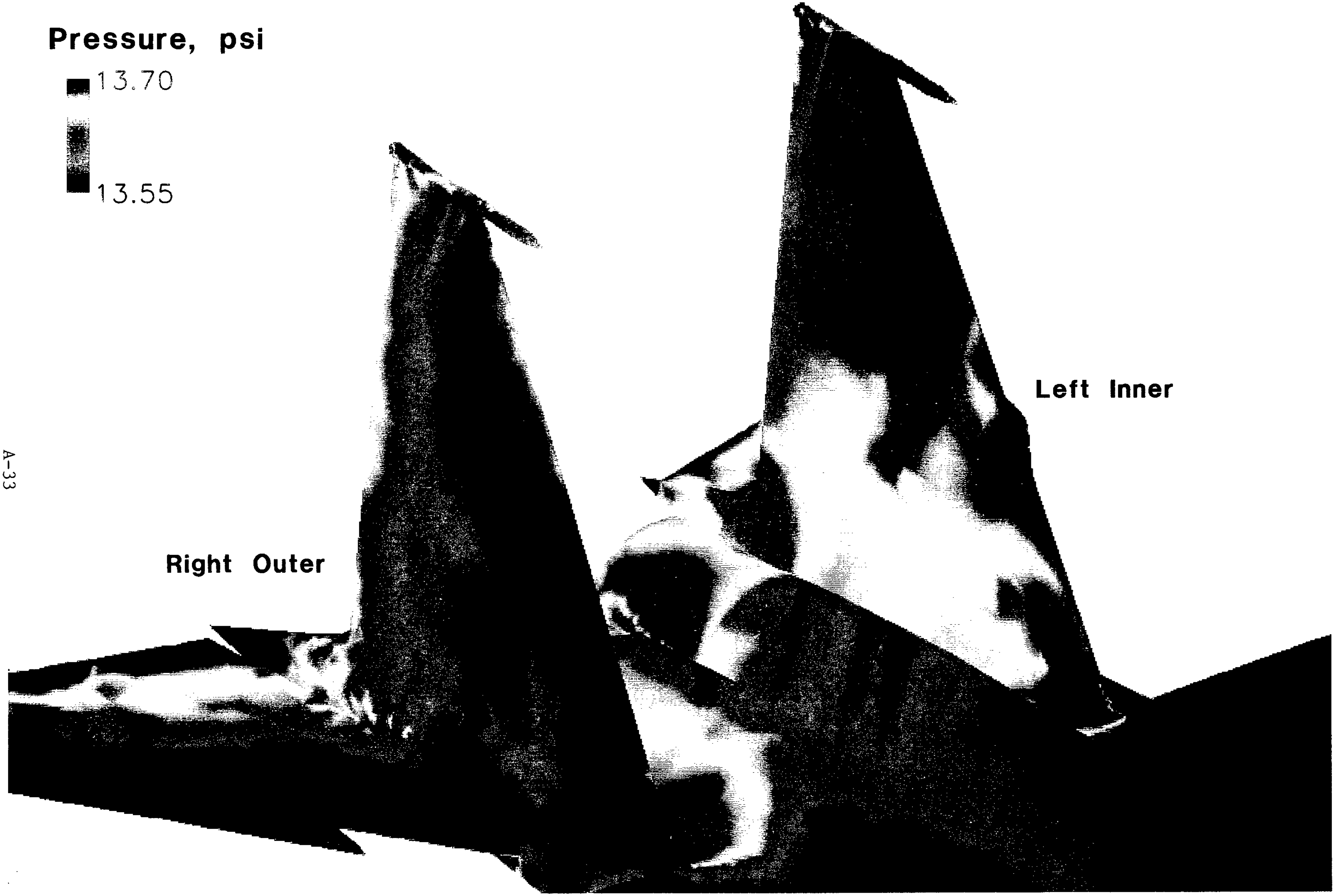

Fig 33. Pressure on Vertical Tails from Aircraft Right

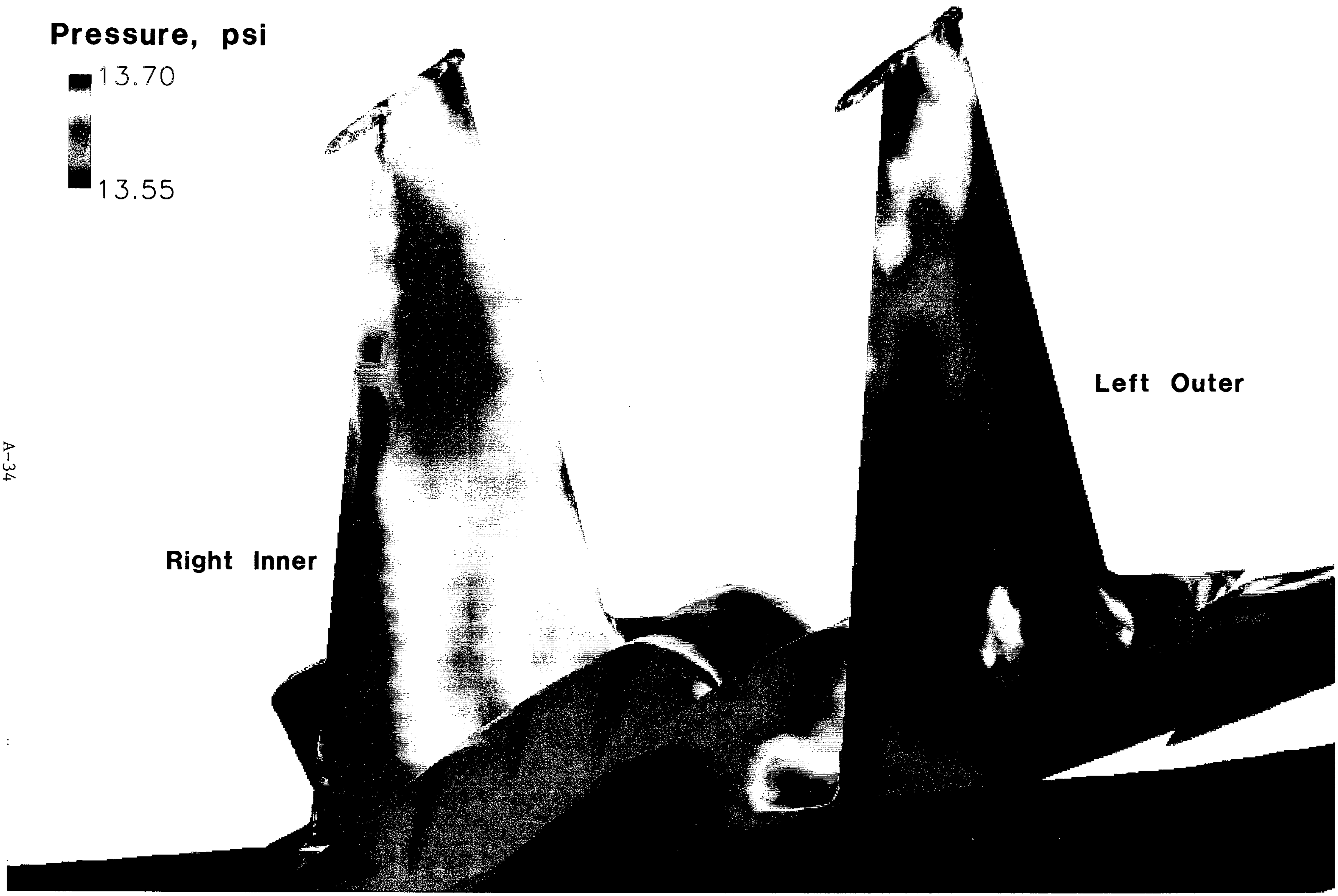

Fig 34. Pressure on Vertical Tails from Aircraft Left

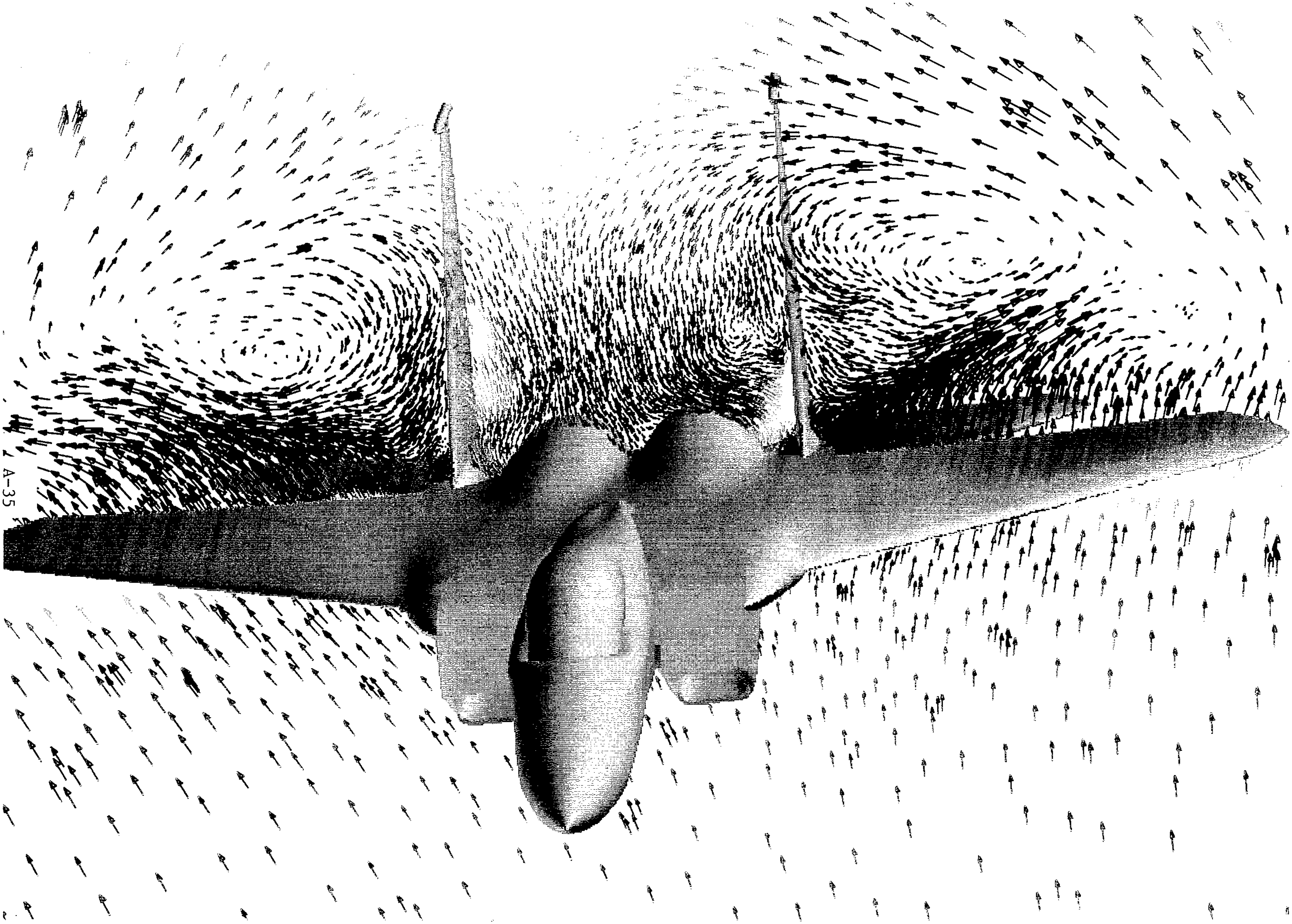

Fig 35. Vortical Flow over the Vertical Tails for the Engine-on Case

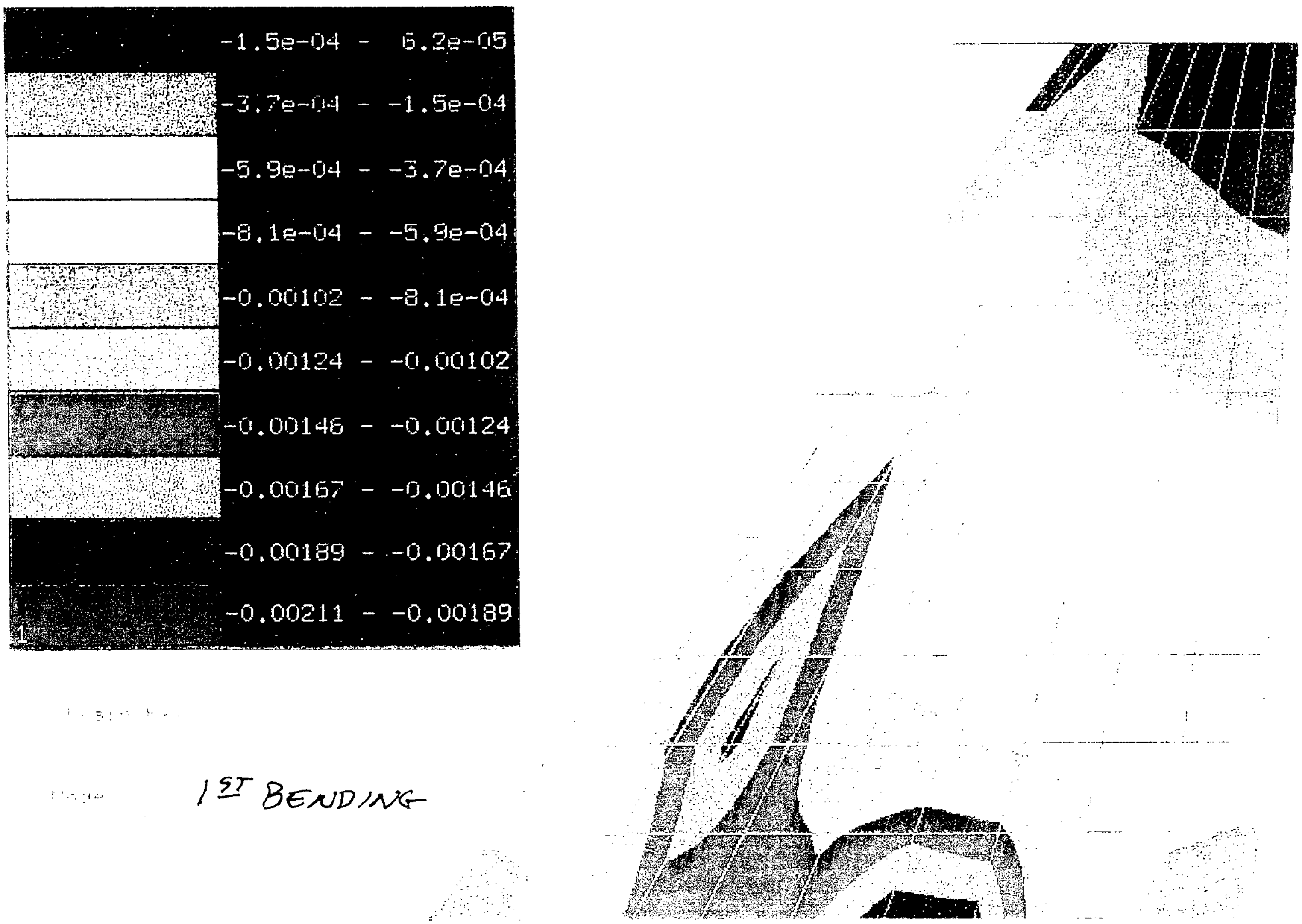

Fig 36. Strain Intensity on the Vertical Tail for the First Bending Mode

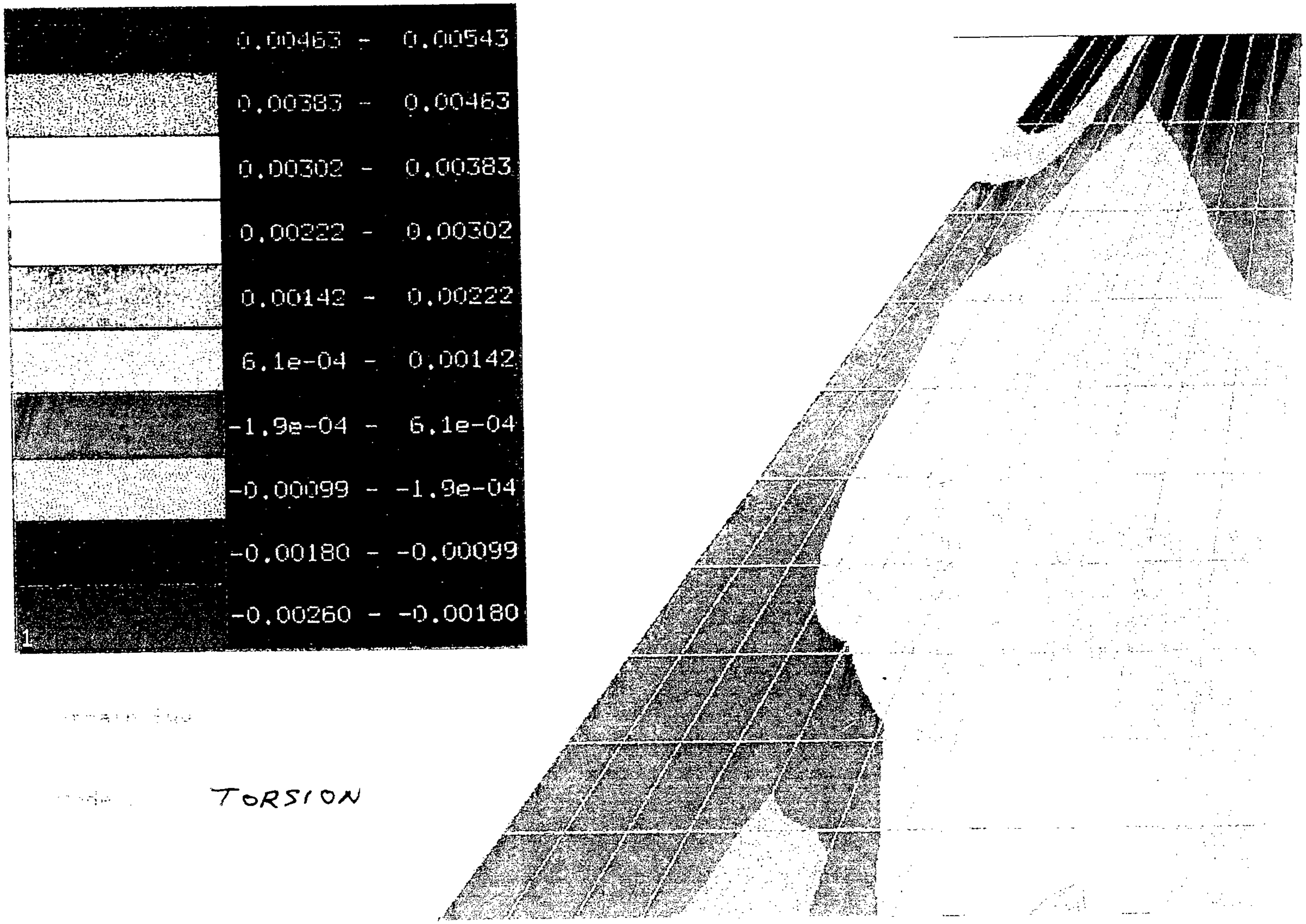

Fig 37. Strain Intensity on the Vertical Tail for the First Torsion Mode

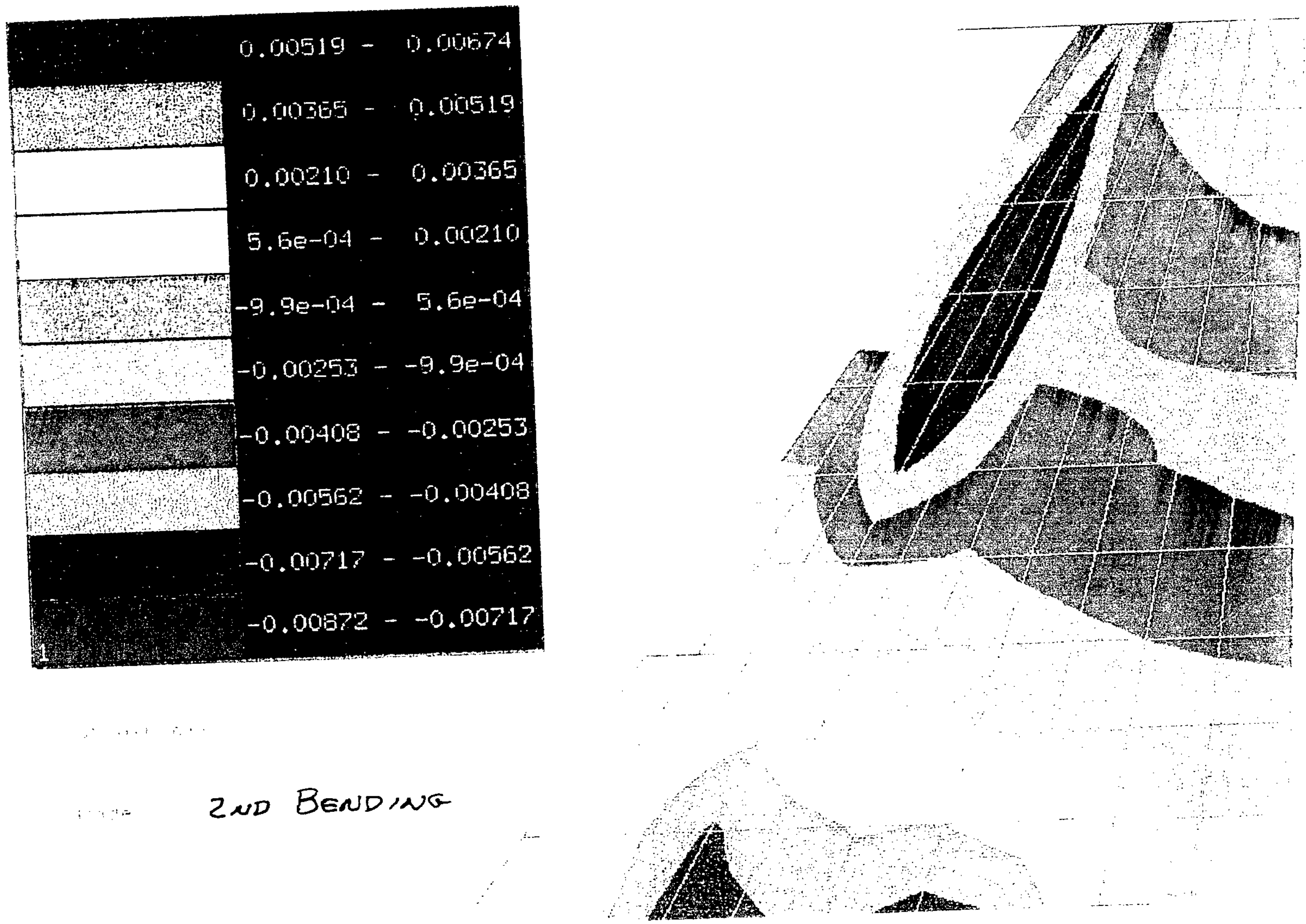

Fig 38. Strain Intensity on the Vertical Tail for the Second Bending Mode

	TPN	Tape#	deg	deg	psf	deg R	psia	psia	psia	psia	C mu	C mu	C mu	C mu		
Date & Time	TPN	Tape#	Alpha	Beta	Q	TOIN	PL_1	PL_2	PL_3	PL_4					Comment	
10/20/95 at 09:05:41	2894	1	0	0	56.1	521.6	13.78	13.74	13.74	13.7					No Blowing	Flex tail installed, Air lines capped
10/20/95 at 09:07:01	2895	1	-3.84	1.97	56.2	521.6	13.77	13.75	13.74	13.8					No Blowing	Flex tail installed, Air lines capped.
10/20/95 at 09:08:02	2896	1	0.12	1.89	55.9	521.7	13.77	13.75	13.74	13.7					No Blowing	Flex tail installed, Air lines capped.
10/20/95 at 09:09:03	2897	1	2.07	1.92	56.2	521.6	13.76	13.74	13.71	13.7					No Blowing	Flex tail installed, Air lines capped.
10/20/95 at 09:09:58	2898	1	4.07	1.95	56.2	521.6	13.77	13.74	13.67	13.6					No Blowing	Flex tail installed, Air lines capped.
10/20/95 at 09:10:49	2899	1	6.09	1.97	55.9	521.6	13.76	13.73	13.6	13.6					No Blowing	Flex tail installed, Air lines capped.
10/20/95 at 09:11:40	2900	1	8.13	1.98	56.3	521.6	13.74	13.73	13.52	13.5					No Blowing	Flex tail installed, Air lines capped.
10/20/95 at 09:12:31	2901	1	10.16	1.97	56.4	521.6	13.73	13.72	13.43	13.4					No Blowing	Flex tail installed, Air lines capped.
10/20/95 at 09:13:22	2902	1	12.18	1.95	56.1	521.6	13.72	13.7	13.35	13.3					No Blowing	Flex tail installed, Air lines capped.
10/20/95 at 09:14:13	2903	1	14.2	1.98	55.9	521.6	13.7	13.67	13.25	13.2					No Blowing	Flex tail installed, Air lines capped.
10/20/95 at 09:15:04	2904	1	16.22	1.97	55.8	521.5	13.69	13.66	13.19	13.1					No Blowing	Flex tail installed, Air lines capped.
10/20/95 at 09:15:55	2905	1	18.25	1.96	55.4	521.6	13.66	13.64	13.28	13.1					No Blowing	Flex tail installed, Air lines capped.
10/20/95 at 09:16:46	2906	1	20.28	1.97	55.3	521.6	13.64	13.61	13.19	13.1					No Blowing	Flex tail installed, Air lines capped.
10/20/95 at 09:17:37	2907	1	22.3	1.93	55.5	521.6	13.6	13.59	13.14	13					No Blowing	Flex tail installed, Air lines capped.
10/20/95 at 09:18:28	2908	1	24.33	1.94	56.4	521.7	13.57	13.56	13.13	13					No Blowing	Flex tail installed, Air lines capped.
10/20/95 at 09:19:21	2909	1	28.37	1.95	55.6	521.6	13.51	13.5	12.95	12.8					No Blowing	Flex tail installed, Air lines capped.
10/20/95 at 09:20:14	2910	1	32.38	1.94	55.4	521.7	13.45	13.43	12.63	12.4					No Blowing	Flex tail installed, Air lines capped.
10/20/95 at 09:21:13	2911	1	0	0	56.1	521.8	13.78	13.75	13.74	13.7					No Blowing	Flex tail installed, Air lines capped.
	TPN	Tape#	deg	deg	psf	deg R	psia	psia	psia	psia	C mu	C mu	C mu	C mu		
Date & Time	TPN	Tape#	Alpha	Beta	Q	TOIN	PL_1	PL_2	PL_3	PL_4					Comment	
10/20/95 at 10:07:03	2912	2	0	0	56.1	522.7	13.76	13.75	13.73	13.7					No Blowing	Flex tail installed, Air lines capped.
10/20/95 at 10:08:42	2913	2	-3.85	3.95	56.5	522.8	13.76	13.77	13.73	13.7					No Blowing	Flex tail installed, Air lines capped.
10/20/95 at 10:09:39	2914	2	0.12	3.89	56.1	522.8	13.75	13.77	13.73	13.7					No Blowing	Flex tail installed, Air lines capped.
10/20/95 at 10:10:34	2915	2	2.1	3.92	56.1	522.8	13.75	13.77	13.71	13.7					No Blowing	Flex tail installed, Air lines capped.
10/20/95 at 10:11:27	2916	2	4.1	3.93	55.9	522.8	13.74	13.76	13.66	13.6					No Blowing	Flex tail installed, Air lines capped.
10/20/95 at 10:12:20	2917	2	6.1	3.94	56	522.8	13.74	13.74	13.59	13.5					No Blowing	Flex tail installed, Air lines capped.
10/20/95 at 10:13:13	2918	2	8.12	3.95	55.8	522.8	13.72	13.74	13.53	13.5					No Blowing	Flex tail installed, Air lines capped.
10/20/95 at 10:14:04	2919	2	10.15	3.93	55.8	522.7	13.71	13.73	13.44	13.4					No Blowing	Flex tail installed, Air lines capped.
10/20/95 at 10:14:55	2920	2	12.17	3.97	55.7	522.5	13.7	13.71	13.36	13.3					No Blowing	Flex tail installed, Air lines capped.
10/20/95 at 10:15:46	2921	2	14.2	3.96	56.8	521.2	13.68	13.69	13.26	13.1					No Blowing	Flex tail installed, Air lines capped.
10/20/95 at 10:16:37	2922	2	16.25	3.93	56.6	520	13.66	13.67	13.21	13.1					No Blowing	Flex tail installed, Air lines capped.
10/20/95 at 10:17:28	2923	2	18.26	3.99	55.8	519.1	13.64	13.64	13.3	13					No Blowing	Flex tail installed, Air lines capped.
10/20/95 at 10:18:19	2924	2	20.28	3.99	55.7	518.2	13.61	13.62	13.25	13					No Blowing	Flex tail installed, Air lines capped.
10/20/95 at 10:19:10	2925	2	22.29	3.98	56.3	517.5	13.59	13.58	13.21	12.9					No Blowing	Flex tail installed, Air lines capped.
10/20/95 at 10:20:01	2926	2	24.32	3.99	55.6	517.1	13.55	13.55	13.2	12.9					No Blowing	Flex tail installed, Air lines capped.
10/20/95 at 10:20:54	2927	2	28.35	3.94	55.3	516.7	13.49	13.49	13.05	12.8					No Blowing	Flex tail installed, Air lines capped.
10/20/95 at 10:21:47	2928	2	32.37	3.96	55.4	516.5	13.43	13.42	12.71	12.4					No Blowing	Flex tail installed, Air lines capped.
10/20/95 at 10:22:46	2929	2	0	0	51	515.9	13.78	13.75	13.76	13.7					No Blowing	Flex tail installed, Air lines capped.
	TPN	Tape#	deg	deg	psf	deg R	psia	psia	psia	psia	C mu	C mu	C mu	C mu		
Date & Time	TPN	Tape#	Alpha	Beta	Q	TOIN	PL_1	PL_2	PL_3	PL_4	L NOSE	R NOSE			Comment	
10/23/95 at 09:03:49	2931	3	0.02	0	1	512.4	14.37	14.37	14.37	14.4					No Flow point	
10/23/95 at 09:43:28	2932	3	28.35	-0.02	56.7	514.3	37.14	34.13	13.18	13.2	0.002085	0.002069			Nose only	Cmu Sweep P1=LN P2=RN P3=LGB P4=RGB
10/23/95 at 09:48:08	2933	3	28.12	-3.94	56.1	514.4	37.18	34.18	13.09	13.4	0.002109	0.002094			Nose only	Cmu Sweep P1=LN P2=RN P3=LGB P4=RGB
10/23/95 at 09:52:14	2934	3	28.1	3.96	56.1	514.9	37.22	34.25	13.41	13.1	0.002111	0.002098			Nose only	Cmu Sweep P1=LN P2=RN P3=LGB P4=RGB
10/23/95 at 09:59:01	2935	3	28.36	-0.01	56.3	515.2	67.61	62.34	13.2	13.2	0.003822	0.003806			Nose only	Cmu Sweep P1=LN P2=RN P3=LGB P4=RGB
10/23/95 at 10:03:26	2936	3	28.35	-3.97	56.3	515.5	67.58	62.36	13.09	13.3	0.00382	0.003807			Nose only	Cmu Sweep P1=LN P2=RN P3=LGB P4=RGB
10/23/95 at 10:07:01	2937	3	28.35	3.94	56.3	515.8	67.59	62.39	13.39	13.1	0.003821	0.003809			Nose only	Cmu Sweep P1=LN P2=RN P3=LGB P4=RGB
10/23/95 at 10:11:15	2938	3	28.37	-0.01	56.2	516.1	90.94	84.46	13.22	13.2	0.00515	0.005165			Nose only	Cmu Sweep P1=LN P2=RN P3=LGB P4=RGB
10/23/95 at 10:14:47	2939	3	28.55	-1.66	55.9	516.2	90.19	83.87	13.1	13.3	0.005135	0.005157			Bad Data Point	
10/23/95 at 10:16:34	2940	3	28.35	-3.87	56.4	516.3	90.08	83.75	13.09	13.3	0.005083	0.005104			Nose only	Cmu Sweep P1=LN P2=RN P3=LGB P4=RGB
10/23/95 at 10:20:15	2941	3	28.34	3.89	56.1	516.5	89.88	83.58	13.39	13.1	0.005099	0.00512			Nose only	Cmu Sweep P1=LN P2=RN P3=LGB P4=RGB
	TPN	Tape#	deg	deg	psf	deg R	psia	psia	psia	psia	C mu	C mu	C mu	C mu		
Date & Time	TPN	Tape#	Alpha	Beta	Q	TOIN	PL_1	PL_2	PL_3	PL_4	L GUN	R GUN			Comment	
10/23/95 at 10:27:17	2942	3	28.36	-0.01	56.1	516.9	13.87	13.9	31.77	29.6	0.002008	0.002213			Gun Bump only	Cmu Sweep P1=LN P2=RN P3=LGB P4=RGB
10/23/95 at 10:30:13	2943	3	28.36	-4.01	56.3	517.1	13.88	13.9	32.02	29.8	0.002017	0.00222			Gun Bump only	Cmu Sweep P1=LN P2=RN P3=LGB P4=RGB
10/23/95 at 10:34:04	2944	3	28.35	3.98	55.8	517.7	13.87	13.94	32.21	30	0.002047	0.002255			Gun Bump only	Cmu Sweep P1=LN P2=RN P3=LGB P4=RGB
10/23/95 at 10:38:49	2945	3	28.36	-0.01	55.8	518.2	13.88	13.93	46.92	43.5	0.002982	0.003269			Gun Bump only	Cmu Sweep P1=LN P2=RN P3=LGB P4=RGB
10/23/95 at 10:41:29	2946	3	28.35	-3.97	55.8	518.3	13.89	13.92	47.13	43.6	0.002995	0.003277			Gun Bump only	Cmu Sweep P1=LN P2=RN P3=LGB P4=RGB
10/23/95 at 10:44:13	2947	3	28.35	3.94	55.7	518.6	13.88	13.96	47.24	43.7	0.003008	0.00329			Gun Bump only	Cmu Sweep P1=LN P2=RN P3=LGB P4=RGB
10/23/95 at 10:50:11	2948	3	28.36	-0.01	56	519.3	13.89	13.96	67.37	61.4	0.004266	0.004598			Gun Bump only	Cmu Sweep P1=LN P2=RN P3=LGB P4=RGB
10/23/95 at 10:52:38	2949	3	28.36	-3.97	56.2	519.5	13.9	13.94	67.21	61.2	0.004241	0.004567			Gun Bump only	Cmu Sweep P1=LN P2=RN P3=LGB P4=RGB

Table 1. Representative Test Conditions with and without Blowing

10/23/95 at 10:55:54	2950	3	28.36	3.94	55.7	520	13.89	13.98	66.99	60.9	0.004265	0.004585			Gun Bump only	Cmu Sweep P1=LN P2=RN P3=LGB P4=RGB
	TPN	Tape#	deg	deg	psf	deg R	psia	psia	psia	psia	C mu	C mu	C mu	C mu		
Date & Time	TPN	Tape#	Alpha	Beta	Q	TOIN	PL_1	PL_2	PL_3	PL_4	L WING	R WING			Comment	
10/23/95 at 12:36:52	2952	3	0.03	0	1	524.3	14.43	14.54	14.37	14.4					No Flow Point	
10/23/95 at 12:51:40	2953	3	28.36	-0.01	56.6	524.8	26.44	33.24	13.19	13.2	0.002123	0.002339			Wing only	Cmu Sweep P1=LW P2=RW P3=LGB P4=RGB
10/23/95 at 12:55:46	2954	3	28.36	-3.96	56.6	524.6	26.35	33.16	13.07	13.3	0.002115	0.002333			Wing only	Cmu Sweep P1=LW P2=RW P3=LGB P4=RGB
10/23/95 at 12:59:43	2955	3	28.35	3.93	56.1	525.4	26.38	33.16	13.38	13.1	0.002137	0.002354			Wing only	Cmu Sweep P1=LW P2=RW P3=LGB P4=RGB
10/23/95 at 13:05:08	2956	3	28.37	-0.01	55.7	524.8	39.74	49.98	13.2	13.2	0.003242	0.003574			Wing only	Cmu Sweep P1=LW P2=RW P3=LGB P4=RGB
10/23/95 at 13:08:28	2957	3	28.35	-3.96	56	524.8	39.73	49.91	13.1	13.4	0.003224	0.003549			Wing only	Cmu Sweep P1=LW P2=RW P3=LGB P4=RGB
10/23/95 at 13:11:41	2958	3	28.34	3.99	55.8	524.9	39.68	49.88	13.39	13.1	0.003231	0.00356			Wing only	Cmu Sweep P1=LW P2=RW P3=LGB P4=RGB
10/23/95 at 13:18:16	2959	3	28.37	-0.01	55.6	524.9	57.14	69.93	13.21	13.2	0.00467	0.005009			Wing only	Cmu Sweep P1=LW P2=RW P3=LGB P4=RGB
10/23/95 at 13:23:03	2960	3	28.34	-4.01	56.3	525.6	56.93	69.56	13.09	13.3	0.004595	0.004921			Wing only	Cmu Sweep P1=LW P2=RW P3=LGB P4=RGB
10/23/95 at 13:27:06	2961	3	28.35	3.94	55.6	525.7	56.86	69.35	13.4	13.1	0.004647	0.004967			Wing only	Cmu Sweep P1=LW P2=RW P3=LGB P4=RGB
10/23/95 at 13:31:30	2962	3	28.35	-0.01	56.2	525.6	13.3	13.47	13.18	13.2					No Blowing	Repeat Runs
10/23/95 at 13:35:47	2963	3	28.36	-3.97	55.3	525.7	13.32	13.38	13.06	13.3					No Blowing	Repeat Runs
10/23/95 at 13:39:52	2964	3	28.36	3.94	55.7	525.6	13.19	13.54	13.38	13.1					No Blowing	Repeat Runs
	TPN	Tape#	deg	deg	psf	deg R	psia	psia	psia	psia	C mu	C mu	C mu	C mu		
Date & Time	TPN	Tape#	Alpha	Beta	Q	TOIN	PL_1	PL_2	PL_3	PL_4	L WING	R WING	L GUN	R GUN	Comment	
10/23/95 at 13:45:25	2965	3	28.38	-0.01	56	525.9	26.58	33.5	31.66	29.5	0.002157	0.002382	0.002005	0.002209	GB & Wing	Cmu Sweep P1=LW P2=RW P3=LGB P4=RGB
10/23/95 at 13:49:59	2966	3	28.37	-3.97	55.6	525.9	26.51	33.41	31.92	29.7	0.002167	0.002393	0.002036	0.00224	GB & Wing	Cmu Sweep P1=LW P2=RW P3=LGB P4=RGB
10/23/95 at 13:53:02	2967	3	28.36	3.94	55.2	526.1	26.49	33.38	32.01	29.8	0.002181	0.002408	0.002057	0.002264	GB & Wing	Cmu Sweep P1=LW P2=RW P3=LGB P4=RGB
10/23/95 at 13:58:39	2968	3	28.35	-0.01	55.4	526	40.37	50.81	46.76	43.2	0.003311	0.003653	0.002993	0.00327	GB & Wing	Cmu Sweep P1=LW P2=RW P3=LGB P4=RGB
10/23/95 at 14:01:39	2969	3	28.36	-3.96	55.3	525.9	40.29	50.7	46.77	43.2	0.003311	0.003651	0.002999	0.003276	GB & Wing	Cmu Sweep P1=LW P2=RW P3=LGB P4=RGB
10/23/95 at 14:05:38	2970	3	28.36	3.95	55.3	526.7	40.17	50.53	46.74	43.1	0.003301	0.003639	0.002997	0.003268	GB & Wing	Cmu Sweep P1=LW P2=RW P3=LGB P4=RGB
10/23/95 at 14:14:39	2971	3	28.35	-0.01	55.5	526.8	57.25	69.98	66.28	60.3	0.004687	0.005022	0.004235	0.004556	GB & Wing	Cmu Sweep P1=LW P2=RW P3=LGB P4=RGB
10/23/95 at 14:18:14	2972	3	28.36	-3.96	55.3	526.8	57.07	69.74	66.1	60	0.004689	0.005022	0.004239	0.00455	GB & Wing	Cmu Sweep P1=LW P2=RW P3=LGB P4=RGB
10/23/95 at 14:25:01	2973	3	28.35	3.99	55.3	526.8	57.02	69.5	65.95	59.9	0.004685	0.005005	0.004229	0.004542	GB & Wing	Cmu Sweep P1=LW P2=RW P3=LGB P4=RGB
10/23/95 at 14:31:24	2974	3	16.24	-0.01	55.7	527.1	57.16	69.61	66.03	59.8	0.004663	0.004977	0.004204	0.004502	GB & Wing	Alpha Sweep P1=LW P2=RW P3=LGB P4=RGB
10/23/95 at 14:35:37	2975	3	18.24	-0.01	55.5	527.2	57.11	69.51	65.93	59.8	0.004676	0.004988	0.004213	0.004519	GB & Wing	Alpha Sweep P1=LW P2=RW P3=LGB P4=RGB
10/23/95 at 14:39:57	2976	3	20.27	-0.01	55.5	527.5	57.07	69.43	65.87	59.7	0.004672	0.004982	0.004209	0.004511	GB & Wing	Alpha Sweep P1=LW P2=RW P3=LGB P4=RGB
10/23/95 at 14:43:17	2977	3	22.29	-0.01	55.5	527.6	57.03	69.34	65.82	59.6	0.004669	0.004976	0.004206	0.004503	GB & Wing	Alpha Sweep P1=LW P2=RW P3=LGB P4=RGB
10/23/95 at 14:47:45	2978	3	24.32	-0.01	56.2	527.9	57	69.31	65.8	59.6	0.004609	0.004912	0.004152	0.004447	GB & Wing	Alpha Sweep P1=LW P2=RW P3=LGB P4=RGB
	TPN	Tape#	deg	deg	psf	deg R	psia	psia	psia	psia	C mu	C mu	C mu	C mu		
Date & Time	TPN	Tape#	Alpha	Beta	Q	TOIN	PL_1	PL_2	PL_3	PL_4	L WING	R WING			Comment	
10/23/95 at 14:54:17	2979	3	16.24	-0.01	56.1	528	57.43	69.69	13.38	13.3	0.004652	0.004947			Wing only	Alpha Sweep P1=LW P2=RW P3=LGB P4=RGB
10/23/95 at 14:57:24	2980	3	18.25	-0.01	56.1	528.2	57.37	69.59	13.4	13.4	0.004647	0.00494			Wing only	Alpha Sweep P1=LW P2=RW P3=LGB P4=RGB
10/23/95 at 15:01:41	2981	3	20.28	-0.01	55.8	528.5	57.29	69.47	13.35	13.4	0.004665	0.004958			Wing only	Alpha Sweep P1=LW P2=RW P3=LGB P4=RGB
10/23/95 at 15:05:59	2982	3	22.31	-0.01	55.5	528.4	57.19	69.32	13.33	13.3	0.004682	0.004974			Wing only	Alpha Sweep P1=LW P2=RW P3=LGB P4=RGB
10/23/95 at 15:09:20	2983	3	24.32	-0.01	55.7	528.3	57.11	69.26	13.3	13.3	0.004659	0.004952			Wing only	Alpha Sweep P1=LW P2=RW P3=LGB P4=RGB
10/23/95 at 15:15:13	2984	3	16.23	-0.01	55.6	529	12.92	13.13	13.38	13.3					No Blowing	Alpha Sweep
10/23/95 at 15:19:56	2985	3	18.26	-0.01	55.6	528.3	13.14	13.38	13.4	13.4					No Blowing	Alpha Sweep
10/23/95 at 15:23:31	2986	3	20.28	-0.01	55.4	528.9	13.16	13.4	13.35	13.3					No Blowing	Alpha Sweep
10/23/95 at 15:27:16	2987	3	22.31	-0.01	55.3	529.2	13.16	13.41	13.32	13.3					No Blowing	Alpha Sweep
10/23/95 at 15:30:24	2988	3	24.34	-0.01	55.2	529.2	13.16	13.4	13.29	13.3					No Blowing	Alpha Sweep
10/24/95 at 09:01:07	2990	3	-0.05	0	1	511.5	14.21	14.27	14.23	14.3					No Flow Point	
	TPN	Tape#	deg	deg	psf	deg R	psia	psia	psia	psia	C mu	C mu	C mu	C mu		
Date & Time	TPN	Tape#	Alpha	Beta	Q	TOIN	PL_1	PL_2	PL_3	PL_4			L GUN	R GUN	Comment	
10/24/95 at 09:12:46	2991	3	0	0	56.4	510	13.79	13.83	66.96	61.2			0.00421	0.00455	Gun Bump only	Alpha Sweep P1=LW P2=RW P3=LGB P4=RGB
10/24/95 at 09:13:43	2992	3	16.24	-3.92	56.2	510	12.92	12.75	66.95	61.1			0.004225	0.004559	Gun Bump only	Alpha Sweep P1=LW P2=RW P3=LGB P4=RGB
10/24/95 at 09:14:34	2993	3	18.25	-3.98	55.8	510	13.02	13	66.93	61.1			0.004254	0.004592	Gun Bump only	Alpha Sweep P1=LW P2=RW P3=LGB P4=RGB
10/24/95 at 09:15:25	2994	3	20.28	-3.94	56	510	13.03	13.02	66.88	61.1			0.004235	0.004576	Gun Bump only	Alpha Sweep P1=LW P2=RW P3=LGB P4=RGB
10/24/95 at 09:16:16	2995	3	22.31	-3.93	56.1	510.1	13.03	13.03	66.91	61.1			0.00423	0.004567	Gun Bump only	Alpha Sweep P1=LW P2=RW P3=LGB P4=RGB
10/24/95 at 09:17:07	2996	3	24.32	-3.93	55.6	510.1	13.08	13.06	66.9	61.1			0.004267	0.004608	Gun Bump only	Alpha Sweep P1=LW P2=RW P3=LGB P4=RGB
10/24/95 at 09:17:57	2997	3	26.35	-3.93	55.8	510.1	13.17	13.09	66.88	61			0.004251	0.004584	Gun Bump only	Alpha Sweep P1=LW P2=RW P3=LGB P4=RGB
10/24/95 at 09:18:54	2998	3	16.21	-0.01	56.6	510	12.78	12.85	66.88	61			0.00419	0.00452	Gun Bump only	Alpha Sweep P1=LW P2=RW P3=LGB P4=RGB
10/24/95 at 09:19:44	2999	3	18.25	-0.01	56.4	510.1	12.98	13.04	66.88	61			0.004205	0.004536	Gun Bump only	Alpha Sweep P1=LW P2=RW P3=LGB P4=RGB
10/24/95 at 09:20:35	3000	3	20.27	-0.01	56.5	510.1	13.01	13.04	66.88	61			0.004198	0.004528	Gun Bump only	Alpha Sweep P1=LW P2=RW P3=LGB P4=RGB
10/24/95 at 09:21:26	3001	3	22.3	-0.01	55.9	510.2	13.01	13.04	66.87	61			0.004242	0.004576	Gun Bump only	Alpha Sweep P1=LW P2=RW P3=LGB P4=RGB
10/24/95 at 09:22:18	3002	3	24.32	-0.01	56.2	510.2	13.04	13.06	66.85	61			0.004218	0.004552	Gun Bump only	Alpha Sweep P1=LW P2=RW P3=LGB P4=RGB
10/24/95 at 09:23:09	3003	3	26.34	-0.01	55.9	510.1	13.09	13.13	66.86	61			0.004242	0.004576	Gun Bump only	Alpha Sweep P1=LW P2=RW P3=LGB P4=RGB
10/24/95 at 09:24:06	3004	3	16.23	3.93	56.7	510.1	12.66	12.94	66.83	60.9			0.00418	0.004504	Gun Bump only	Alpha Sweep P1=LW P2=RW P3=LGB P4=RGB
10/24/95 at 09:24:57	3005	3	18.25	3.99	56.3	510	12.92	13.04	66.87	60.9			0.004212	0.004536	Gun Bump only	Alpha Sweep P1=LW P2=RW P3=LGB P4=RGB
10/24/95 at 09:25:48	3006	3	20.27	3.98	56.7	510	12.96	13.06	66.75	60.9			0.004175	0.004504	Gun Bump only	Alpha Sweep P1=LW P2=RW P3=LGB P4=RGB

Table 2. Representative Test Conditions with and without Blowing

10/24/95 at 09:26:39	3007	3	22.3	3.94	56.3	510	12.98	13.04	66.74	60.9			0.004204	0.004536	Gun Bump only	Alpha Sweep P1=LW P2=RW P3=LGB P4=RGB
10/24/95 at 09:27:30	3008	3	24.33	3.95	56.5	510	12.98	13.08	66.53	60.7			0.004176	0.004505	Gun Bump only	Alpha Sweep P1=LW P2=RW P3=LGB P4=RGB
10/24/95 at 09:28:21	3009	3	26.35	3.99	56.1	509.9	13.02	13.16	66.53	60.7			0.004206	0.004537	Gun Bump only	Alpha Sweep P1=LW P2=RW P3=LGB P4=RGB
10/24/95 at 09:29:20	3010	3	0	0	56.2	510	13.78	13.79	66.53	60.7			0.004198	0.004529	Gun Bump only	Alpha Sweep P1=LW P2=RW P3=LGB P4=RGB
	TPN	Tape#	deg	deg	psf	deg R	psia	psia	psia	psia	C mu	C mu	C mu	C mu		
Date & Time	TPN	Tape#	Alpha	Beta	Q	T0IN	PL_1	PL_2	PL_3	PL_4	L WING	R WING	L GUN	R GUN	Comment	
10/24/95 at 09:33:10	3011	3	0	0	56.6	509.7	57.16	70.72	66.02	60.2	0.004589	0.004976	0.004137	0.00446	GB & Wing	Alpha Sweep P1=LW P2=RW P3=LGB P4=RGB
10/24/95 at 09:34:07	3012	3	16.24	-3.92	56.2	509.8	57	70.48	65.91	60.1	0.004609	0.004994	0.004159	0.004485	GB & Wing	Alpha Sweep P1=LW P2=RW P3=LGB P4=RGB
10/24/95 at 09:34:57	3013	3	18.25	-3.97	56	509.8	56.86	70.3	65.88	60	0.004614	0.004999	0.004172	0.004493	GB & Wing	Alpha Sweep P1=LW P2=RW P3=LGB P4=RGB
10/24/95 at 09:35:48	3014	3	20.28	-3.94	55.7	509.8	56.99	70.39	66	60.2	0.004649	0.005033	0.004202	0.004532	GB & Wing	Alpha Sweep P1=LW P2=RW P3=LGB P4=RGB
10/24/95 at 09:36:38	3015	3	22.3	-3.93	55.8	509.8	56.85	70.19	65.91	60.1	0.004629	0.00501	0.004189	0.004517	GB & Wing	Alpha Sweep P1=LW P2=RW P3=LGB P4=RGB
10/24/95 at 09:37:29	3016	3	24.31	-3.97	55.8	509.8	57.03	70.41	66.06	60.2	0.004644	0.005025	0.004198	0.004524	GB & Wing	Alpha Sweep P1=LW P2=RW P3=LGB P4=RGB
10/24/95 at 09:38:20	3017	3	26.35	-3.93	55.8	509.8	57.03	70.37	66.04	60.2	0.004644	0.005022	0.004197	0.004524	GB & Wing	Alpha Sweep P1=LW P2=RW P3=LGB P4=RGB
10/24/95 at 09:39:15	3018	3	16.21	-0.01	55.9	509.8	56.9	70.15	65.97	60.1	0.004625	0.004998	0.004185	0.004509	GB & Wing	Alpha Sweep P1=LW P2=RW P3=LGB P4=RGB
10/24/95 at 09:40:06	3019	3	18.24	-0.01	55.9	509.8	56.96	70.21	66.04	60.2	0.00463	0.005002	0.00419	0.004516	GB & Wing	Alpha Sweep P1=LW P2=RW P3=LGB P4=RGB
10/24/95 at 09:40:57	3020	3	20.27	-0.01	55.7	509.8	56.91	70.14	65.99	60.1	0.004643	0.005015	0.004202	0.004525	GB & Wing	Alpha Sweep P1=LW P2=RW P3=LGB P4=RGB
10/24/95 at 09:41:48	3021	3	22.3	-0.01	55.7	509.5	56.8	69.98	65.88	60.1	0.004634	0.005004	0.004195	0.004525	GB & Wing	Alpha Sweep P1=LW P2=RW P3=LGB P4=RGB
10/24/95 at 09:42:39	3022	3	24.31	-0.01	56.3	509	57.08	70.3	66.14	60.2	0.004607	0.004973	0.004166	0.004484	GB & Wing	Alpha Sweep P1=LW P2=RW P3=LGB P4=RGB
10/24/95 at 09:43:29	3023	3	26.33	-0.01	55.8	508.8	57	70.17	66.04	60.2	0.004642	0.005008	0.004197	0.004524	GB & Wing	Alpha Sweep P1=LW P2=RW P3=LGB P4=RGB
10/24/95 at 09:44:26	3024	3	16.23	3.93	56.2	508.6	56.89	70.02	66	60.1	0.0046	0.004962	0.004165	0.004485	GB & Wing	Alpha Sweep P1=LW P2=RW P3=LGB P4=RGB
10/24/95 at 09:45:17	3025	3	18.24	3.99	56	508.5	56.96	70.1	66.04	60.2	0.004622	0.004985	0.004182	0.004508	GB & Wing	Alpha Sweep P1=LW P2=RW P3=LGB P4=RGB
10/24/95 at 09:46:08	3026	3	20.27	3.99	55.8	508.4	56.91	70.04	66	60.1	0.004634	0.004999	0.004195	0.004517	GB & Wing	Alpha Sweep P1=LW P2=RW P3=LGB P4=RGB
10/24/95 at 09:46:59	3027	3	22.3	3.94	56	508.2	56.83	69.91	65.93	60.1	0.004611	0.004972	0.004175	0.004501	GB & Wing	Alpha Sweep P1=LW P2=RW P3=LGB P4=RGB
10/24/95 at 09:47:50	3028	3	24.32	3.95	55.8	508	57.06	70.18	66.15	60.2	0.004646	0.005009	0.004204	0.004524	GB & Wing	Alpha Sweep P1=LW P2=RW P3=LGB P4=RGB
10/24/95 at 09:48:41	3029	3	26.35	3.95	55.8	508.1	57	70.09	66.06	60.2	0.004642	0.005002	0.004198	0.004524	GB & Wing	Alpha Sweep P1=LW P2=RW P3=LGB P4=RGB
10/24/95 at 09:49:40	3030	3	0	0	56.6	508	56.85	69.9	66	60.1	0.004564	0.004918	0.004135	0.004453	GB & Wing	Alpha Sweep P1=LW P2=RW P3=LGB P4=RGB
	TPN	Tape#	deg	deg	psf	deg R	psia	psia	psia	psia	C mu	C mu	C mu	C mu		
Date & Time	TPN	Tape#	Alpha	Beta	Q	T0IN	PL_1	PL_2	PL_3	PL_4	L WING	R WING			Comment	
10/24/95 at 09:53:21	3031	3	0	0	55.9	507.8	56.99	70.02	13.88	13.9	0.004632	0.004988			Wing only	Alpha Sweep P1=LW P2=RW P3=LGB P4=RGB
10/24/95 at 09:54:18	3032	3	16.24	-3.92	55.5	507.7	57.06	69.77	13.31	13.4	0.004672	0.005007			Wing only	Alpha Sweep P1=LW P2=RW P3=LGB P4=RGB
10/24/95 at 09:55:09	3033	3	18.25	-3.97	55.9	507.7	56.88	69.87	13.27	13.5	0.004624	0.004978			Wing only	Alpha Sweep P1=LW P2=RW P3=LGB P4=RGB
10/24/95 at 09:56:00	3034	3	20.29	-3.94	56.1	507.8	57.08	70.14	13.21	13.5	0.004623	0.004979			Wing only	Alpha Sweep P1=LW P2=RW P3=LGB P4=RGB
10/24/95 at 09:56:51	3035	3	22.3	-3.93	56.2	507.8	57.12	70.17	13.13	13.5	0.004618	0.004972			Wing only	Alpha Sweep P1=LW P2=RW P3=LGB P4=RGB
10/24/95 at 09:57:42	3036	3	24.34	-3.93	56	507.9	57.02	70.06	13.12	13.4	0.004627	0.004982			Wing only	Alpha Sweep P1=LW P2=RW P3=LGB P4=RGB
10/24/95 at 09:58:33	3037	3	26.34	-3.97	55.7	507.9	56.99	69.99	13.06	13.4	0.004649	0.005004			Wing only	Alpha Sweep P1=LW P2=RW P3=LGB P4=RGB
10/24/95 at 09:59:28	3038	3	16.22	-0.01	56	507.9	56.93	69.9	13.35	13.3	0.004619	0.004971			Wing only	Alpha Sweep P1=LW P2=RW P3=LGB P4=RGB
10/24/95 at 10:00:19	3039	3	18.25	-0.01	55.9	507.7	56.89	69.84	13.34	13.4	0.004624	0.004976			Wing only	Alpha Sweep P1=LW P2=RW P3=LGB P4=RGB
10/24/95 at 10:01:10	3040	3	20.27	-0.01	55.8	507.7	56.85	69.8	13.33	13.3	0.004629	0.004982			Wing only	Alpha Sweep P1=LW P2=RW P3=LGB P4=RGB
10/24/95 at 10:02:01	3041	3	22.29	-0.01	56	507.7	56.81	69.74	13.29	13.3	0.00461	0.00496			Wing only	Alpha Sweep P1=LW P2=RW P3=LGB P4=RGB
10/24/95 at 10:02:52	3042	3	24.32	-0.01	56	507.7	56.8	69.72	13.27	13.3	0.004609	0.004958			Wing only	Alpha Sweep P1=LW P2=RW P3=LGB P4=RGB
10/24/95 at 10:03:43	3043	3	26.33	-0.01	55.5	507.7	56.79	69.7	13.18	13.2	0.004649	0.005001			Wing only	Alpha Sweep P1=LW P2=RW P3=LGB P4=RGB
10/24/95 at 10:04:39	3044	3	16.23	3.93	56.4	507.7	56.76	69.68	13.44	13.3	0.004573	0.00492			Wing only	Alpha Sweep P1=LW P2=RW P3=LGB P4=RGB
10/24/95 at 10:05:30	3045	3	18.25	3.98	55.9	507.7	56.77	69.67	13.52	13.2	0.004615	0.004964			Wing only	Alpha Sweep P1=LW P2=RW P3=LGB P4=RGB
10/24/95 at 10:06:21	3046	3	20.27	3.98	56	507.8	56.75	69.65	13.47	13.2	0.004605	0.004953			Wing only	Alpha Sweep P1=LW P2=RW P3=LGB P4=RGB
10/24/95 at 10:07:12	3047	3	22.29	3.98	55.8	507.9	56.74	69.65	13.45	13.1	0.00462	0.004971			Wing only	Alpha Sweep P1=LW P2=RW P3=LGB P4=RGB
10/24/95 at 10:08:02	3048	3	24.33	3.95	56	508	56.74	69.62	13.42	13.2	0.004604	0.004951			Wing only	Alpha Sweep P1=LW P2=RW P3=LGB P4=RGB
10/24/95 at 10:08:52	3049	3	26.34	3.95	55.7	508	56.76	69.66	13.39	13.1	0.00463	0.004981			Wing only	Alpha Sweep P1=LW P2=RW P3=LGB P4=RGB
10/24/95 at 10:09:51	3050	3	0	0	56.6	508	56.69	69.57	13.87	13.9	0.004551	0.004895			Wing only	Alpha Sweep P1=LW P2=RW P3=LGB P4=RGB
	TPN	Tape#	deg	deg	psf	deg R	psia	psia	psia	psia	C mu	C mu	C mu	C mu		
Date & Time	TPN	Tape#	Alpha	Beta	Q	T0IN	PL_1	PL_2	PL_3	PL_4	L NOSE	R NOSE			Comment	
10/24/95 at 10:35:38	3051	3	0	0	55.6	508.8	89.87	83.42	13.89	13.9	0.005144	0.005157			Nose only	Alpha Sweep P1=LN P2=RN P3=LGB P4=RGB
10/24/95 at 10:36:35	3052	3	16.23	-3.95	55.5	508.8	89.7	83.31	13.32	13.4	0.005144	0.005159			Nose only	Alpha Sweep P1=LN P2=RN P3=LGB P4=RGB
10/24/95 at 10:37:26	3053	3	18.26	-3.98	55.6	508.6	89.7	83.23	13.27	13.5	0.005134	0.005145			Nose only	Alpha Sweep P1=LN P2=RN P3=LGB P4=RGB
10/24/95 at 10:38:17	3054	3	20.27	-3.94	55.7	508.7	89.61	83.2	13.23	13.5	0.00512	0.005134			Nose only	Alpha Sweep P1=LN P2=RN P3=LGB P4=RGB
10/24/95 at 10:39:07	3055	3	22.3	-3.93	56.1	508.7	89.52	83.16	13.13	13.4	0.005078	0.005095			Nose only	Alpha Sweep P1=LN P2=RN P3=LGB P4=RGB
10/24/95 at 10:39:57	3056	3	24.33	-3.94	55.7	508.8	89.5	83.08	13.13	13.4	0.005114	0.005126			Nose only	Alpha Sweep P1=LN P2=RN P3=LGB P4=RGB
10/24/95 at 10:40:48	3057	3	26.34	-3.98	55.7	508.6	89.43	83	13.05	13.3	0.00511	0.005121			Nose only	Alpha Sweep P1=LN P2=RN P3=LGB P4=RGB
10/24/95 at 10:41:43	3058	3	16.22	-0.01	56.4	508.7	89.41	83.02	13.35	13.3	0.005045	0.005059			Nose only	Alpha Sweep P1=LN P2=RN P3=LGB P4=RGB
10/24/95 at 10:42:34	3059	3	18.25	-0.01	56	508.8	89.3	82.95	13.35	13.4	0.005075	0.005091			Nose only	Alpha Sweep P1=LN P2=RN P3=LGB P4=RGB
10/24/95 at 10:43:25	3060	3	20.26	-0.01	55.7	508.9	89.33	82.93	13.32	13.3	0.005104	0.005117			Nose only	Alpha Sweep P1=LN P2=RN P3=LGB P4=RGB
10/24/95 at 10:44:16	3061	3	22.29	-0.01	56.1	508.9	89.26	82.89	13.29	13.3	0.005064	0.005078			Nose only	Alpha Sweep P1=LN P2=RN P3=LGB P4=RGB
10/24/95 at 10:45:06	3062	3	24.32	-0.01	55.7	508.9	89.22	82.84	13.28	13.3	0.005098	0.005112			Nose only	Alpha Sweep P1=LN P2=RN P3=LGB P4=RGB
10/24/95 at 10:45:57	3063	3	26.33	-0.01	55.1	508.8	89.15	82.81	13.2	13.2	0.005149	0.005165			Nose only	Alpha Sweep P1=LN P2=RN P3=LGB P4=RGB

Table 3. Representative Test Conditions with and without Blowing

10/24/95 at 10:46:54	3064	3	16.24	3.93	56	508.9	89.16	82.85	13.44	13.3	0.005067	0.005085			Nose only	Alpha Sweep P1=LN P2=RN P3=LGB P4=RGB
10/24/95 at 10:47:45	3065	3	18.26	3.99	56.2	509.1	89.15	82.8	13.5	13.2	0.005048	0.005064			Nose only	Alpha Sweep P1=LN P2=RN P3=LGB P4=RGB
10/24/95 at 10:48:36	3066	3	20.26	3.99	55.9	509.3	89.11	82.77	13.47	13.2	0.005073	0.005089			Nose only	Alpha Sweep P1=LN P2=RN P3=LGB P4=RGB
10/24/95 at 10:49:27	3067	3	22.29	3.98	56	509.3	89.09	82.73	13.44	13.1	0.005063	0.005077			Nose only	Alpha Sweep P1=LN P2=RN P3=LGB P4=RGB
10/24/95 at 10:50:18	3068	3	24.3	3.99	55.3	509.4	88.99	82.72	13.42	13.1	0.005121	0.005141			Nose only	Alpha Sweep P1=LN P2=RN P3=LGB P4=RGB
10/24/95 at 10:51:09	3069	3	26.33	3.99	55.5	509.4	89.04	82.68	13.38	13.1	0.005106	0.00512			Nose only	Alpha Sweep P1=LN P2=RN P3=LGB P4=RGB
10/24/95 at 10:52:08	3070	3	0	0	56.1	509.2	88.95	82.68	13.88	13.9	0.005046	0.005065			Nose only	Alpha Sweep P1=LN P2=RN P3=LGB P4=RGB
	TPN	Tape#	deg	deg	psf	deg R	psia	psia	psia	psia	C mu	C mu	C mu	C mu		
Date & Time	TPN	Tape#	Alpha	Beta	Q	TOIN	PL_1	PL_2	PL_3	PL_4	L NOSE	R NOSE	L GUN	R GUN	Comment	
10/24/95 at 11:01:06	3071	3	0	0	56.5	509.2	89.19	82.91	66.61	60.8	0.005024	0.005043	0.004181	0.004513	Nose & GB	Alpha Sweep P1=LN P2=RN P3=LGB P4=RGB
10/24/95 at 11:01:53	3072	3	0	0	56.3	509.1	89.24	82.92	66.6	60.7	0.005044	0.005062	0.004195	0.004521	Nose & GB	Alpha Sweep P1=LN P2=RN P3=LGB P4=RGB
10/24/95 at 11:02:50	3073	3	16.24	-3.93	55.6	509.5	89.23	82.94	66.59	60.7	0.005107	0.005127	0.004247	0.004578	Nose & GB	Alpha Sweep P1=LN P2=RN P3=LGB P4=RGB
10/24/95 at 11:03:41	3074	3	18.25	-3.98	56.2	509.4	89.17	82.91	66.55	60.6	0.005049	0.00507	0.004199	0.004522	Nose & GB	Alpha Sweep P1=LN P2=RN P3=LGB P4=RGB
10/24/95 at 11:04:32	3075	3	20.27	-3.94	56	509.4	89.19	82.93	66.54	60.6	0.005069	0.00509	0.004214	0.004538	Nose & GB	Alpha Sweep P1=LN P2=RN P3=LGB P4=RGB
10/24/95 at 11:05:23	3076	3	22.29	-3.93	55.9	509.5	89.18	82.91	66.52	60.6	0.005077	0.005098	0.00422	0.004546	Nose & GB	Alpha Sweep P1=LN P2=RN P3=LGB P4=RGB
10/24/95 at 11:06:14	3077	3	24.31	-3.98	55.6	509.4	89.23	82.97	66.52	60.6	0.005107	0.005129	0.004243	0.004571	Nose & GB	Alpha Sweep P1=LN P2=RN P3=LGB P4=RGB
10/24/95 at 11:07:05	3078	3	26.35	-3.93	55.8	509.4	89.24	82.97	66.48	60.6	0.00509	0.00511	0.004225	0.004554	Nose & GB	Alpha Sweep P1=LN P2=RN P3=LGB P4=RGB
10/24/95 at 11:08:00	3079	3	16.21	-0.01	56	509.3	89.16	82.93	66.47	60.6	0.005067	0.00509	0.004209	0.004538	Nose & GB	Alpha Sweep P1=LN P2=RN P3=LGB P4=RGB
10/24/95 at 11:08:51	3080	3	18.24	-0.01	55.7	509.4	89.23	82.96	66.46	60.6	0.005098	0.005119	0.004231	0.004563	Nose & GB	Alpha Sweep P1=LN P2=RN P3=LGB P4=RGB
10/24/95 at 11:09:42	3081	3	20.26	-0.01	55.7	509.3	89.18	82.93	66.4	60.5	0.005095	0.005117	0.004228	0.004555	Nose & GB	Alpha Sweep P1=LN P2=RN P3=LGB P4=RGB
10/24/95 at 11:10:33	3082	3	22.29	-0.02	55.6	509.3	89.19	82.93	66.43	60.5	0.005105	0.005126	0.004237	0.004563	Nose & GB	Alpha Sweep P1=LN P2=RN P3=LGB P4=RGB
10/24/95 at 11:11:24	3083	3	24.32	-0.01	55.7	509.3	89.25	82.95	66.43	60.5	0.005099	0.005118	0.00423	0.004555	Nose & GB	Alpha Sweep P1=LN P2=RN P3=LGB P4=RGB
10/24/95 at 11:12:15	3084	3	26.32	-0.01	55.4	509.3	89.25	82.94	66.42	60.5	0.005127	0.005145	0.004252	0.00458	Nose & GB	Alpha Sweep P1=LN P2=RN P3=LGB P4=RGB
10/24/95 at 11:13:11	3085	3	16.23	3.94	55.7	509.4	89.24	82.95	66.4	60.4	0.005099	0.005118	0.004228	0.004547	Nose & GB	Alpha Sweep P1=LN P2=RN P3=LGB P4=RGB
10/24/95 at 11:14:02	3086	3	18.25	3.96	55.9	509.4	89.25	82.99	66.4	60.4	0.005081	0.005102	0.004212	0.004531	Nose & GB	Alpha Sweep P1=LN P2=RN P3=LGB P4=RGB
10/24/95 at 11:14:53	3087	3	20.26	3.99	55.8	509.5	89.27	83	66.39	60.4	0.005091	0.005112	0.004219	0.004539	Nose & GB	Alpha Sweep P1=LN P2=RN P3=LGB P4=RGB
10/24/95 at 11:15:44	3088	3	22.29	3.98	55.6	509.4	89.27	83.01	66.39	60.4	0.00511	0.005131	0.004235	0.004556	Nose & GB	Alpha Sweep P1=LN P2=RN P3=LGB P4=RGB
10/24/95 at 11:16:35	3089	3	24.32	3.95	55.6	509.3	89.2	82.95	66.38	60.4	0.005106	0.005128	0.004234	0.004556	Nose & GB	Alpha Sweep P1=LN P2=RN P3=LGB P4=RGB
10/24/95 at 11:17:26	3090	3	26.34	3.94	55.3	509.2	89.2	82.97	66.35	60.4	0.005133	0.005157	0.004255	0.00458	Nose & GB	Alpha Sweep P1=LN P2=RN P3=LGB P4=RGB
10/24/95 at 11:18:25	3091	3	0	0	56.2	509.2	89.18	82.98	66.35	60.4	0.00505	0.005075	0.004187	0.004507	Nose & GB	Alpha Sweep P1=LN P2=RN P3=LGB P4=RGB
	TPN	Tape#	deg	deg	psf	deg R	psia	psia	psia	psia	C mu	C mu	C mu	C mu		
Date & Time	TPN	Tape#	Alpha	Beta	Q	TOIN	PL_1	PL_2	PL_3	PL_4	L NOSE	R NOSE	L WING	R WING	Comment	
10/24/95 at 12:50:30	3093	3	0	0	56.2	510	89.17	82.85	57.7	71.1	0.005049	0.005067	0.004665	0.005038	Nose & Wing	Alpha Sweep P1=LN P2=RN P3=LW P4=RW
10/24/95 at 12:51:48	3094	3	16.24	-3.92	55.7	510.2	89.16	82.8	57.73	71.2	0.005094	0.005109	0.004709	0.005091	Nose & Wing	Alpha Sweep P1=LN P2=RN P3=LW P4=RW
10/24/95 at 12:52:39	3095	3	18.25	-3.98	55.2	510.3	89.16	82.79	57.74	71.1	0.00514	0.005155	0.004753	0.00513	Nose & Wing	Alpha Sweep P1=LN P2=RN P3=LW P4=RW
10/24/95 at 12:53:30	3096	3	20.28	-3.94	55.6	510.2	89.08	82.73	57.72	71.1	0.005099	0.005114	0.004717	0.005093	Nose & Wing	Alpha Sweep P1=LN P2=RN P3=LW P4=RW
10/24/95 at 12:54:21	3097	3	22.3	-3.93	55.5	510.1	88.98	82.69	57.7	71.1	0.005102	0.005121	0.004724	0.005102	Nose & Wing	Alpha Sweep P1=LN P2=RN P3=LW P4=RW
10/24/95 at 12:55:12	3098	3	24.34	-3.93	55.8	510.1	88.98	82.65	57.71	71.1	0.005075	0.005091	0.004699	0.005075	Nose & Wing	Alpha Sweep P1=LN P2=RN P3=LW P4=RW
10/24/95 at 12:56:03	3099	3	26.36	-3.92	56	510	88.98	82.67	57.7	71.1	0.005057	0.005074	0.004682	0.005056	Nose & Wing	Alpha Sweep P1=LN P2=RN P3=LW P4=RW
10/24/95 at 12:56:58	3100	3	16.23	-0.01	56.4	509.9	88.92	82.6	57.73	71.1	0.005017	0.005033	0.004651	0.005021	Nose & Wing	Alpha Sweep P1=LN P2=RN P3=LW P4=RW
10/24/95 at 12:57:49	3101	3	18.25	-0.01	56.2	510	88.84	82.57	57.72	71.1	0.005031	0.00505	0.004667	0.005038	Nose & Wing	Alpha Sweep P1=LN P2=RN P3=LW P4=RW
10/24/95 at 12:58:40	3102	3	20.27	-0.01	56.5	510	88.86	82.56	57.91	71.1	0.005005	0.005022	0.004657	0.005012	Nose & Wing	Alpha Sweep P1=LN P2=RN P3=LW P4=RW
10/24/95 at 12:59:31	3103	3	22.3	-0.01	56.2	509.9	88.83	82.54	57.71	71	0.00503	0.005048	0.004666	0.005031	Nose & Wing	Alpha Sweep P1=LN P2=RN P3=LW P4=RW
10/24/95 at 13:00:22	3104	3	24.32	-0.01	56.6	509.8	88.8	82.52	57.72	71	0.004993	0.005011	0.004634	0.004996	Nose & Wing	Alpha Sweep P1=LN P2=RN P3=LW P4=RW
10/24/95 at 13:01:13	3105	3	26.33	-0.01	55.9	510	88.78	82.49	57.71	71	0.005054	0.005072	0.004691	0.005058	Nose & Wing	Alpha Sweep P1=LN P2=RN P3=LW P4=RW
10/24/95 at 13:02:08	3106	3	16.23	3.93	57	510.2	88.78	82.47	57.7	71	0.004957	0.004973	0.0046	0.004961	Nose & Wing	Alpha Sweep P1=LN P2=RN P3=LW P4=RW
10/24/95 at 13:02:59	3107	3	18.25	3.99	56.5	510.3	88.75	82.49	57.71	71	0.004999	0.005018	0.004641	0.005005	Nose & Wing	Alpha Sweep P1=LN P2=RN P3=LW P4=RW
10/24/95 at 13:03:50	3108	3	20.27	3.99	56.7	510.1	88.7	82.43	57.76	71	0.004979	0.004997	0.004629	0.004987	Nose & Wing	Alpha Sweep P1=LN P2=RN P3=LW P4=RW
10/24/95 at 13:04:40	3109	3	22.31	3.94	56.9	510	88.69	82.44	57.71	71	0.004961	0.00498	0.004609	0.004969	Nose & Wing	Alpha Sweep P1=LN P2=RN P3=LW P4=RW
10/24/95 at 13:05:31	3110	3	24.32	3.99	55.4	510	88.64	82.41	57.7	71	0.005092	0.005113	0.004732	0.005104	Nose & Wing	Alpha Sweep P1=LN P2=RN P3=LW P4=RW
10/24/95 at 13:06:22	3111	3	26.34	3.99	55.6	509.9	88.62	82.4	57.7	71	0.005072	0.005094	0.004715	0.005086	Nose & Wing	Alpha Sweep P1=LN P2=RN P3=LW P4=RW
10/24/95 at 13:07:21	3112	3	0	0	57	509.9	88.6	82.4	57.64	70.9	0.004947	0.004968	0.004595	0.004954	Nose & Wing	Alpha Sweep P1=LN P2=RN P3=LW P4=RW
	TPN	Tape#	deg	deg	psf	deg R	psia	psia	psia	psia	C mu	C mu	C mu	C mu		
Date & Time	TPN	Tape#	Alpha	Beta	Q	TOIN	PL_1	PL_2	PL_3	PL_4	L WING	R WING	L GUN	R GUN	Comment	
10/24/95 at 13:25:37	3113	3	0	0	55.9	510.1	40.05	50.44	46.62	43.1	0.003255	0.003594	0.002958	0.003233	GB & Wing	Alpha Sweep P1=LW P2=RW P3=LGB P4=RGB
10/24/95 at 13:26:55	3114	3	16.24	-3.92	56	510	39.97	50.36	46.61	43.1	0.003243	0.003581	0.002952	0.003228	GB & Wing	Alpha Sweep P1=LW P2=RW P3=LGB P4=RGB
10/24/95 at 13:27:46	3115	3	18.26	-3.94	55.6	509.9	39.89	50.25	46.6	43.1	0.00326	0.003599	0.002972	0.003251	GB & Wing	Alpha Sweep P1=LW P2=RW P3=LGB P4=RGB
10/24/95 at 13:28:37	3116	3	20.28	-3.94	55.7	509.8	39.81	50.15	46.57	43.1	0.003248	0.003586	0.002965	0.003245	GB & Wing	Alpha Sweep P1=LW P2=RW P3=LGB P4=RGB
10/24/95 at 13:29:28	3117	3	22.31	-3.97	55.8	509.8	39.78	50.1	46.56	43.1	0.003239	0.003576	0.002959	0.003239	GB & Wing	Alpha Sweep P1=LW P2=RW P3=LGB P4=RGB
10/24/95 at 13:30:19	3118	3	24.33	-3.93	55.5	509.7	39.72	50.05	46.57	43.1	0.003252	0.003591	0.002976	0.003257	GB & Wing	Alpha Sweep P1=LW P2=RW P3=LGB P4=RGB
10/24/95 at 13:31:10	3119	3	26.36	-3.93	55.5	509.5	39.69	50	46.57	43	0.003249	0.003588	0.002976	0.003249	GB & Wing	Alpha Sweep P1=LW P2=RW P3=LGB P4=RGB
10/24/95 at 13:32:05	3120	3	16.24	-0.01	56.3	509.5	39.67	49.94	46.59	43.1	0.003202	0.003533	0.002935	0.00321	GB & Wing	Alpha Sweep P1=LW P2=RW P3=LGB P4=RGB
10/24/95 at 13:32:56	3121	3	18.25	-0.01	55.9	509.3	39.65	49.91	46.59	43.1	0.003223	0.003556	0.002956	0.003233	GB & Wing	Alpha Sweep P1=LW P2=RW P3=LGB P4=RGB

Table 4. Representative Test Conditions with and without Blowing

F-15 Vertical Tail Buffet Test: RMS (in-lbs) & Peak PSD (in-lbs**2/Hz)

1st Bending: 35-65 Hz

S1-BENDING: No Blowing Pressure					Wing Blowing Pressure					
Beta	Alpha	rms	peak	freq	B.P.	Beta	Alpha	rms	peak	freq
-4	20	.4719	3.268E-02	49.4						
-4	22	.6473	4.857E-02	50.0						
-4	24	.8462	1.104E-01	48.2						
-4	28	1.1270	2.024E-01	48.2						
-4	32	1.5490	3.856E-01	48.8	45	-4	32	1.5620	4.819E-01	51.3
0	20	.4131	2.155E-02	50.0						
0	22	.5085	3.832E-02	50.0						
0	24	.6262	4.925E-02	48.8	45	0	24	.6672	6.118E-02	51.3
0	28	1.0190	1.584E-01	48.2	65	0	24	.6224	4.609E-02	47.0
0	32	1.6110	5.005E-01	47.6	45	0	32	1.5644	4.996E-01	51.3
4	20	.2885	8.435E-03	50.7						
4	22	.4207	2.526E-02	50.7						
4	24	.6123	6.338E-02	50.7						
4	28	.9290	1.363E-01	50.0						
4	32	1.3960	3.659E-01	48.8	45	4	32	1.5402	3.871E-01	50.0

1st Torsion: 180-210 Hz

S2-TORSION: No Blowing Pressure					Wing Blowing Pressure					
Beta	Alpha	rms	peak	freq	B.P.	Beta	Alpha	rms	peak	freq
-4	20	.5690	2.721E-02	190.4						
-4	22	.6756	3.987E-02	191.0						
-4	24	.5643	2.557E-02	191.6						
-4	28	.2354	4.128E-03	194.7						
-4	32	.2240	4.622E-03	193.5	45	-4	32	.2372	5.284E-03	204.5
0	20	.3817	1.632E-02	190.4						
0	22	.5708	3.368E-02	189.8						
0	24	.7279	5.535E-02	191.0	45	0	24	.6712	5.378E-02	201.4
0	28	.4221	1.556E-02	191.0	65	0	24	.6099	3.122E-02	187.4
0	32	.2695	5.935E-03	193.5	45	0	32	.3151	1.124E-02	205.7
4	20	.2140	4.036E-03	192.3						
4	22	.3882	1.423E-02	191.6						
4	24	.6070	3.559E-02	193.5						
4	28	.7277	4.453E-02	192.9						
4	32	.3947	1.381E-02	195.3	45	4	32	.4154	2.289E-02	204.5

2nd Bending: 210-240 Hz

S1-BENDING: No Blowing Pressure					Wing Blowing Pressure					
Beta	Alpha	rms	peak	freq	B.P.	Beta	Alpha	rms	peak	freq
-4	20	.3241	6.926E-03	230.1						
-4	22	.3698	9.630E-03	226.4						
-4	24	.3158	7.514E-03	227.1						
-4	28	.4941	1.790E-03	227.7						
-4	32	.3532	9.624E-03	227.1	45	-4	32	.3313	1.299E-02	237.4
0	20	.2478	4.503E-03	228.9						
0	22	.3145	6.206E-03	228.9						
0	24	.3090	5.511E-03	228.9	45	0	24	.3143	8.208E-03	232.5
0	28	.4908	1.687E-02	228.9	65	0	24	.3136	7.744E-03	216.7
0	32	.4465	1.303E-02	231.3	45	0	32	.3797	1.529E-02	239.3
4	20	.1100	8.259E-04	229.5						
4	22	.1812	2.647E-03	232.5						
4	24	.2640	5.177E-03	231.9						
4	28	.3367	9.148E-03	233.2						
4	32	.5290	1.955E-02	228.3	45	4	32	.4909	2.343E-02	236.8

Table 5. Additional Data for Different Test Conditions

COMPARISON OF ANALYSIS AND TEST

Coefficient	Computation	Test
Lift	1.30	1.29
Side Force	0.039	0.051
Drag	0.582	0.824
Pitching Moment	-.173	-.186
Yawing Moment	0.005	0.003
Rolling Moment	-.008	0.011

Conditions: M=0.2, 24 deg angle of attack, & -4 deg sideslip

Table 6. Comparison of Analysis and Test

96149TMF-12LH

Table 7. Vertical Tail Pressure Comparisons (Flow Through Inlet Computations to Wind Tunnel Test)

Gauge	Test Pressure psi	Computational Pressure psi	Percentage Difference	Test Pressure Coefficient	Computational Pressure Coefficient	Percentage Difference	Within Experimental Uncertainty
Right Inner							
K147 2	13.436	13.620	1.4	-0.725	-0.251	-65.4	*
K148 3	13.576	13.620	0.3	-0.365	-0.251	-31.3	*
K149 4	13.400	13.643	1.8	-0.817	-0.194	-76.3	*
K145 5	13.480	13.668	1.4	-0.612	-0.127	-79.2	*
K150 6	13.555	13.644	0.7	-0.419	-0.189	-54.8	*
Right Outer							
K152 2	13.524	13.525	0.0	-0.499	-0.497	-0.3	*
K153 3	13.533	13.567	0.2	-0.475	-0.389	-18.1	*
K154 4	13.404	13.571	1.2	-0.807	-0.377	-53.3	*
K151 5	13.224	13.591	2.8	-1.269	-0.323	-74.3	
K155 6	13.454	13.603	1.1	-0.678	-0.296	-56.4	*
Left Inner							
K122 1	13.656	13.624	-0.2	-0.159	-0.242	52.1	*
K121 2	13.604	13.602	0.0	-0.293	-0.298	1.8	*
K115 3	13.601	13.576	-0.2	-0.301	-0.365	21.3	*
K119 4	13.541	13.579	0.3	-0.455	-0.358	-21.3	*
K114 5	13.533	13.581	0.4	-0.475	-0.352	-25.9	*
K113 6	13.622	13.617	0.0	-0.247	-0.260	5.3	*
Left Outer							
K144 1	13.545	13.562	0.1	-0.445	-0.402	-9.6	*
K143 2	13.591	13.586	0.0	-0.326	-0.340	4.3	*
K120 3	13.629	13.627	0.0	-0.229	-0.233	1.9	*
K117 4	13.641	13.677	0.3	-0.198	-0.105	-47.1	*
K142 5	13.596	13.644	0.4	-0.314	-0.191	-39.0	*
K118 6	13.653	13.640	-0.1	-0.167	-0.200	20.0	*

Table 7. Vertical Tail Static Pressure Comparison